ELUCIDATION OF microRNA miR-6744-5p REGULATION OF ANOIKIS IN BREAST CANCER CELL LINES AND POTENTIAL FOR THERAPEUTIC APPLICATIONS

SHARAN MALAGOBADAN

FACULTY OF SCIENCE
UNIVERSITY OF MALAYA
KUALA LUMPUR

2019

ELUCIDATION OF microRNA miR-6744-5p REGULATION OF ANOIKIS IN BREAST CANCER CELL LINES AND POTENTIAL FOR THERAPEUTIC APPLICATIONS

SHARAN MALAGOBADAN

THESIS SUBMITTED IN FULFILMENT OF THE REQUIREMENTS FOR THE DEGREE OF DOCTOR OF PHILOSOPHY

INSTITUTE OF BIOLOGICAL SCIENCES
FACULTY OF SCIENCE
UNIVERSITY OF MALAYA
KUALA LUMPUR

2019

UNIVERSITY OF MALAYA

ORIGINAL LITERARY WORK DECLARATION

Name of Candidate: **Sharan Malagobadan**

Matric No: **SHC140032**

Name of Degree: **Doctor of Philosophy**

Title of Project Paper/Research Report/Dissertation/Thesis ("this Work"):

ELUCIDATION OF microRNA miR6744-5p REGULATION OF ANOIKIS IN BREAST CANCER CELL LINES AND POTENTIAL FOR THERAPEUTIC APPLICATIONS

Field of Study: **Molecular Oncology**

I do solemnly and sincerely declare that:

(1) I am the sole author/writer of this Work;
(2) This Work is original;
(3) Any use of any work in which copyright exists was done by way of fair dealing and for permitted purposes and any excerpt or extract from, or reference to or reproduction of any copyright work has been disclosed expressly and sufficiently and the title of the Work and its authorship have been acknowledged in this Work;
(4) I do not have any actual knowledge nor do I ought reasonably to know that the making of this work constitutes an infringement of any copyright work;
(5) I hereby assign all and every rights in the copyright to this Work to the University of Malaya ("UM"), who henceforth shall be owner of the copyright in this Work and that any reproduction or use in any form or by any means whatsoever is prohibited without the written consent of UM having been first had and obtained;
(6) I am fully aware that if in the course of making this Work I have infringed any copyright whether intentionally or otherwise, I may be subject to legal action or any other action as may be determined by UM.

Candidate's Signature Date:

Subscribed and solemnly declared before,

Witness's Signature Date:

Name:

Designation:

ELUCIDATION OF microRNA miR-6744-5p REGULATION OF ANOIKIS IN BREAST CANCER CELL LINES AND POTENTIAL FOR THERAPEUTIC APPLICATIONS

ABSTRACT

Anoikis is apoptosis induced when cells are detached from the extracellular matrix and neighbouring cells. Since anoikis serves as a regulatory barrier, cancer cells often acquire resistance towards anoikis during tumorigenesis to become metastatic. MicroRNAs (miRNAs) are short strand of RNA molecules regulating genes post-transcriptionally, by binding to mRNAs and reducing the expression of its target genes. This study aims to elucidate the role of a novel miRNA, miR-6744-5p, in regulating anoikis in breast cancer and identify its target gene. Anoikis resistant variant of luminal A type breast cancer MCF-7 cell line (MCF-7-AR) was generated by selecting and amplifying surviving cells after repeated exposure to growth in suspension. miRNA microarray revealed a list of dysregulated miRNAs, from which miR-6744-5p was chosen for overexpression and knockdown studies. In MCF-7, overexpression of miR-6744-5p increased anoikis as shown by viability and caspase-3/7 activity assay, inhibited cell migration as shown by wound healing assay and increased E-cadherin expression as shown by Western blotting. Knockdown of miR-6744-5p decreased anoikis, increased cell migration and decreased E-cadherin expression. In the invasive triple-negative breast cancer cell line MDA-MB-231, overexpression of miR-6744-5p promoted anoikis and inhibited cell migration but knockdown of miR-6744-5p produced no effect. Additionally, overexpression of miR-6744-5p also induced morphological changes of MDA-MB-231 cells and inhibited invasiveness of the cells *in vitro* in transwell invasion assay and *in vivo* in zebrafish larva metastasis model. Furthermore, N-acetyltransferase 1 (NAT1) has been identified and validated as the direct target of miR-6744-5p using luciferase reporter assay and western

blot. Overall, this study has proven the ability of miR-6744-5p to increase anoikis in both luminal A and triple negative breast cancer cell lines, highlighting its therapeutic potential in treating breast cancer.

Keywords: anoikis, miRNA, breast cancer

PENYELIDIKAN KE ATAS mikroRNA miR-6744-5p YANG MENGAWAL SELIA ANOIKIS DALAM SEL SEL KANSER PAYUDARA DAN POTENSI TERAPEUTIKNYA

ABSTRAK

Anoikis adalah proses kematian sel yang disebabkan apabila sel-sel terpisah dari matrik luar sel dan dari sel-sel berhampiran. Oleh kerana anoikis bertindak sebagai penghalang pengaturan, sel-sel kanser sering memperoleh ketahanan terhadap anoikis semasa melalui proses perubahan tumor untuk menjadi metastatik. MikroRNA (miRNA) adalah sejenis molekul RNA pendek yang mengawal selia gen selepas proses transkripsi, melalui perikatan dengan mRNA dan mengurangkan ekspresi gen sasarannya. Kajian ini bertujuan untuk menjelaskan peranan mikroRNA baru, iaitu miR-6744-5p, dalam mengawal selia anoikis dalam kanser payudara dan mengenalpasti gen sasarannya. Sejenis varian sel kanser yang boleh menahan anoikis (MCF-7-AR6) telah dihasilkan dari sel kanser payudara jenis "luminal A", MCF-7, dengan memilih dan menguatkan sel yang masih hidup selepas pendedahan berulang kepada pertumbuhan dalam penggantungan. Perbandingan menggunakan "microarray" miRNA telah mendedahkan senarai miRNA yang mengalami perubahan, dari mana miR-6744-5p dipilih untuk kajian peningkatan ekspresi dan perencatan dalam MCF-7. Selain itu, peningkatan ekspresi miR-6744-5p dalam sel kanser payudara jenis "triple-negative", MDA-MB-231, juga telah dijalankan untuk menilai keupayaannya dalam menganggu potensi metastatik sel kanser payudara. Kajian ini menunjukkan bahawa peningkatan ekspresi dan perencatan miR-6744-5p dalam MCF-7 masing-masing telah meningkatkan dan menurunkan kepekaan terhadap anoikis. Keputusan yang sama diperhatikan dalam MDA-MB-231, di mana peningkatan miR-6744-5p telah menyebabkan perubahan bentuk sel dan mengurangkan pencerobohan sel-sel kanser. Selain itu, enzim N-acetyltransferase 1 telah dikenalpasti dan disahkan

sebagai sasaran langsung bagi miR-6744-5p. Secara keseluruhannya, kajian ini telah membuktikan keupayaan miR-6744-5p untuk meningkatkan kepekaan terhadap anoikis pada kedua-dua "luminal A" dan "triple-negative" sel-sel kanser payudara, menunjukkan potensi terapeutiknya dalam merawat kanser payudara.

Kata kunci: anoikis, miRNA, kanser payudara

ACKNOWLEDGEMENTS

I would like to thank and acknowledge the roles of various individuals and parties that have supported my journey as a postgraduate, both directly and indirectly, without whom this project would not have been successfully completed. First and foremost, I would like to thank my supervisor, Professor Dr. Noor Hasima Nagoor, who has guided and supervised this project from the very beginning. Her vision and guidance have always been available throughout this project, for which I am eternally grateful.

I would also like to acknowledge and thank the members of the Cancer Research Lab for their camaraderie during our time together in the lab. Especially noteworthy are the senior members of the lab, Phuah Neoh Hun, Norahayu Othman and Ho Chai San, whose advices and guidance were invaluable during the various difficulties faced during this project.

Next, I would like to thank all the generous financial assistance and grants that made this project possible, such as the MyBrain MyPhD scholarship from the Ministry of Education, the University of Malaya Postgraduate Research grant (PG021-2016A) and the Research University CEBAR grant (RU015-2016). Last but not the least, I would like to thank everyone else who has been there for me throughout this journey, both friends and family, for their support and motivation. Thank you.

TABLE OF CONTENTS

LIST OF FIGURES

LIST OF TABLES

LIST OF SYMBOLS AND ABBREVIATIONS

α	:	Alpha
β	:	Beta
cm	:	Centimetre
℃	:	Degree Celsius
Δ	:	Delta
hpa	:	Hectopascals
h	:	Hours
<	:	Less than
µL	:	Microliter
µm	:	Micrometre
µM	:	Micromolar
mA	:	Milliampere
mg	:	Milligram
mL	:	Millilitre
mm	:	Millimetre
mM	:	Millimolar
>	:	More than
×	:	Multiplication
ng	:	Nanogram
nM	:	Nanomolar
%	:	Percentage
P_c	:	Pressure for compensation
P_i	:	Pressure for injection
g	:	Relative centrifugal force

t_i	:	Time for injection
Akt	:	Ak thymoma/Protein kinase B
AMPA	:	α-amino-3-hydroxy-5-methyl-4-isoxazolepropionic acid
APS	:	Ammonium persulfate
ANOVA	:	Analysis of variance
ATG5	:	Autophagy related 5
BCA	:	Bicinchoninic acid
BCDNIN3D	:	Bicoid-interacting 3 domain-containing protein
Bcl-2	:	B-cell lymphoma 2
Bim	:	Bcl-2-like protein 11
Bit1	:	Bcl-2 inhibitor of transcription 1
Bmf	:	Bcl-2 modifying factor
BNIP3	:	Bcl-2/adenovirus E1B 19 kDa protein-interacting protein 3
BRCA2	:	BCL2/adenovirus E1B 19 kDa protein-interacting protein 3
BSA	:	Bovine serum albumin
CACNG8	:	Calcium voltage-dependent channel gamma-8 subunit
CAM	:	Cell adhesion molecule
CCR4-NOT	:	Carbon catabolite repressor 4- Negative on TATA
CD45	:	Cluster of differentiation 45
cDNA	:	Complementary DNA
CELF2	:	CUGBP Elav-Like Family Member 2
CSC	:	Cancer stem cell
CTC	:	Circulating tumour cell
CYP1A2	:	Cytochrome P450
DiI	:	1,1'-dioctadecyl-3,3,3',3'-tetramethylindocarbo-cyanine perchlorate

DNA	:	Deoxyribonucleic acid
dNTP	:	Deoxynucleotide triphosphate
DPBS	:	Dulbecco's phosphate-buffered saline
DTT	:	Dithiothreitol
dTTP	:	Deoxythymidine triphosphate
E-cadherin	:	Epithelial cadherin
ECM	:	Extracellular matrix
EGFR	:	Epidermal growth factor receptor
EMT	:	Epithelial-to-mesenchymal transition
Ep-CAM	:	Epithelial cell adhesion molecule
EPOR	:	Erythropoietin receptor
ER	:	Estrogen receptor
ErbB	:	EGFR structurally related receptor tyrosine kinase family
ERK	:	Extracellular signal-regulated kinases
FBS	:	Fetal bovine serum
FGF5	:	Fibroblast growth factor 5
FGFR	:	Fibroblast growth factor receptor
GAPDH	:	Glyceraldehyde 3-phosphate dehydrogenase
GNB1	:	G Protein Subunit Beta 1
GW182	:	Glycine-tryptophan protein of 182 kDa
HEK293T	:	Human embryonic kidney-293-T-antigen
HER2	:	Human epidermal growth factor receptor 2
hpf	:	Hours post fertilisation
HRP	:	Horseradish peroxidase
ICAM1	:	Intercellular adhesion molecule 1
IGF	:	Insulin growth factor

IGF1R	:	Insulin growth factor-1 receptor
IgG	:	Immunoglobulin G
Ki-67	:	Kiel-67 proliferation marker
LNA	:	Locked nucleic acid
MAPK	:	Mitogen-activated protein kinases
MCF-7	:	Michigan cancer foundation-7
MDA-MB-231	:	MD Anderson-metastatic breast cancer-231
MEM	:	Minimum essential media
MET	:	Mesenchymal-to-epithelial transition
miRISC	:	miRNA-induced silencing complex
miRNA	:	MicroRNA
MMP	:	Metalloproteinases
MRE	:	mRNA response element
mRNA	:	Messenger RNA
NAT1	:	N-acetyltransferase 1
ncRNA	:	Non-coding RNA
NSCLC	:	Non-small-cell lung carcinoma
nt	:	Nucleotide
ORF	:	Open reading frame
p53	:	Tumour protein p53
PACT	:	Protein Activator of the interferon-induced protein kinase
PAGE	:	Polyacrylamide gel electrophoresis
PAN	:	Poly(A)-nuclease deadenylation complex subunit
PBS	:	Phosphate-buffered saline
PI3K	:	Phosphoinositide 3-kinase
PR	:	Progesterone receptor

PTEN	:	Phosphatase and tensin homolog
PTU	:	Phenyl 2-thiourea
RACK1	:	Receptor for activated C kinase 1
RIPA	:	Radioimmunoprecipitation assay
RNA	:	Ribonucleic acid
RPM	:	Rotation per minute
RPMI	:	Roswell Park Memorial Institute
RT-qPCR	:	Reverse transcription-quantitative polymerase chain reaction
SD	:	Standard deviation
SDS	:	Sodium dodecyl sulfate
SOX7	:	SRY-Box 7
siRNA	:	Small interfering RNA
TARBP2	:	Trans-activation-responsive RNA-binding protein 2
TBS	:	Tris-buffered saline
TCTP	:	Translationally-controlled tumour protein
TEMED	:	Tetramethyl-ethylenediamine
TGF-β	:	Transforming growth factor beta
TGS	:	Tris/Glycine/SDS
TNFR	:	Tumour necrosis factor receptor
ULA	:	Ultra-Low Attachment
UTR	:	Untranslated region
v/v	:	Volume/volume
w/v	:	Weight/volume
Xrn1	:	5'-3' exoribonuclease 1
YAP1	:	Yes Associated Protein 1
ZEB	:	Zinc finger E-box-binding homeobox

LIST OF APPENDICES

CHAPTER 1: INTRODUCTION

Breast cancer remains among the top cancer types worldwide, affecting women predominantly. A recent analysis done in Europe has placed breast cancer as the most common cancer in Europe, revealing a worrying trend (Ferlay et al., 2018). As such, despite having a relatively better prognosis, breast cancer is one of the biggest contributors to overall cancer death at 6.4%. Based on molecular expression, breast cancer can be grouped into several subtypes, such as luminal, HER2-enriched and basal-like (Engstrom et al., 2013). Classifying breast cancer into these groups enables treatment decision, although it does not guarantee efficiency due to breast cancer heterogeneity.

Anoikis is the cell death that occurs when cells are removed from the attachment to the extracellular matrix (ECM) and other neighbouring cells, mediated by cell adhesion molecules (CAMs) (Paoli et al., 2013). This detachment severs the survival signals from CAMs, resulting in apoptotic cell death. As such, anoikis is a barrier that cancer cells often attempt to break during tumorigenesis before being able to metastasise (Kim et al., 2012). Monitoring anoikis related biomarkers and targeting anoikis resistance in developing cancer therapeutics will no doubt prove to be a more effective strategy in reducing the aggressiveness of cancer and decreasing the probabilities of cancer recurrence.

MicroRNAs (miRNAs) are short strand of RNA molecules that are involved in the regulation of myriads of cellular processes (Macfarlane & Murphy, 2010). By binding to an mRNA 3' untranslated region (UTR) with a complementary sequence, miRNAs downregulate the expression of target genes post-transcriptionally. In cancer, the expression of miRNAs has been shown to be dysregulated, with the increase in expression of miRNAs that promote tumorigenesis and decrease in the expression of miRNAs that inhibit tumorigenesis (Iorio & Croce, 2012).

Although studies of dysregulated miRNA in breast cancer are not new, there are relatively few studies that have analysed the link between anoikis resistance and miRNA in breast cancer. As such, this project hypothesises that novel miRNAs regulate anoikis in breast cancer cells by targeting anoikis-related genes.

. Thus, the objectives of this thesis are:

i. To generate an anoikis resistant variant of MCF-7 breast cancer cell line.
ii. To list differential miRNA expression in anoikis resistant MCF-7 using miRNA microarray and select miRNA candidates for further studies.
iii. To identify the effects of the selected miRNA in regulating anoikis and migration in the non-invasive MCF-7.
iv. To investigate the effects of the selected miRNA in regulating anoikis, migration and invasion in the invasive MDA-MB-231 breast cancer cell line.
v. To establish potential target genes and signalling network regulated by the selected miRNA.
vi. To confirm the miRNA-target gene interaction and validate the downregulation of the target gene by the selected miRNA.

CHAPTER 2: LITERATURE REVIEW

2.1 Breast cancer

2.1.1 Overview

Although cancer is often seen as a single disease affecting various parts of the body, a major consensus on cancer is that it collectively refers to a group of genetic diseases unified by the six major criteria at a cellular level (Hanahan & Weinberg, 2011). These are the hallmarks of cancer, which are the evasion of cell death, continuous survival signalling, indomitable growth, invasive and metastatic spread, unlimited replication and induction of angiogenesis. These characteristics endow cancer with the ability to resist the internal immune response and many existing therapeutic options, putting cancer as one of the leading causes of death globally.

Breast cancer is reportedly well known to have highly favourable prognosis among the different cancer types. Unfortunately, despite predominantly affecting only women, an analysis from 2012 found breast cancer to be the second most common cancer overall and is prevalent almost equally in both less- and well-developed parts of the world (Ferlay et al., 2015). As such, the high frequency of breast cancer has placed it as the fifth most common cause of cancer death in 2012, representing 6.4% of overall cancer death. A more recent analysis carried out in Europe has revealed the worsening of this worrying trend, with breast cancer taking the first place as the most common cancer in 2018 (Ferlay et al., 2018). Similarly, breast cancer ranks as the top cancer in Malaysia, with 24,012 new cases reported in 2018, representing 18.63% of all cancer cases (Bray et al., 2018).

Even with comprehensive genomic profiling, understanding the dysregulated molecular network in breast cancer is not an easy feat and remains an ongoing challenge. However, knowledge accumulated so far has enabled classifying breast cancer into four major subtypes based on the expression of key biomarkers, such as estrogen receptor

(ER), progesterone receptor (PR), human epidermal growth factor receptor 2 (HER2) and cell proliferation marker Ki-67 (Cancer Genome Atlas, 2012). These subtypes are luminal A, luminal B, HER2-enriched and basal-like; however, additional biomarkers can be taken into consideration to derive more subtypes (Engstrom et al., 2013; Godone et al., 2018). Since the objective of classifying breast cancer is to determine effective treatments, this grouping enables informed clinical decision based on predicted responsiveness to known therapeutic approach (Coates et al., 2015). As of now, common breast cancer treatments include cytotoxic chemotherapy, endocrine therapy and HER2-targeted therapy.

2.1.2 Breast cancer biomarkers

The four broadly identified breast cancer markers are the hormone receptor ER and PR, HER2 and Ki67. In addition to these, there are other markers that can be used to expand the existing molecular classification of breast cancer, such as cytokeratin 5/6 and claudin proteins (Godone et al., 2018). However, although the analysis of these biomarkers can greatly assist breast cancer treatment, commonly available immunohistochemistry tools are incapable of correctly distinguishing the molecular subtype of breast cancer, restricting accurate classification to the availability of the more expensive and advanced genetic assays (Vieira & Schmitt, 2018).

2.1.2.1 Hormone receptors

As the presence of hormone receptors ER and PR marks majority of the reported breast cancer cases, the understanding of the role of these receptors in cancer development and growth is important. ER is a receptor activated by the ligands known as estrogen. Estrogen is a type of hormone produced naturally in the body in the forms of estrone, estradiol and estriol. Due to its lipophilic nature, estrogen is able to pass through the plasma membrane to ligate and activate genomic signalling through ER isoforms, which are expressed as

ERα or ERβ (Hua et al., 2018). Upon activation, the ER receptors form either homo- or heterodimers before proceeding into the nucleus to act as transcriptional activators. Meanwhile, PR is another hormone receptor used as a biomarker for breast cancer. Similar to ER, PR is ligated by a hormone, progesterone, resulting in its activation as a transcriptional factor (Daniel et al., 2011). Together, these hormone receptors have been implicated to promote tumourigenesis by promoting the expression of various oncogenes to stimulate proliferation and metastasis when activated (Saha Roy & Vadlamudi, 2012). Endocrine therapy is a relatively safe cancer treatment that serves to suppress the effects of these hormone receptors. This works either by the use of agonist such as tamoxifen to competitively inhibit hormones from binding to the receptors, or aromatase inhibitors such as anastrozole to lower hormone production (Lumachi et al., 2011).

2.1.2.2 HER2

HER2 is another important receptor and biomarker in classifying several types of cancers including breast cancer. It belongs to the ErbB family, a group of structurally related receptor tyrosine kinases, well known to modulate a wide variety of cellular processes related to survival and proliferation (Burstein, 2005). As such, HER2 acts as an oncogene when overexpressed in breast cancer and provides an anti-apoptotic advantage (Mitri et al., 2012). HER2-targeted therapy using anti-HER2 monoclonal antibody or HER2 inhibitor is the recommended treatment for cancers exhibiting overexpression of HER2, as determined through immunohistochemistry on tumour sample.

2.1.2.3 Ki67

Although breast cancer cells are rapidly dividing, determining the proliferative nature to be either high or low plays a significant role in choosing the effective treatment and reducing the need and risk of cytotoxic chemotherapy. Ki-67 is a biomarker that is used for this very purpose. As a nuclear protein, Ki-67's expression is correlated with the

process of cell division, and its presence is used to denote high proliferation of tumour cells in breast cancer patients (Soliman & Yussif, 2016). A threshold for Ki-67 at 15% (compared to positive control) is commonly used as a cut-off point to determine rate of proliferation, where ≤15% is considered low Ki-67 and >15% is considered high Ki-67. However, establishing an exact cut-off point as a good prognostic marker remains controversial (Coates et al., 2015; Acs et al., 2017).

2.1.3 Types of breast cancer

The luminal type breast cancer, named after its hypothesised origin from luminal progenitor cells, represents the largest percentage of reported breast cancer and incidentally has the best prognosis compared to the other breast cancer types. Luminal A is the first of the luminal type breast cancer, which can be characterised by the expression of ER and PR, and low expression of Ki67 by the cancer cells (Cho, 2016). As a result of responsiveness to hormones and lower proliferative nature of the cancer cells, patients with luminal A breast cancer often exhibit relatively higher survival rates when given the recommended treatment of endocrine therapy (Prat et al., 2015).

Luminal B is the second of the luminal type breast cancer, which is also characterised by the expression of ER and PR. However, unlike luminal A type, luminal B type expresses a high level of Ki67 and may or may not overexpress HER2 receptors (Cho, 2016). These differences contribute to the poorer prognosis and long-term survival among patients with luminal B type breast cancer. As with luminal A type breast cancer, patients with luminal B type breast cancer can benefit from endocrine therapy due to the expression of hormone receptors by the cancer cells. Depending on the specific phenotype of the luminal B cancer cells, additional treatment can also be carried out, such as cytotoxic chemotherapy and HER2-targeted therapy (Coates et al., 2015).

HER2-enriched is the next breast cancer subtype, which represents breast cancer that overexpresses HER2 with minimal expression of hormone receptors. Although this subtype does not respond well to endocrine therapy, the high expression of HER2 has enabled targeted treatment options through anti-HER2 therapy in addition to cytotoxic chemotherapy (Coates et al., 2015).

Finally, basal-like subtype, named after its hypothesised origin from basal progenitor cells, is negative for both ER and PR and has normal HER2 expression (Cho, 2016). Due to the lack of a specifically targetable element, this subtype has the poorest prognosis among the breast cancer subtypes with limited treatment options.

2.1.4 Breast cancer heterogeneity

As with other cancer types, intertumour and intratumour heterogeneities introduce complexities to type-specific chemotherapy for breast cancer (Polyak, 2011). Intertumour heterogeneity refers to the differences within a specific type of cancer between patients, whereas intratumour heterogeneity refers to the differences within a single tumour. The fact that such heterogeneities exist is not surprising considering that cancer cells are continuously undergoing genetic and epigenetic changes. For example, although the previous understanding was that luminal type breast cancer originates from luminal progenitor cells, and basal-like breast cancer originates from basal progenitor cells, the possibility of luminal progenitor cells transforming into basal-like breast cancer cells has been demonstrated using an animal model and human tissue samples (Lim et al., 2009; Molyneux et al., 2010). From a clinical perspective, this issue can be a challenge when devising appropriate treatment regimen for cancer patients as the current histopathological and molecular subtyping of breast cancer relies on tumour biopsy, which do not accurately reflect the entire population of the tumour (Rivenbark et al., 2013). As such, due to both intra- and intertumour heterogeneity, a recommended

treatment for a breast cancer subtype may not be effective in all patients due to the presence of undetected subpopulation of tumour cells of a different subtype.

Various solutions have been proposed to increase our understanding of the varying cellular makeup in a tumour sample. Currently, a number of genomic profiling platforms are available for breast cancer analysis, such as BreastPRS, Mammaprint and Oncotype DX, which can provide additional insights on risk of recurrence and benefits of specific cancer treatment (Fayanju et al., 2018). Furthermore, single-cell sequencing of representative cells derived from the primary tumour and analysis of cells from secondary sources other than the primary tumour have also shown some promise in revealing the diverse characteristics of breast cancer, as well as identifying the existence of various subtypes within the same patient (Navin et al., 2011; Ellsworth et al., 2017). Cells from secondary sources, such as the metastases and circulating tumour cells (CTCs), undergo changes to survive in the circulatory system and metastasise, acquiring marked genetic differences compared to the primary tumour. For example, discrepancies in HER2 status have been observed during the analysis of CTCs, where HER2-enriched CTCs were discovered in HER2-negative breast cancer patients (De Gregorio et al., 2017; Jaeger et al., 2017). Such detections provide additional information that must be accounted for, which may enable earlier prediction of poor response to endocrine or HER2-targeted therapy. However, while comprehensive analysis enables discerning the diverse subtype composition of the breast cancer, further evidence is still needed to support the usefulness of this information in cancer treatment and prognostics before its clinical application (Van Poznak et al., 2015). Overall, disregarding breast cancer heterogeneity may underestimate the actual tumour burden, resulting in poor prognosis and higher chances of recurrence. Regardless of the platform used, solving this issue will lead to more personalized and effective cancer treatments.

2.2 Anoikis

Most cells in the human body are found affixed to a specific location within the context of their cellular functions. This is enabled by the extracellular matrix (ECM), a tissue-specific scaffold primarily made of collagen and other components secreted by fibroblasts (Mouw et al., 2014). The ECM not only provides structural support by assembling cell populations but also houses the necessary ligands and growth factors to potentiate survival signals, such as fibronectin, hyaluronic acid and laminins. As such, ECM prevents inadvertently-detached cells from reattaching at a different niche and initiating the growth of the wrong type of tissues. Anoikis is the apoptotic cell death that is induced when cells are detached from their surrounding ECM and neighbouring cells.

The term 'anoikis', coined by Steven M. Frisch and Hunter Francis in 1994, combines the Greek words 'home' and 'without' to refer to the homelessness of the detached cells. This was based on their discoveries on apoptosis that was induced in epithelial cells when the connection to the ECM was disrupted (Frisch & Francis, 1994). This finding became the foundation to the existing understanding on how anoikis plays an important role in the survival of cancer cells during metastatic progression. This study also demonstrated how anoikis can be inhibited through various means, such as the overexpression of anti-apoptotic Bcl-2, transformation by tumour-promoting agents and exposure to proteins promoting motility and ECM invasion.

Cells are able to interact with the ECM through receptors expressed on the plasma membranes, such as the cell adhesion molecules (CAMs). One of the major groups of CAMs is integrins (Vachon, 2011). The integrins are ligated by the ECM components such as collagen, fibronectin and laminins, and can be found within structures known as the focal adhesion, a large multi-protein complex that anchors the cell to the ECM (Wu, 2007). Also found within this structure are the adaptor proteins and kinases that regulate

various downstream signalling pathway. Thus, by forming a transmembrane bridge connecting the ligands in the ECM with the CAM and actin cytoskeleton in the cells, the focal adhesion enables cells to receive survival signals when attached to the ECM. In addition to the cell-ECM bond, cell-cell interactions also form a crucial part of anoikis signalling network through receptors such as the cadherin family. A member of this family, E-cadherin, is another CAM that is expressed by epithelial cells. When ligated, E-cadherin plays an important role in survival and adhesion, as it regulates various signalling pathways and mediates the contact between the actin filaments of connecting cells (Paoli et al., 2013).

Due to the tight interconnection between the ECM and anoikis, disruption in the ECM landscape has shown to cause erroneous activation of anoikis in several diseases. For example, in aneurysm, which is the weakening of the artery's wall, it is shown that the enzyme plasmin causes fibronectin degradation in the ECM, resulting in the detachment and death of smooth muscle cells (Michel et al., 2018). On the other hand, inhibition of anoikis can also prove to be pathogenic, which is evident from cancer cells acquiring resistance to anoikis during tumourigenesis. As survival in the circulatory system in an anchorage-independent state is necessary for metastasising cancer cells, anoikis is one of the early barriers required to be broken before metastasis can occur.

2.2.1 Apoptosis

Since the discovery that anoikis takes place through apoptosis, investigations have shown the involvement of both caspase-dependent and caspase-independent apoptotic pathways. The caspase-dependent apoptotic pathway can be either intrinsic or extrinsic (Kim et al., 2012).

In the intrinsic pathway during anoikis, disturbance to the cytoskeleton and increase in cellular stress cause the activation of pro-apoptotic BH3-only proteins Bim and Bid,

which facilitate other pro-apoptotic proteins Bax and Bak to cause mitochondrial membrane permeabilisation. This is followed by the release of cytochrome c from the mitochondria, formation of apoptosome and subsequently the activation of caspases.

Meanwhile, the extrinsic pathway involves the activation of tumour necrosis factor receptor (TNFR) superfamily. Detachment from the ECM has shown to produce overexpression of these receptors and their ligands, thus causing increased activation of TNFR and the downstream caspases (Aoudjit & Vuori, 2001). The eventualities of both the intrinsic and extrinsic pathways are the same, which are the activation of the caspase cascade and orderly destruction of the cells.

On the other hand, there are also emerging evidence supporting caspase-independent apoptosis in anoikis. For example, Bit1, a mitochondrial protein, is suggested to promote anoikis upon loss of attachment to the ECM, although the exact mechanism of cell death is yet to be elucidated (Jenning et al., 2013).

2.2.2 Regulation of anoikis

The initiation of anoikis begins at the cell-surface level, a task handled by a multitude of receptors. These receptors can be those that mediate cell-ECM interactions, such as the integrins, or cell-cell interaction, such as E-cadherin, or growth-related transmembrane receptors, such as the epidermal growth factor receptor (EGFR), HER2 and insulin-like growth factor 1 receptor (IGF1R). The role of each of these receptors and how they translate ECM detachment into apoptosis has been shown to occur through the regulation of various survival signalling pathways such as the PI3K/Akt and MAPK/ERK pathways (Slabáková et al., 2017), and the interactions are summarised in Figure 2.1.

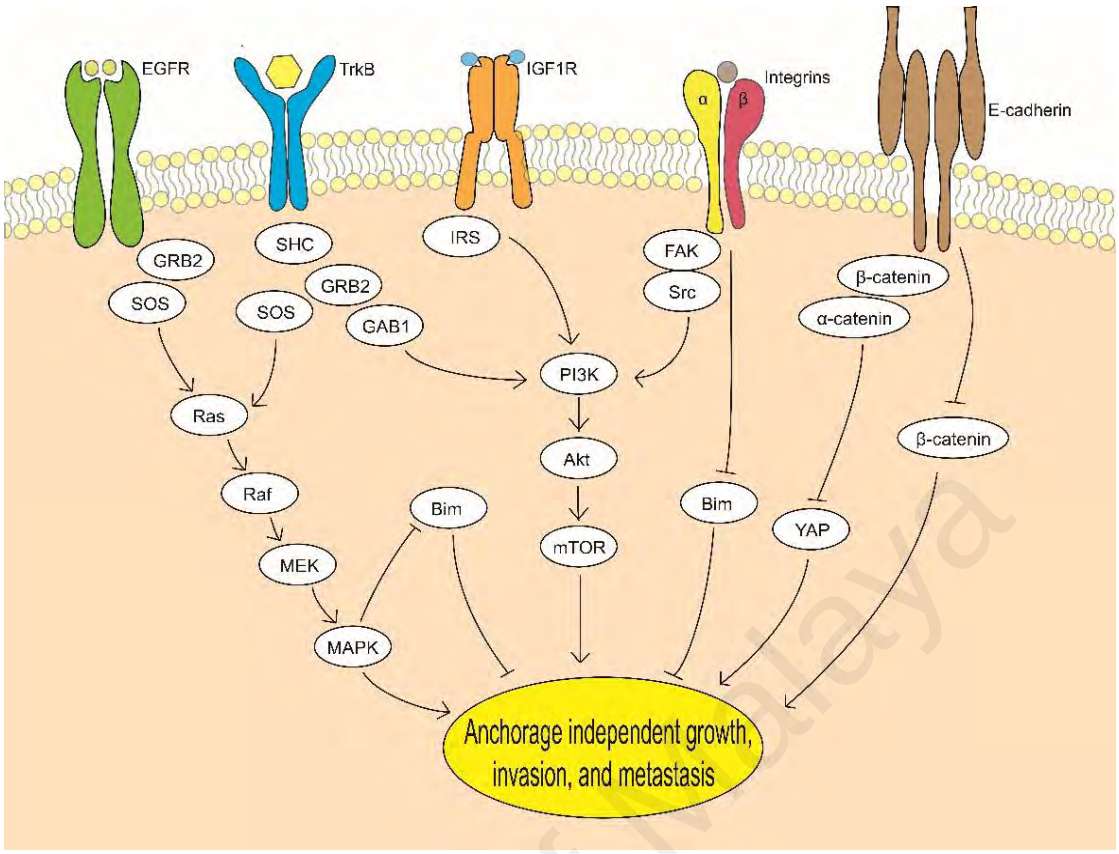

Figure 2.1: Signalling pathways regulating anoikis (adapted with permission from Malagobadan & Nagoor, 2019)

2.2.2.1 Integrins

Integrins are heterodimers found within the focal adhesion assembly and are made up of the α- and β-subunits. This pair of subunits can exist in 24 different combinations depending on cell type and responds to different ligands. Upon activation, the integrins can activate the FAK/Src complex and recruit various other proteins to eventually activate the PI3K/Akt pathway and promote cell survival (Vachon, 2011). Since the detachment from the ECM deprives exposure to the ligands necessary to activate the integrins, cancer cells have been observed to manipulate its expression to favour integrins that can be activated by self-produced ligands. For example, integrin α5β1, also known as the fibronectin receptor, is upregulated in various types of cancer such as lung, skin and breast cancer (Schaffner et al., 2013). This integrin is ligated by the mesenchymal marker

fibronectin, which the cancer cells synthesise as it undergoes EMT, allowing the cells to compensate for the detachment from the ECM and inhibit anoikis.

2.2.2.2 Growth-related transmembrane receptors

EGFR and HER2 are members of the ErbB family widely reported to be overexpressed in different cancer types (Wang, 2017). In breast cancer especially, overexpression of EGFR in HER2-enriched cancer is correlated with poor prognosis and lower overall disease-free survival (Lee et al., 2015). As transmembrane receptors, the role of EGFR and HER2 in regulating anoikis can take place independently of ligation when cells are detached from the ECM with the help of integrins. The tyrosine-protein kinase Src recruited by activated integrin phosphorylates both EGFR and HER2, which then transduce signalling for PI3K/Akt and MAPK/ERK pathways to promote survival while in suspension (Reginato et al., 2003; Haenssen et al., 2010). Additionally, phosphorylation of these receptors has also been demonstrated to inhibit anoikis by suppressing the pro-apoptotic regulator Bim.

Meanwhile, IGF1R is another closely-linked receptor capable of promoting cell survival during ECM detachment. The ability of IGF1R to inhibit anoikis is primarily through the activation of PI3K/Akt pathway. In fact, the overexpression of IGF1R has been repeatedly associated with drug resistance in HER2-enriched breast cancer subtypes, through the formation of heterodimer with EGFR and the upregulation of the PI3K/Akt pathway (Nahta et al., 2005; Gallardo et al., 2012). Furthermore, IGF1R was also shown to suppress anoikis in luminal type breast cancer when activated by its ligand, the insulin-like growth factor (IGF) (Luey & May, 2016).

2.2.2.3 E-cadherin

E-cadherin is an epithelial marker that enables cell adhesion, activated by homophilic ligation with E-cadherin of neighbouring cells (Kovacs et al., 2002). As the activation of E-cadherin requires cell-cell contact, its expression is a liability to cancer cells attempting to detach and metastasise. This receptor regulates cytoskeletal dynamics through a complex formed with α-catenin, a cell-adhesion protein. Through this complex, E-cadherin also sequesters β-catenin, another cell-adhesion protein and transcriptional activator. Consequently, this interaction prevents β-catenin from translocating to the nucleus and activating the expression of proteins necessary for EMT and inhibition of anoikis (Lamouille et al., 2014). Furthermore, E-cadherin is also involved in the PI3K/Akt pathway through its modulation of the tumour suppressor protein PTEN (Lau et al., 2011). A negative regulator of the PI3K/Akt pathway, PTEN is a phosphatase that is repressed by β-catenin. By restricting β-catenin's function, E-cadherin is able to prevent the dysregulation of PI3K/Akt pathway in cancer cells. Unsurprisingly, the loss of E-cadherin expression is the hallmark of the epithelial-to-mesenchymal transition (EMT), a process cancer cells undergo to become less differentiated during metastasis.

2.2.3 EMT and anoikis

To further understand the regulation of anoikis in cancer, it is imperative to clarify the interaction between anoikis and various cellular processes implicated in cancer phenotypes. One of such interactions is between anoikis and EMT. During EMT, cancer cells lose the expression of epithelial markers, such as E-cadherin and α-catenin, and gain the expression of mesenchymal markers, such as N-cadherin, vimentin and fibronectin (Tsai & Yang, 2013). While it is necessary for normal bodily functions such as wound healing and tissue regeneration, EMT is also exploited by cancer cells for metastatic progression. To metastasise, cancer cells need to undergo dedifferentiation to lose

epithelial characteristics and become more motive. This allows the cells to relinquish the expression of cell surface receptor attaching them to the ECM and other cells, to adopt a more mesenchymal-like morphology. The cancer cells are now able to invade the circulatory system as they are no longer reliant on adherent growth condition to survive. Although EMT provides an invasive advantage, cancer cells eventually undergo the reversion of EMT, named mesenchymal-to-epithelial transition (MET) to attach themselves to a different environment to form secondary tumours.

EMT and anoikis resistance are mainly linked by the first stage of EMT, which is the loss of E-cadherin. As E-cadherin plays a primary role in mediating cell-cell attachment, losing its expression facilitates cancer cell detachment from the original tumour and inhibition of anoikis (Frisch et al., 2013). Additionally, cell-ECM interaction is also altered during EMT, through the change in the landscape of integrin expression. Downregulation of epithelial integrins and increased expression of integrins conducive for metastasis have been observed in various cancer types (Lamouille et al., 2014).

The overexpression of metastasis-promoting integrins during EMT has also shown to assist the degradation of the ECM by promoting the expression of matrix metalloproteinases (MMP). For instance, integrin α5β1 was necessary for MMP-2 mediated breast cancer invasion, through the upregulation of survival signalling pathways and direct interaction with MMP-2 (Morozevich et al., 2009). This integrin, which promotes cancer cell migration and invasion, was also observed to have an inverse relationship with E-cadherin, where the expression of E-cadherin suppressed the expression of integrin α5β1 (Wu et al., 2006).

2.2.4 Autophagy and anoikis

In addition to EMT, autophagy is another cellular process that is related to anoikis. Autophagy is a self-preservation mechanism that allows cells to degrade cellular

components for recycling purpose or as a compromise in the event of stresses such as nutrient starvation (Saha et al., 2018). As such, autophagy maintains cellular homeostasis and contributes to increased resistance to cell death in the event of detachment from the ECM. The relationship of autophagy and anoikis is especially important as it determines what happens in the gap between ECM detachment and successful activation of anoikis. During this cytoskeletal stress condition, cancer cells are able to invoke autophagy as a defence against anoikis.

Studies have demonstrated how this is achieved, through the association between the pro-apoptotic proteins Bim and Bmf, and pro-autophagy regulator Beclin-1 (Delgado & Tesfaigzi, 2013). These pro-apoptotic proteins are usually associated with the cytoskeletal microtubule in adherent condition. In this configuration, Bim and Bmf are able to sequester and suppress the function of Beclin-1. However, upon detachment from the ECM, this inhibition is repressed, allowing Beclin-1 to be released and initiate autophagy. Additionally, Beclin-1 is also inhibited through a complex with the anti-apoptotic protein Bcl-2. A recent study showed that detachment from the ECM can cause the increase in the expression of the pro-apoptotic protein BNIP3, which also releases the inhibition of Beclin-1 and activate autophagy (Chen et al., 2017).

Unsurprisingly, Beclin-1 is also documented to be necessary for the formation of CSC using breast cancer cell lines, where Beclin-1 expression was found to be high in mammospheres when compared to the adherent parental cells (Gong et al., 2012). However, this tumour promoting role may be restricted to a limited number of circumstances such as anoikis inhibition, as some findings suggest the possible tumour suppressive role of Beclin-1 (Avalos et al., 2014).

For example, the expression of Beclin-1 is downregulated in a variety of cancer types due to the monoallelic loss of its gene. Moreover, the overexpression of Beclin-1 has also

been shown to restrict proliferation and induce apoptosis in cervical and lung cancer models (Sun et al., 2011; Shin et al., 2013). As such, although cancer cells are able to resort to autophagy to circumvent anoikis in anchorage-independent condition, autophagy in cancer as a whole requires further delineation in establishing its function in tumourigenesis.

2.2.5 Anoikis resistance in cancer stem cells (CSCs) and circulating tumour cells (CTCs)

CSCs are cancer cells with stem-cell like features, such as self-renewal and differentiation, which endow them with the prominent role in maintaining tumours and enabling the formation of metastases (Yu et al., 2012). Notably, CSCs are also well known for their ability to form tumoursphere in cell culture by inhibiting anoikis. Tumourspheres are spherical colony of cells derived from a single progenitor cancer stem cell in a non-adherent growth condition. The formation of tumourspheres using breast cancer cells, aptly termed mammosphere, is particularly interesting, as it provides several advantages for *in vitro* analysis of CSCs that is otherwise not feasible. For example, mammosphere formation assay has shown to be a promising model to enrich for CSCs and characterise them in tumourigenic breast cancer cell lines (Iglesias et al., 2013; Piscitelli et al., 2015). Furthermore, as targeting CSCs is an important strategy in cancer treatment, this model also allows for faster and more effective anti-cancer drug screening against CSCs (Lee et al., 2016).

CTCs are cancer cells that have detached from their originating tumour and successfully survived while suspended in the circulatory system. As such, CTCs represent what happens when cancer cells acquire resistance to anoikis. Unlike normal cells, cancer cells are able to reattach in various organs depending on the makeup of the original tumour and proliferate, resulting in the formation of secondary tumours. However, CTCs

as a whole is not intrinsically capable of forming metastases and is highly heterogenous (Bulfoni et al., 2016). For that purpose, CTCs need to undergo further phenotypic changes before seeding the growth of secondary tumours by becoming CSCs. Indeed, cellular- and molecular-based analysis of CTCs have revealed that CSCs make up a significant population of CTCs (Toloudi et al., 2011).

Currently, analysis of CTCs for diagnostic and prognostic purposes are still unachievable due to various obstacles, such as limited blood sample, insufficient number of captured CTCs and inefficient separation of CTCs from the hematopoietic cells in the blood samples (Bulfoni et al., 2016). Several interesting developments are being made in this front by targeting various molecular markers which may yield more information from the liquid biopsy for treatment decision, such as epithelial cell adhesion molecule (Ep-CAM), receptor CD45 and HER2 (Ferreira et al., 2016). For instance, in line with the findings on tumour heterogeneity, HER2-enriched CTCs were detected in both HER2-enriched and HER2-negative gastric cancer cases, suggesting the usefulness of HER2-targeted therapy for these patients regardless of their primary tumour status (Matsusaka et al., 2012; Mishima et al., 2017).

It is also worth noting that while CTCs are in suspension, most resources are being used for survival, pushing proliferation lower in terms of priority. Unfortunately, since most conventional chemotherapies are aimed at rapidly proliferating cells, CTCs are likely able to evade existing drugs and contribute to relapse (Mitra et al., 2015). Since these cells exist by inhibiting anoikis, detection of CTCs and biomarkers that can be specifically associated with anoikis resistance, such as miRNAs, may give a better perspective on the likelihood of metastasis or cancer recurrence.

2.3 MicroRNA (miRNA)

The discovery of non-coding RNAs (ncRNA) that are functional came as a surprise, as these were generally dismissed as 'junk RNA.' As of now, ncRNAs are not only found to be generously expressed but are also found in various forms and roles, among which is miRNA. Based on the latest miRNA database (miRbase release 22), 1917 miRNAs have been annotated in human, although much of these are in need of verification and *in vitro* validation to remove false annotations.

First characterised in 1993 in *Caenorhabditis elegans* (*C. elegans)*, miRNAs are short strands of RNA molecules that can regulate genes by binding to a messenger RNA (mRNA) with a complementary sequence (Lee et al., 1993). This binding results in a post-transcriptional downregulation of a miRNA's target gene, as the mRNA can no longer be translated into a protein. Theoretically, a single miRNA can target multiple target genes, and multiple miRNAs can target the same gene. Elucidating this network of regulation is a convoluted process requiring extensive *in silico* and *in vitro* validation. In addition to the cellular level function of miRNAs, they are also known to be secreted into the extracellular surroundings through exosomal packaging to be taken up by neighbouring cells. Not only does this turn miRNAs into autocrine and/or paracrine signalling regulators but also makes them ideal candidates as biomarkers through a fluid biopsy for cancer prognosis.

2.3.1 Biogenesis of mature miRNA

The generation of a functional miRNA begins in the nucleus, where miRNAs are found encoded in both intergenic and intronic region (Perron, 2008; O'Brien et al., 2018). Transcription of miRNA is carried out by RNA polymerase II/III, which creates a stable pri-miRNA with a large stem loop and overhangs on both 5' and 3' ends. While still in the nucleus, the pri-miRNA is next processed by the microprocessor complex, made up

of DGCR8, an RNA binding protein, and Drosha, a type III ribonuclease (Han et al., 2004). The former works to identify and recognize the junction where the overhang meets the stem in the pri-miRNA, and then recruits and directs the latter to cleave the overhangs in a specific manner, producing pre-miRNA with a 3' overhang that is 2 nucleotide (nt) long. The next step is handled by the transporter complex Exportin5/RanGTP, which identifies pre-miRNA based on its structure and exports it into the cytoplasm for further processing.

Here onwards, the pre-miRNA is processed by a complex made of endoribonucleases Dicer and argonaute-2 (Ago2), and RISC-loading complex subunit TARBP2 into a miRNA duplex through the removal of the stem loop (Cifuentes et al., 2010; Macfarlane & Murphy, 2010). The miRNA duplex pairing may or may not be perfect, and each strand in the duplex represents the original 5' arm (5p) and 3' arm (3p) of the pre-miRNA. One of the strands will become the mature miRNA, while the other, designated as the passenger strand or miRNA*, will be unwound from the duplex and degraded. Although the eventual fate of each of the strands in the duplex is predominantly determined by intrinsic factors, such as binding affinity and nucleotide bias, various external factors have also been suggested to be involved, such as the type of cell and the developmental stages the cell is in (Meijer et al., 2014).

2.3.2 Target mRNA downregulation by miRNA

A miRNA downregulates a target gene by RNA interference, identical to that of small-interfering RNA (siRNA) in mammals (Filipowicz et al., 2005). Upon processing and maturation, the miRNA is loaded into Ago2 to form the miRNA-induced silencing complex (miRISC), also composed of Dicer, TARBP2 and interferon-inducible double-stranded RNA-dependent protein kinase activator A (PACT). Within the RISC assembly, the miRNA acts as a guide strand to direct the activated assembly to a target mRNA.

The interaction between the miRNA and target mRNA is mediated by the complementary base pairing between the seed sequence of the miRNA, which spans the length of 6 nt from the second base (position 2 to 7), and the miRNA response element (MRE) located in the 3' UTR of the target mRNA. The complementary pairing can be categorised by specific nomenclatures to describe the length and complementarity of the MRE (Grimson et al., 2007). The first is the 8mer, which denotes a complementary match with position 2 to 8 in the miRNA (seed and position 8) followed by an adenosine base. Next are the 7mers, which can be either 7mer-m8, denoting match with position 2-8 in the miRNA (seed and position 8), or 7mer-A1, denoting match with position 2 to 7 followed by an adenosine base. Finally, the 6mer denotes a complementary match with position 2 to 7. The length of complementary bases between the 3' UTR of target mRNA and the seed, however, does not seem to affect the stability or strength of downregulation, presumably due to the additional role played by Ago2 in stabilizing the interaction (Jo et al., 2015; Mullany et al., 2016).

After the base pairing between the miRNA and the target mRNA, the miRISC recruits more proteins which ultimately results in target mRNA repression and degradation (Jonas & Izaurralde, 2015). These proteins are the scaffolding protein GW182 and poly(A) deadenylation complex PAN2-PAN3 and CCR4-NOT, which results in target mRNA deadenylation. Decapping of the target mRNA also takes place, carried out by the mRNA-decapping enzymes to prepare the mRNA for 5' to 3' degradation by the exoribonuclease Xrn1. Overall, the binding of the miRNA to its target gene results in the target gene downregulation.

2.3.3 Regulation of miRNA's expression and function

Differential miRNA expression has been noted among different cell types and during certain diseases such as cancer. In-depth studies into how miRNA expression is

manipulated has revealed regulation at various stages of miRNA development, such as at the DNA or post-transcriptional levels. There are several DNA-level alterations that can affect the expression of a miRNA. For instance, epigenetic changes such as hypermethylation or histone modification can reduce the general expression of the miRNA, while single-nucleotide polymorphism can cause changes in the secondary structure of pri-miRNA to interfere with its processing or reduce the miRNA's complementarity with its target mRNA (Auyeung et al., 2013).

On the other hand, post-transcriptional regulation can also exert effects on a miRNA's expression level, chiefly through the destabilization of the miRNA, preventing it from effectively interacting with miRNA-processing proteins in order to mature and carry out its function (Ha & Kim, 2014). For example, editing of the pri-miRNA by adenosine deaminases and methylation of pre-miRNA by the methyltransferase BCDIN3D impedes miRNA interaction with Drosha and Dicer respectively.

Additionally, regulation of miRNA function can also occur when the target mRNA's 3'UTR region is changed due to alternative polyadenylation or alternative splicing. Alternative polyadenylation, which results in variable mRNA transcript length, has been demonstrated to be the reason for tissue-specific role of miRNA, as cells were shown to switch the expression of target mRNA to contain shorter 3' UTR isoforms as a way to evade miRNAs in different cell types (Nam et al., 2014). For example, a study in *C. elegans* found that RACK1 and TCTP, proteins involved in calcium signalling, showed increased expression in body muscle tissues by switching to shorter 3' UTR isoforms to prevent downregulation by miRNAs (Blazie et al., 2017).

2.3.4 miRNA regulating anoikis in breast cancer

The dysregulation of miRNA expression is widely reported in various cancer types including breast cancer (Iorio & Croce, 2012). This has allowed identification of miRNAs

playing the role of oncogenes, termed oncomiRs, and miRNAs that play the opposite role, termed tumour suppressor miRNAs. Further studies into these miRNAs have also highlighted important players involved in cancer phenotypes such as anoikis.

Several of these miRNAs have been shown to explicitly regulate anoikis in cancer (Malagobadan & Nagoor, 2015). From the analysis of such miRNAs, it was possible to identify key proteins and signalling pathways that are frequently targeted and downregulated (Figure 2.2). Among these, some miRNAs have been demonstrated to regulate anoikis in breast cancer. Examples of such miRNAs are the miR-200 family and miR-181a.

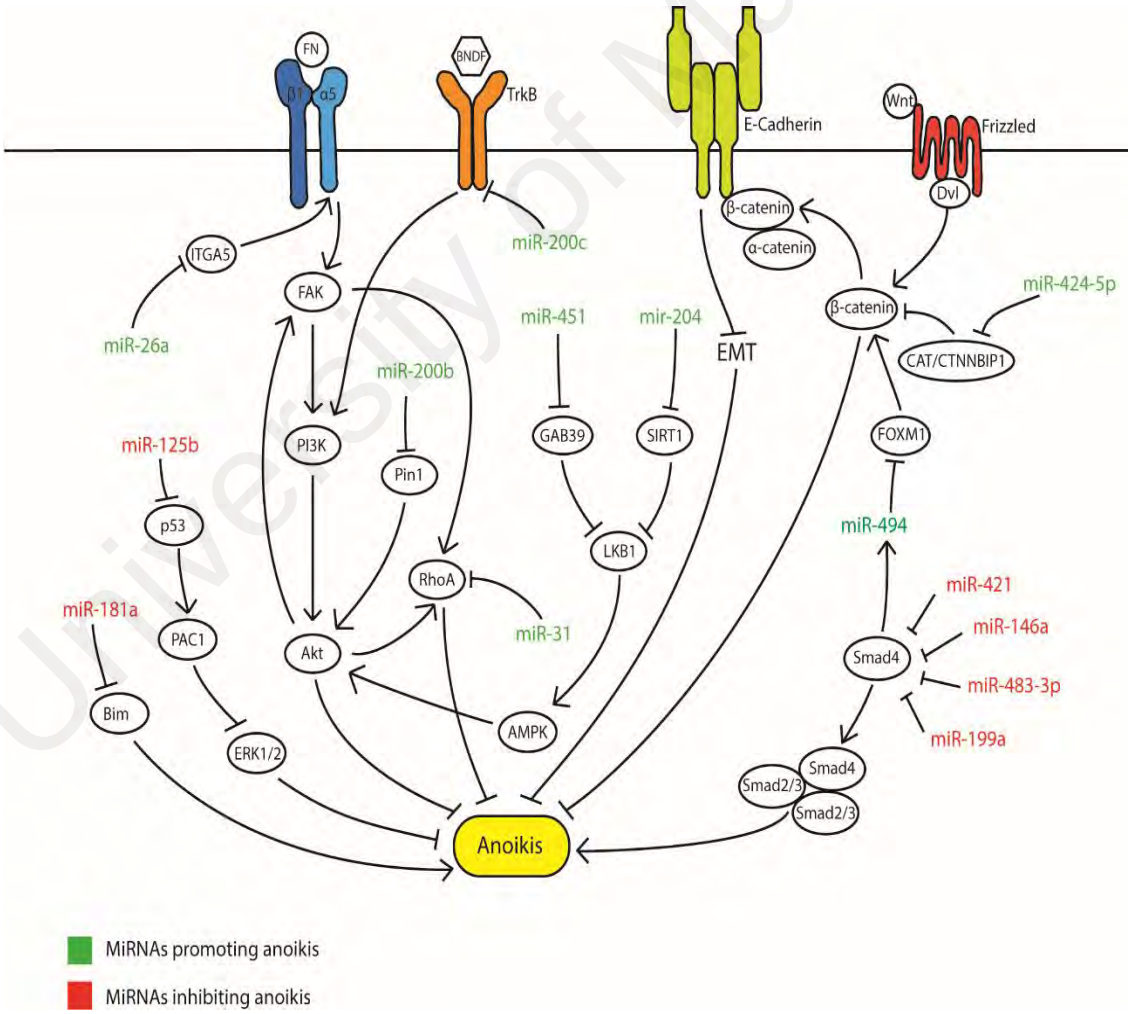

Figure 2.2: Example of the signalling networks regulated by miRNA involved in anoikis in various cancer types (adapted from Malagobadan & Nagoor, 2015)

2.3.4.1 miR-200 family

The miR-200 family is made of four miRNAs whose nearly identical sequences have resulted in similar functions in various cancer types. These miRNAs, which are miR-200a, miR-200b, miR-200c, miR141 and miR-429, have been repeatedly shown to have tumour suppressive characteristics when overexpressed in cancer cells, namely through MET. Separate studies exploring the individual members of the miR-200 family in breast cancer have identified various target proteins of these miRNAs which enable the miRNAs to increase anoikis sensitivity. For example, transcriptional coactivator YAP1 is targeted by miR-200a, isomerase Pin1 is targeted by miR-200b and transcriptional inhibitors ZEB1 and ZEB2 are targeted by miR-200c (Howe et al., 2011; Yu et al., 2013; Zhang et al., 2013). As these targets are intimately linked to EMT, the overall actions of these members of the miR-200 family culminate in the restoration of E-cadherin expression, which enables MET while promoting anoikis (Jabbari et al., 2014).

2.3.4.2 miR-181a

miR-181a is one of the most frequently studied miRNAs in cancer and is known to play significant roles in various cellular processes, such as cell proliferation, apoptosis and senescence. As such, regulation of anoikis in breast cancer by miR-181a has been well explored, revealing the paradoxical role of being oncogenic and tumour suppressive depending on the cell line (Yang et al., 2017). For example, miR-181a was found to be tumour suppressive and promote anoikis in MCF-7, a luminal A type breast cancer cell line (Wei et al., 2016). Interestingly, although its direct target was not validated, miR-181a was shown to suppress autophagy to promote anoikis in MCF-7 through the downregulation of autophagy regulator ATG5.

On the other hand, miR-181a was also shown to be oncogenic by inhibiting anoikis through the targeting of the pro-apoptotic protein Bim in several breast cancer cell lines

(Taylor et al., 2013). This study builds upon findings from earlier studies demonstrating the upregulation of miR-181a and induction of tumoursphere upon the exposure to transforming growth factor TGF-β (Wang et al., 2011). As anoikis resistance and formation of tumoursphere are some of the hallmarks of CSC formation, these findings portray miR-181a as a potential therapeutic target in treating breast cancer. However, the contrasting function of miR-181a emphasises the necessity to establish a miRNA's cell-type dependent role before determining its usefulness in cancer therapeutics.

2.3.5 miRNA in cancer therapeutics

The understanding of the dysregulation of miRNAs in cancer has provided two avenues through which miRNA-based therapeutic approach can be applied, namely through the introduction of miRNA mimetics to mimic the effect of tumour suppressive miRNAs and miRNA inhibitors to inhibit the action of oncomiRs. There are no shortages of miRNAs holding the potential for miRNA-based therapeutics, as can be seen from a myriad of publications on oncomiRs or tumour suppressive miRNAs. However, contextual roles in different cell lines of the same type of cancer are often seen in many of these instances, which may translate into deleterious effects when dealing with the heterogeneity of cancer in patients. As of now, several pharmaceutical companies have spearheaded the efforts to bring miRNA-based therapeutics into clinical application, although many of these are still in the early stages of the development pipeline (Chakraborty et al., 2017). These developments are also aimed at various other diseases in addition to cancer, such as renal fibrosis, atherosclerosis and myocardial infarction.

RNA strands that act as miRNA mimics and inhibitors by themselves are unsuitable for *in vivo* application, as these molecules are subjected to rapid degradation by nucleases in the blood (Chen et al., 2015). As such, several modifications have been developed to deliver a more stable and longer lasting effect in patients, such as locked-nucleic acid

(LNA), 2'-O-methyl and 2'-O-methoxyethyl modification and peptide-nucleic acid (Christopher et al., 2016; Shah et al., 2016). As for the delivery, there are several major mechanisms that have been shown to be successful through *in vivo* models for both miRNA mimics and inhibitors, such as vectors, amphoteric liposomes and nanoparticles. All these examples are summarised with description (Table 2.1).

Table 2.1: Summary of the development of miRNA therapeutics

Developments	**Type**	**Description**	**Reference**
Oligonucleotide modification	LNA	The ribose of the RNA is locked with a methylene bridge between the 2'-O and 4'-C. This conformation enables higher resistance to nucleases and better target affinity.	(Obad et al., 2011)
	2'-O-methyl modified	A methyl group is added to the 2'-O for increased stability against nucleases.	(Kumar et al., 2014)
	2'-O-methoxyethyl modified	A methoxyethyl group is added to the 2'-O for increased stability against nucleases with improved activity over 2'-O-methyl modification.	(Esau et al., 2006)
	Peptide-nucleic acid	A DNA-resembling molecule with 2-aminoethyl-glycine polymer as a backbone, capable of anti-miRNA activity, with significantly higher resistance to degradation and tighter binding.	(Amato et al., 2014)
Delivery mechanisms	Vectors	Vectors act as carrier for miRNA mimics or inhibitors for a longer and more stable expression in target cells. Examples are adenovirus-associated vector widely used for systemic delivery and plasmids carrying miRNA sponges which are inhibitors containing binding sites to target miRNA seed regions.	(Ebert & Sharp, 2010; Xie et al., 2015)

Table 2.1, continued

Developments	Type	Description	Reference
Delivery mechanisms	Amphoteric liposomes	A phospholipid enclosure in the form of a spherical vesicle with high stability in the serum for systemic delivery.	(Daige et al., 2014)
	Nanoparticles	Nanosized particles encapsulating miRNA mimics or inhibitors that can be used for tumour-targeted delivery.	(Zhang et al., 2013)

Presently, no miRNA-based drug for cancer treatment is available in clinical trial after the abrupt termination of MRX34, a mimic of the tumour suppressor miR-34a, due to adverse response in patients. Nevertheless, interest and advancement of miRNA-based therapeutics for cancer remain firm, especially for breast cancer, as is evident from the highest number of patents granted compared to other cancer types (Chakraborty et al., 2017). Such developments will undoubtedly introduce a novel method aimed to exploit miRNA expression to restore normal cellular functions, which would not only be applicable in cancer treatment but also in various other diseases.

2.3.6 miRNA as cancer biomarker

While miRNA-based therapeutics is still lagging, studies based on patients' blood sample have shown significant progress in using miRNAs for cancer diagnostics and prognosis. The expression of miRNAs goes beyond intracellular function as they are also excreted into the circulatory system through exosomes. This provides a way to monitor changes in the expression of miRNAs, which can then be correlated with either malignancy of the tumour or response to cancer treatments. Although still in the early

developmental stages, the use of miRNAs as biomarkers has already been proven to have high potential in monitoring breast cancer.

In the case of cancer diagnostics, multiple studies have shown the success of using combinations of miRNA as biomarkers for specific cancer types. For example, three separate studies using unique panels of miRNAs were able to distinguish early breast cancer patients from healthy controls with significantly high predictive values, including the detection of stage I and stage II breast cancer (Cuk et al., 2013; Ng et al., 2013; Kodahl et al., 2014). Furthermore, analysis of miRNAs associated with senescence and metastasis was also found to be useful for early prediction based on plasma samples obtained after tumour removal and before adjuvant chemotherapy. This was shown in a recent study analysing the expression of miR-21, miR-23b, miR-190 and miR-200c in old samples collected from breast cancer patients, which showed high correlation with cancer relapse and overall survival when compared to actual clinical data (Papadaki et al., 2018).

Even with limited starting material, quantification of serum miRNA can be carried out in several ways, such as reverse transcriptase-quantitative polymerase chain reaction (RT-qPCR), miRNA microarray, next-generation sequencing and NanoString nCounter platform (Hamam et al., 2017). As such, further development of these platforms may lead to automated systems using liquid biopsy to provide faster and easier breast cancer diagnosis and prognosis as compared to the existing manual analysis of tumour biopsy.

CHAPTER 3: MATERIALS AND METHODS

3.1 Cell culture and maintenance

Two breast cancer cell lines, MCF-7 and MDA-MB-231, were obtained from American Type Culture Collection (VA, USA). MCF-7 was cultured in α-MEM media (Nacalai Tesque, Kyoto, Japan) while MDA-MB-231 was cultured in RPMI media (Hyclone, UT, USA). Both cell culture media were supplemented with 10.0% fetal bovine serum (FBS) (Hyclone, UT, USA) and 1.0% penicillin/streptomycin mix (Lonza, Basel, Switzerland) unless otherwise stated. The cells were maintained in a carbon dioxide (CO_2) incubator, with humidity set at 95.0%, temperature at 37.0°C, and CO_2 at 5.0%. Cells were passaged whenever a confluency of approximately 80% was reached.

3.1.1 Cell culture sub-cultivation

Each cell line was split every three to four days or when approximately 80% confluency was reached in the cell culture flask. The harvesting of cells was done by first aspirating spent culture medium and discarding it. The surface of the culture flask with the cell monolayer was then rinsed with sterile phosphate-buffered saline (PBS) to remove traces of cell culture medium. After aspirating and discarding the PBS, 0.25% trypsin enzyme solution (Gibco, CA, USA) with 0.53 mM ethylenediaminetetraacetic acid (EDTA) (Gibco, CA, USA) was added to dissociate the bonds between the cells in the monolayer with each other and the culture flask. The culture flask was placed in the CO_2 incubator at 37.0°C for 5 minutes to facilitate the enzymatic dissociation process. Once the cells were confirmed to have detached from the flask as observed using an inverted microscope, equal volume of respective culture medium was mixed with the trypsin solution containing the suspended cells to inactivate the enzymes. The entire suspension was aspirated and transferred into a 15 mL Falcon tube followed by centrifugation at 1500 RPM in the Eppendorf Centrifuge 5702 (Eppendorf, Hamburg,

Germany) to pellet the cells. The supernatant was gently aspirated and discarded, while the cell pellet was resuspended in fresh culture medium. Upon gentle mixing, the cell suspension was either counted and plated in cell culture plates for experimental purpose or transferred into a new cell culture flask for maintenance purpose.

3.1.2 Cell counting

The concentration of cells in suspension was calculated using dye exclusion viability assay and a haemocytometer. Firstly, the cell suspension was gently mixed to ensure even distribution of cells. Then, 20.0 µL of the suspension was mixed with 20.0 µL of 0.08% trypan blue stain solution (Sigma Aldrich, MO, USA) in a 1.5 mL microcentrifuge tube. The mixture was left at room temperature for 3 minutes to allow penetration of the stain into dead cells. After pipetting the mixture up and down several times, 10.0 µL of the mixture was transferred into the chamber between a haemocytometer and the cover slip. Using 100× magnification under the inverted microscope, the number of viable cells in four square grids at each corner was counted. Dead cells, which are stained blue, were not counted. The total number of viable cells from the four grids was divided by four to obtain the average number of cells per grid, and the cell concentration was calculated using the following formula:

$$\text{Cell concentration (cell/ml)} = \frac{\text{Number of cells}}{\text{Number of grids}} \times \text{Dilution factor} \times 10^4 \qquad (3.1)$$

3.2 Anoikis resistant sub-cell line generation

MCF-7 cells were harvested from normal tissue culture flask using trypsin and counted. A total of 0.6×10^6 cells in 2.0 mL of complete medium was transferred into a well in the 6-well Costar Ultra Low Attachment (ULA) plate (Corning, NY, USA) to induce anoikis. After 72 hours (h), the cells were transferred into normal tissue culture plate to enable viable cells to attach and proliferate. After 24 h, the media was replaced

to discard floating dead cells. The cells were then harvested again, and this cycle was repeated for a total of six times before establishing a new anoikis resistant sub-cell line labelled as MCF-7-AR6. This sub-cell line was cultured similarly as MCF-7 cell line.

3.3 Cell viability assay

To measure proliferation of transfected cells, viable cells were quantified using CellTiter-Glo Luminescent Cell Viability Assay kit (Promega, WI, USA) at 24 h interval for a total of 6 days. First, MCF-7 and MDA-MB-231 cells were harvested using trypsin and counted 24 h after transfection. The cells were resuspended into complete growth medium at a concentration of 1.0×10^5 cells/mL. Each transfection group was plated into 5 separate wells in a 24-well plate labelled Day 1 – Day 5, at a volume of 500 uL per each well, and incubated at 37.0°C. Simultaneously, another 100.0 uL of the suspension was mixed with an equal volume of CellTiter-Glo Reagent in a microcentrifuge tube and placed in a shaker for 2 minutes. After an additional 10 minutes of incubation at room temperature, the luminescence for Day 0 was recorded using GloMax-Multi Jr Single Tube Multimode Reader (Promega, WI, USA).

After 24 h, spent media from Day 1 well was collected in a 15 mL falcon tube, and the cells were harvested using trypsin and mixed into the same tube. The cells were centrifuged to obtain the pellet, which was resuspended in fresh 500.0 mL growth medium. Then, 100.0 uL of the cell suspension was mixed with an equal volume of CellTiter-Glo Reagent and placed in a shaker for 2 minutes. After an additional 10 minutes of incubation at room temperature, the luminescence for Day 1 was recorded using GloMax-Multi Jr Single Tube Multimode Reader (Promega, WI, USA). This step was repeated at every 24 h interval until Day 5 measurement was collected.

To measure cell viability after induction of anoikis, CellTiter-Glo Luminescent Cell Viability Assay kit (Promega, WI, USA) was used. A total of 0.3×10^6 cells of MCF-7 or

MCF-7-AR6 were suspended in 1 mL of respective media and transferred to a well in 24-well ULA plate for 48 h of incubation at 37.0°C to induce anoikis. For transfected cells, at 48 h post transfection, cells from each well of a 6-well tissue culture plate were harvested using trypsin and mixed with spent media from respective wells. The cells were then centrifuged and resuspended in 2.0 mL of respective growth medium before being transferred into a well in a 6-well ULA plate for 48 h of incubation at 37.0°C in suspension. To measure the viability of cells, the cell suspension was mixed thoroughly by pipetting to break up clumps of cells and ensure even distribution of cells. Then, 100.0 µL of the cell suspension was mixed with an equal volume of CellTiter-Glo Reagent in a microcentrifuge tube and placed in a shaker for 2 minutes. After an additional 10 minutes of incubation at room temperature, the luminescence was recorded using GloMax-Multi Jr Single Tube Multimode Reader (Promega, WI, USA).

3.4 Caspase-3/7 activity assay

Caspase-3/7 activity was detected using Caspase-Glo 3/7 Assay kit (Promega, WI, USA). A total of 0.3×10^6 cells of MCF-7 or MCF-7-AR6 were suspended in 1.0 mL of recommended media and transferred to a well in 24-well ULA plate for 24 h of incubation at 37.0°C in suspension. For transfected cells, at 48 h post transfection, cells from each well of a 6-well tissue culture plate were harvested using trypsin and combined with spent media. The cells were then centrifuged and resuspended in 2.0 mL of respective growth medium before being transferred into a well in a 6-well ULA plate for 24 h of incubation at 37.0°C to induce anoikis. The caspase-3/7 activity in each sample was then measured according to manufacturer's protocol. The cell suspension was thoroughly mixed by pipetting to break up clumps of cells and ensure even distribution of cells. Then, 100.0 µL of the cell suspension was mixed with an equal volume of Caspase-3/7 Glo Reagent in a microcentrifuge tube and incubated in the dark at room temperature for 1 h. The

resulting luminescence in the samples was measured using GloMax-Multi Jr Single Tube Multimode Reader.

3.5 Wound healing assay

Cells were grown to confluency in a 6-well tissue culture plate. A scratch was made on the monolayer by dragging a p200 pipette tip across the well. The well was rinsed twice with PBS to remove the dislodged cell debris and the culture media supplemented with 1.0% FBS was added to the well. The wound gap was photographed at 40× magnification at 0 h and 24 h at specific predefined point in the well. The relative wound area was measured using TScratch v1.0 software (ETH, Zurich, Switzerland), which calculates the area of the scratch. Area recovered at 24 h was calculated based on the following equation:

$$\text{Area recovered (\%)} = \frac{\text{Scratch area at 0 h} - \text{Scratch area at 24 h}}{\text{Scratch area at 0 h}} \times 100 \qquad (3.2)$$

3.6 Total RNA extraction

Total RNA extraction was done on cell pellets using Qiagen miRNeasy mini kit (Qiagen, Hilden, Germany), containing QIAzol Lysis Reagent, RNeasy Mini spin column and Buffer RPE. The cell pellet was resuspended in 700.0 µL of QIAzol Lysis Reagent in a 1.5 mL microcentrifuge tube. After vortexing the suspension for 15 seconds and mixing it well, the suspension was incubated at room temperature. After 5 minutes, 140.0 µL of chloroform was mixed with the solution, and the microcentrifuge tube was shaken vigorously for 15 seconds. After an additional 2-3 minutes incubation at room temperature, the microcentrifuge tube was centrifuged at 4.0°C for 15 minutes at 12000×*g*. The solution separates into upper, middle and lower phases. The upper aqueous phase, which contains RNA, was gently aspirated and transferred into a new collection tube, and 1.5× volume of 100% ethanol (Fisher Scientific, MA, USA) was mixed with the aqueous phase. The solution was then transferred an RNeasy Mini spin column placed

in a collection tube and centrifuged for 15 seconds at 8000×*g*. The flow-through in the column was discarded, and 500.0 µL of Buffer RPE was added into the column. After centrifuging for 2 minutes at 8000×*g*, the column was taken out of the collection tube and placed in a 1.5 mL microcentrifuge tube. Then, 30.0 µL of RNase-free water was pipetted onto the membrane in the column, and the tube was centrifuged for 1 minute at 8000×*g*. The flow through solution which eluted the RNA was either stored at -20.0°C or used immediately for experimental purposes.

3.6.1 RNA quantitation and quality analysis

Quality and quantity analysis of the extracted RNA were done using NanoDrop Spectrophotometer (Thermo Fisher Scientific, MA, USA) for RT-qPCR and Agilent 2200 TapeStation System (Agilent Technologies, CA, USA) for miRNA microarray. In the NanoDrop Spectrophotometer, 1.0 µL of the extracted RNA was pipetted onto the pedestal and the concentration was measured for each sample at OD_{260}. In the Agilent 2200 TapeStation, a mixture of 1.0 µL of the sample and 4.0 µL of R6K sample buffer in a microcentrifuge tube was heated for 3 minutes at 72.0°C to denature the sample. The solution was then cooled on ice for 2 minutes and briefly centrifuged to collect the samples at the bottom of the tube. The entire solution was then transferred into the ScreenTape R6K and loaded into the Agilent 2200 TapeStation to measure the RNA concentration and integrity.

3.7 miRNA microarray

3.7.1 RNA preparation

To screen for miRNAs regulating anoikis resistance, the differential expression of miRNA in MCF-7-AR6 compared to MCF-7 was analysed using GeneChip miRNA Arrays (Affymetrix, CA, USA) kit based on manufacturer's recommended protocol. Firstly, poly (A) tailing was conducted on the extracted total RNA from MCF-7 and MCF-7-AR6. For each sample, 1000 ng of RNA was diluted in 8.0 µL of nuclease-free water and mixed with 2.0 µL of RNA Spike Control Oligos while on ice. In a separate tube, ATP mix was prepared at 1:500 dilution in I mM Tris. Next, a master mix for poly (A) tailing was prepared in the order listed in Table 3.1. The master mix was added the RNA mixture and incubated at 37.0°C for 15 minutes to complete the poly (A) tailing reaction. The tailed RNA was then mixed with 4.0 µL of 5× FlashTag Biotin HSR Ligation Mix and 2.0 uL of T4 DNA Ligase. This mixture was incubated at room temperature for 30 minutes. Then, 2.5 uL of HSR Stop Solution was mixed with the sample and the biotin-labelled RNA sample was kept on ice until next step.

Table 3.1: Poly (A) tailing master mix

Ingredients	**Volume (**uL)
10× Reaction Buffer	1.5
25 mM $MnCl_2$	1.5
Diluted ATP mix	1.0
PAP Enzyme	1.0
Total Volume	5.0

3.7.2 Hybridisation

The reagents for hybridisation cocktail were thawed to room temperature, and the 20× Hybridisation Controls was heated at 65.0°C for 5 minutes. The reagents were added to the tube containing biotin-labelled RNA sample by the order and volume listed in Table 3.2 to prepare the hybridisation cocktail.

Table 3.2: Hybridisation cocktail components

Ingredients	**Volume (**uL)
2× Hybridisation Mix	50.0
27.5% Formamide	15.0
DMSO	10.0
20× Hybridisation Controls	5.0
Control Oligo B2, 3nM	1.7
Total Volume	81.7

The mixture was incubated at 99.0°C for 5 minutes and 45.0°C for 5 minutes. From the mixture, 100 uL of sample was injected into the GeneChip Array cartridge. The cartridge was then loaded into the GeneChip Hybridisation Oven 640 (Affymetrix, CA, USA) and incubated at 48.0°C and 60 rpm for 18 h. After the incubation, the sample was aspirated out of the cartridge, and Array Holding Buffer was filled into the cartridge completely, ensuring that no bubbles formed inside. After 10 minutes of incubation at room temperature, the cartridge was loaded into the GeneChip Fluidics Station 450 (Affymetrix, CA, USA) for washing and staining using the default 100 format array protocol. The cartridge was then scanned using GeneChip Scanner 300 (Affymetrix, CA, USA) using default settings.

3.7.3 Microarray analysis

Affymetrix Transcriptome Analysis Console v3.0 (Affymetrix Inc, CA, US) was used to analyse the results and compare the differential miRNA expression between MCF-7-AR6 and MCF-7 using one-way between-subject ANOVA, with ANOVA p-value <0.05, and fold change threshold set at >2.5 or <-2.5.

3.8 Reverse transcription polymerase chain reaction (RT-PCR)

RT-PCR of miRNA was carried out with TaqMan MicroRNA Reverse Transcription Kit (Applied Biosystems, CA, USA) and TaqMan MicroRNA Assays (Applied Biosystems, CA, USA) (Table 3.3).

Table 3.3: TaqMan MicroRNA assays

Assay ID	Accession Number	Assay Name
002178	MI0005757	hsa-miR-935
466929	MI0022589	hsa-miR-6744-5p
001093	-	RNU6B

The RT master mix was prepared according to manufacturer's protocol as listed in Table 3.4. Once the master mix was prepared, it was mixed thoroughly and centrifuged briefly to collect the mixture at the bottom of the microcentrifuge tube. The RT master mix was place on ice while the RNA sample was prepared.

Table 3.4: RT master mix composition

Component	Master mix volume
100 nM dNTPs (with dTTP)	0.10 µL
MultiScribe™ Reverse Transcriptase, 50 U/µL	0.67 µL
10× Reverse Transcription Buffer	1.00 µL
RNase Inhibitor 20 U/ µL	0.13 µL
Nuclease-free water	2.78 µL
Total Volume	4.68 µL

For each miRNA, the 5× RT primer and RNA sample were thawed on ice. After thawing, 1000 ng of total RNA in 3.3 µL was mixed with 4.68 µL of RT master mix. Then, 2.0 µL of RT primer of respective miRNAs was added to the mixture, and the tube containing the reaction was briefly centrifuged and placed on ice for 5 minutes. The tube was then loaded into a thermal cycler, set to run with settings for cDNA synthesis (Table 3.5).

Table 3.5: Thermal cycler settings

Time	Temperature
30 minutes	16°C
30 minutes	42°C
5 minutes	85°C
∞	4°C

3.9 Quantitative PCR (qPCR)

The product of RT reaction was used for qPCR by mixing it with the following components (Table 3.6).

Table 3.6: Composition of qPCR master mix

Component	Master mix volume
TaqMan Fast Advanced PCR Master Mix	5.00 µL
Nuclease-free water	3.84 µL
TaqMan MicroRNA Assay (20)	0.50 µL
Product from RT reaction	0.67 µL
Total Volume	10.01 µL

The master mix for qPCR was prepared in a low-profile microcentrifuge tube. The mixture was mixed well and centrifuged to collect the samples at the bottom of the tube. After sealing, the tubes were loaded into CFX96™ Real-Time PCR Detection System (Bio-Rad Laboratories, CA, USA), set to run with the following settings (Table 3.7).

Table 3.7: Real-time PCR settings

Step	Enzyme Activation	PCR	
	HOLD	CYCLE (40 Cycles)	
		Denature	Anneal/Extend
Temperature	95°C	95°C	60°C
Time	10 min	15 sec	60 sec

The results were analysed with Bio-Rad CFX Manager™ v1.6 (Bio-Rad Laboratories, CA, USA) to obtain cycle threshold (Ct) values for the tested miRNAs.

3.10 Transfection

For the overexpression and knockdown of selected miRNAs, cells were transfected with miRIDIAN miRNA mimics and hairpin inhibitors (GE Healthcare Dharmacon, CO, USA) (Table 3.8). The miRNA mimics are double-stranded nucleotides that functions similarly as the chosen miRNAs, whereas the hairpin inhibitors are oligonucleotides that binds to the target miRNA and suppresses its function. Negative controls for mimics and inhibitors are based on the sequence of *C. elegans* miRNA (cel-miR-67), a miRNA with minimal known activity in human.

Table 3.8: Accession number and sequences of mature chosen miRNAs

ID	Accession Number	Sequence (5'----3')
hsa-miR-935	MIMAT0004978	CCAGUUACCGCUUCCGCUACCGC
hsa-miR-6744-5p	MIMAT0027389	UGGAUGACAGUGGAGGCCU
cel-mir-67	MIMAT0000039	UCACAACCUCCUAGAAAGAGUAGA

Cells used for transfection were first harvested and counted. In a well in 6-well plate, 0.3×10^6 cells were plated in 2.0 mL of complete medium for 24 h. Stock solution for the miRNA mimics, inhibitors and respective controls were prepared at 20 μM aliquots. During transfection, 2.5 μL of 20 μM stock solution of each transfection reaction was mixed with 197.5 μL serum- and antibody free media and kept in a microcentrifuge tube for 5 minutes at room temperature. In another tube, 2.0 μL Dharmafect 1 transfection reagent (GE Healthcare Dharmacon CA, USA) was mixed with 198.0 μL serum- and antibody free medium. The contents of both tubes were mixed thoroughly to make up a total volume of 400.0 μL and kept at room temperature for 15 minutes. Then, the solution was mixed with 1.6 mL full growth medium without antibody and mixed thoroughly to create the transfection medium with a final concentration of 25 nM. The existing medium in the 6-well plate with the plated cells was aspirated and discarded, and the wells were

rinsed with 2.0 mL of PBS. Then, the transfection medium with either miRNA mimics, inhibitors or controls were added to the appropriate wells for transfection.

3.11 Western blot

3.11.1 Protein extraction

Total protein was harvested from cells 72 h after transfection using RIPA buffer (Thermo Fisher Scientific, MA, USA). Before use, RIPA buffer was mixed with Halt Protease Inhibitor Cocktail (Thermo Fisher Scientific, MA, USA) and Halt Phosphatase Inhibitor Cocktail (Thermo Fisher Scientific, MA, USA) at 1:1000 dilution each and placed on ice. Next, media from the wells containing transfected cells in 6-well plate was aspirated and discarded. The plate was placed on ice, and each well was rinsed with 1.0 mL ice-cold PBS twice. Then, 100.0 µL of RIPA buffer was added to the surface of each well and the plate was gently swirled to uniformly spread the buffer throughout the well. After 5 minutes of incubation on ice, the cells were scraped from the 6-well plate using a cell scraper and immediately transferred into a 1.5 mL microcentrifuge tube on ice. The tubes were then centrifuged at 14000×*g* for 15 minutes. The supernatant, which contained total protein, was gently aspirated without disturbing the cell pellet and transferred into another 1.5 mL microcentrifuge tube. The protein sample was then used for protein quantification and western blot analysis.

3.11.2 Protein quantification

To quantify the concentration of protein in each extracted sample, Pierce BCA Protein Assay Kit (Thermo Fisher Scientific, MA, USA) was used. A standard curve for protein concentration was first prepared using the provided bovine serum albumin (BSA) solution with a concentration of 2000 µg/mL. BSA samples with concentrations of 2,000, 1,500, 1,000, 750, 500, 250, 125, and 25 µg/ml were prepared to establish a standard curve. Meanwhile, BCA working reagent was mixed as recommended by combining 50 parts of

BCA Reagent A and 1 part of BCA Reagent B. For each measurement, 200.0 µL of working reagent was mixed with 20.0 µL sample and incubated for 30 minutes at 37.0°C. The absorbance was measured using NanoDrop 2000 at 560 nm and protein concentration was determined based on the standard curve.

3.11.3 Sample preparation

To denature the complex protein structures into linear forms for sodium dodecyl sulfate-polyacrylamide gel electrophoresis (SDS-PAGE), Lane Marker Reducing Sample Buffer (Thermo Fisher Scientific, MA, USA), which contains 100mM dithiothreitol (DTT) and 5% SDS, was used. DTT reduces proteins down to its primary structures by breaking the inter- and intramolecular disulphide bonds, while SDS attaches to amino acids uniformly on a protein to provide a constant charge-to-mass ratio. To prepare the protein samples for SDS-PAGE, the concentration of the protein was adjusted to 2.0 µg/µL in a final volume of 20.0 µL. The adjusted sample was mixed thoroughly with 5.0 µL of the sample buffer which was cooled down to room temperature. The mixture was boiled for 5 minutes at 95.0°C in a heat block and allowed to cool down to room temperature before SDS-PAGE.

3.11.4 Gel preparation

Once the protein samples have been denatured and prepared with a uniform concentration, the samples were loaded into a polyacrylamide gel to separate proteins based on their sizes using electrophoresis. Due to the negative charge imparted by SDS, proteins in the samples will migrate towards the anode. Meanwhile, pores within the gel ensures that proteins migrate at a speed that is determined by their respective sizes, enabling efficient separation. For this analysis, 4.0% stacking gel and 7.5% resolving gel were used. The gels were prepared using ingredients in the order listed in Table 3.9. The

last two ingredients, ammonium persulfate (APS) and tetramethyl-ethylenediamine (TEMED), were added right before pouring the gel mixture into its cast.

Table 3.9: Polyacrylamide gel ingredients

Ingredients	Stacking Gel (4.0%) (µl)	Resolving Gel (7.5%) (µl)
Distilled H_2O (dH_2O)	3167.5	5460.0
0.5M Tris-HCl (pH 6.8)	1,250.0	-
1.5M Tris-HCl (pH 8.8)	-	2500.0
10% SDS	50.0	100.0
40% Acrylamide (Promega, WI, USA)	500.0	1880.0
10% (w/v) Fresh ammonium persulfate (APS)	25.0	50.0
Tetramethyl-ethylenediamine (TEMED) (Acros, MA, USA)	7.5	10.0
Total Volume	5000.0	10000.0

Glass plates of 1 mm thickness and 18 cm×16 cm dimension (Bio-Rad Laboratories, CA, USA) were set into the provided casting tray, ensuring that the plates are aligned parallel to each other to prevent leaks. Then, 5.0 mL of resolving gel solution that was prepared was immediately and gently poured into the space between the glass plates. To ensure that the top layer of the gel is even, 2.0 mL of 70.0% ethanol solution was poured gently on top of the resolving gel. After 30 minutes, once a clear line is visible separating the solidified gel from the ethanol layer on top, the cast was tilted to pour out the ethanol, and Kim-wipes were used to gently blot out the remaining ethanol residues in the cast. Next, the stacking gel solution was prepared accordingly and poured immediately on top of the resolving gel, all the way to the brim of the glass plates. A 10-well gel comb of 1 mm thickness was then inserted quickly into the space between the glass plates while ensuring that air bubbles were not formed during this step. The stacking gel was allowed to solidify for another 30 minutes before the casted gel was ready for SDS-PAGE.

3.11.5 SDS-PAGE

Before the protein samples were loaded into the gel, two casted gels in glass plates were transferred into the Mini PROTEAN Tetra System (Bio-Rad Laboratories, CA, USA) into a single cassette in the tank. The glass plates are placed in the correct orientation, in which the sides where samples are loaded face each other. The entire set up is filled with Tris/Glycine/SDS (TGS) running buffer, including the space between the glass plates. The combs were gently lifted from the plates, and each well in the gels was flushed with the running buffer to clear the wells of undesired gel residues. The first well of the gel was loaded with 8.0 μL of biotinylated protein ladder (Cell Signaling Technology, USA), while 20.0 μL of denatured protein samples were loaded into the remaining wells. Once all samples were loaded, the set up was connected to the Power Pack (Bio-Rad Laboratories, CA, USA), and electrophoresis was carried out at 110 volts and a maximum of 400 mA for 15 minutes, followed by 150 volts and a maximum of 400 mA for another 40 minutes or until the bright pink dye of the sample buffer reaches the bottom of the gel.

3.11.6 Protein transfer

Once separated by electrophoresis in the gel, the proteins were transferred from the gel into a nitrocellulose membrane. A 2.0 μm nitrocellulose membrane and two blot absorbent filter papers (Bio-Rad Laboratories, CA, USA) were cut approximately the same size as the resolving gel and soaked in transfer buffer mixed with 20.0% (v/v) methanol (Merck, Darmstadt, Germany) for small proteins (<100kDa) or 10% (v/v) for large proteins (>100kDa), for 10 minutes. The gel from SDS-PAGE was obtained by prying open and removing one of the glass plates. Before removing the resolving gel, the stacking gel was cut and discarded from the glass plate. Then, the resolving gel was gently lifted and transferred into a container with transfer buffer and methanol similar to the membrane and filter papers for 10 minutes. On the platinum anode plate of Trans-Blot

SD Semi-Dry Transfer Cell (Bio-Rad Laboratories, CA, USA), the gel sandwich was prepared by placing the first filter paper, membrane, gel and the second filter paper, in that order. As each layer was placed, a roller was used to push out any air bubble that has formed from underneath. Once the sandwich of layers was set, the top stainless-steel cathode was gently fixed, and the safety cover was placed on top of it. Then, the transfer was run at 50 mA and 25 volts for every gel used for 90 minutes using MP-2AP Power Supply (Major Science, Taiwan). After the completion of the transfer, the membrane was removed and stained with 0.1% (w/v) Ponceau S (Sigma Aldrich, MO, USA) for 30 seconds to visualise the proteins on the membrane. Successful transfer of protein was indicated by visibility of clear protein bands uniformly in each lane in the membrane. The membrane was then washed twice with tris-buffered saline (TBS) for 5 minutes per each wash to remove the stain while shaking on the Reciprocal Shaker MS-RC (Major Science, Taiwan). Once clear of stains, the membrane was blocked with blocking buffer made of 5.0% (w/v) non-fat skim milk powder (Merck, Darmstadt, Germany), 0.05% (v/v) Tween 20 (Promega, WI, USA) in tris-buffered saline (TBS) for 1 h at room temperature while shaking on the shaker. After blocking, the membrane was washed thrice using TBST, made of TBS with 0.05% (v/v) Tween 20, for 5 minutes per each wash. The membrane was incubated in 10.0 mL of solution containing primary antibody at appropriate dilution (Table 3.10) for 1 h in room temperature on the shaker and overnight at 4.0°C.

Table 3.10: Antibody dilution buffer composition

Antibody	Dilution Buffer	Dilution
E-cadherin (24E10) Rabbit mAb	5.0% w/v BSA in 1×TBS with 0.1% Tween 20	1:5000
Vimentin (D21H3) Rabbit mAb	5.0% w/v BSA in 1×TBS with 0.1% Tween 20	1:5000
N-acetyltransferase 1 (NAT1) (ab175088) Rabbit pAb	5.0% w/v non-fat dry milk in 1×TBS with 0.1% Tween 20	1:1000
GAPDH (14C10) Rabbit mAb	5.0% w/v BSA in 1×TBS with 0.1% Tween 20	1:5000
Anti-rabbit IgG HRP-linked	5.0% w/v BSA in 1×TBS with 0.1% Tween 20	1:5000
Anti-biotin HRP-linked	5.0% w/v BSA in 1×TBS with 0.1% Tween 20	1:5000

The next day, the membrane was washed thrice using TBST for 5 minutes per each wash and incubated in 10.0 mL of solution containing secondary antibodies, which are the anti-rabbit IgG HRP-linked antibody (Cell Signaling Technology, USA) and anti-biotin HRP-linked antibody (Cell Signaling Technology, USA) (Table 3.10), for 1 h. Then, the membrane was washed thrice using TBST for 5 minutes per each wash and placed in TBS until the next step.

3.11.7 Protein band visualisation

To visualise the bands of interest on the membrane, Western Bright Quantum (Advansta, CA, USA) was used. This kit provides a substrate for the horseradish peroxidase (HRP) enzyme conjugated to the secondary antibodies. The reaction results in the release of chemiluminescence signal, which can be captured by an imaging system to visualise the protein bands. The reagent from the kit was prepared according to manufacturer's protocol, and 1.0 mL of the reagent was added to the top of the membrane in a container. After 2 minutes of incubation, the membrane was placed under a charged couple device (CCD) camera and imaged using a chemiluminescent imaging system, the Fusion FX7 system (Vilber Lourmat, France). The intensity of the visualised bands was quantified using ImageJ v1.50i software (NIH, MD, USA). The relative expression of

protein was calculated by normalising the intensity of the protein band to the intensity of GAPDH band for each sample.

3.12 Transwell-invasion assay

After 48 h of transfection, MDA-MB-231 cells were serum starved for 24 h, and the Matrigel (Corning, NY, USA) was thawed overnight at 4.0°C before the beginning of the assay. On the first day of the assay, the Matrigel was diluted to achieve a concentration of 1.5 mg/mL in cold dilution buffer. Each 24-well transwell insert (8.0 μm pore size; BD Biosciences, NJ, USA) was prepared with a coating of 20.0 μL of Matrigel (30.0 μg). After ensuring even coating at the bottom, the inserts, together with the companion 24-well plate, were incubated in the CO_2 incubator at 37.0°C for more than 2 h to facilitate solidification of the Matrigel. Once the Matrigel had solidified, the serum-starved transfected cells were harvested by trypsin and counted before being resuspended into low-serum media (growth media supplemented with 0.1% serum). The concentration of the cells was adjusted to 0.2×10^6 cells/mL. In the companion 24-well plates, each well was filled with 1mL of high-serum media (growth media supplemented with 20% FBS). The inserts were gently placed into the well in the companion 24-well plates before being incubated at 37.0°C for 24 h. Then, 500.0 μl of the cell suspension was seeded into the upper chamber of the insert. After 24 h of incubation at 37.0°C, the non-invading cells were removed by rinsing the inserts in PBS and wiping the inside of the inserts with a cotton swab. To visualize the invading cells, the cells were fixed in 100% ethanol (Fisher Scientific, MA, USA) for 2 minutes and stained with methylene blue (Sigma Aldrich, MO, USA) solution (1.0% w/v in dH_2O) for 20 minutes. After staining, the inserts were rinsed twice with distilled water. After the stained inserts had air dried, five random fields in each insert were photographed using an inverted microscope at 100× magnification for every replicate and the number of cells were counted using ImageJ v1.50i software for analysis.

3.13 Zebrafish care and maintenance

The handling of zebrafish (wild-type *Danio rerio*) for this experiment was in accordance to the protocol approved by University of Malaya, Faculty of Medicine, Institutional Animal Care and Use Committee (Ethics reference number: 2017-181108/IBS/R/SM). The maintenance and care of zebrafish adults were in the Zebrafish Laboratory, Department of Biomedical Science, Faculty of Medicine, University of Malaya. The zebrafish was maintained in a ZebTEC zebrafish housing system (Tecniplast, Italy) at regulated conductivity (500 µS), pH (7.0) and temperature (28.0°C). The set up was maintained at 14 h:10 h light:dark cycle, and the zebrafish were fed with Hikari dry food pellets twice and live *Artemia salina* (brine shrimp) once daily.

3.13.1 Zebrafish breeding

To obtain zebrafish embryos for metastasis assay, adult zebrafish were randomly chosen for mating. Three female zebrafish and two male zebrafish were placed in a special breeding tank with an overlay of marbles at the bottom before 4 pm. The zebrafish were placed in the tank overnight to allow mating ritual which results in laying and fertilisation of eggs at the onset of light the next day. The zebrafish were then returned to their respective tanks based on their gender, and the eggs were harvested into a 200 mL beaker and rinsed with system water thrice. The eggs were then gently collected from the beaker using a Pasteur pipette into a 60 mm×15 mm petri dish containing system water. After 2 h of incubation at 28.5°C, the collected embryos were examined under Leica EZ4 dissecting microscope (Leica Microsystems, Hesse, Germany) to identify and remove dead or unviable embryos, which appear white instead of translucent. The viable embryos were transferred into a petri dish containing system water with 0.1% (v/v) methylene blue (Sigma Aldrich, USA). The next day, at 24 h post fertilisation (hpf), the embryos were rinsed thrice with system water and placed into system water mixed with 75.0 µM N-

phenylthiourea (PTU) (Sigma Aldrich, MO, USA) to suppress pigmentation. The embryos were placed back in the incubator at 28.5°C for 24 h before microinjection.

3.14 Zebrafish metastasis assay

3.14.1 Cell preparation

MDA-MB-231 cells were transfected with either miR-6744-5p mimic or mimic control in 6-well plates. After 24 h, the cells were labelled with 1,1'-dioctadecyl-3,3,3',3'-tetramethylindocarbo-cyanine perchlorate (DiI) stain (Invitrogen, CA, USA) prior to microinjection. The stain was prepared from a stock solution (20.0 mg/mL), which was diluted in Dulbecco's phosphate-buffered saline (DPBS) with calcium and magnesium at 1:1000 dilution. The media used on the transfected cells was removed from the wells, and the wells were rinsed with 1.0 mL PBS twice. Then, 2.0 mL of the stain solution was added to each well and allowed to incubate at 37.0°C in the dark. After 30 minutes, the stain solution was removed, and each well was rinsed with 1.0 mL of PBS twice before adding fresh media. The cells were checked under an inverted fluorescence microscope to ensure successful staining. The cells were incubated overnight in normal cell culture condition.

3.14.2 Zebrafish embryo preparation

At 48 hpf, some of the zebrafish embryos naturally hatch out of the outer shell of the embryo known as the chorion. These zebrafish were picked up and transferred into a new petri dish using a Pasteur pipette. The remaining zebrafish were liberated from the chorion by the use of sharp microsurgical forceps (Watchmaker #5) (Samco, UK). Forceps were used to hold down and gently make a tear in the chorion, allowing the zebrafish to squeeze out of the shell. The collected zebrafish were rinsed thrice with system water to remove traces of broken chorions and transferred to fresh system water with PTU.

3.14.3 Microinjection

The labelled MDA-MB-231 cells were harvested using trypsin and counted. The cells were then resuspended in culture media with 1.0% FBS without antibiotics at a concentration of 4.0×10^5 cells/mL. The cells were kept in the dark and on ice until they were ready for microinjection. The 48 hpf zebrafish were first anaesthetised by transferring them into 2 mL of 10.0% benzocaine (Sigma Aldrich, USA) in system water for 2 minutes. When the zebrafish no longer displayed movement after two minutes, they were picked up and placed onto 1.0% (w/v) agarose gel plate. Using a microloader (Eppendorf, Hamburg, Germany), 10.0 µL of the cell suspension that was thoroughly mixed was loaded into a 20 µm TransferTip (Eppendorf, Hamburg, Germany) attached to a FemtoJet Microinjector (Eppendorf, Hamburg, Germany). By monitoring using a stereo microscope (Leica Microsystems, Hesse, Germany), the InjectMan NI 2 Micromanipulator (Eppendorf, Hamburg, Germany) was used to inject the cell suspension into the yolk sac region of the zebrafish with constant injection pressure (P_i) (120 hpa), compensation pressure (P_c) (30 hpa) and injection time (t_i) (0.3 seconds). The instrument settings were set to inject approximately 200 cells per injection into each embryo. The zebrafish were rinsed with system water and placed back into appropriately labelled petri dish containing fresh system water with PTU. The petri dish was covered with aluminium foil and incubated at 33.0°C for 48 h.

3.14.4 Zebrafish serial imaging

The 48 hpi zebrafish were euthanised in 10.0% benzocaine (Sigma Aldrich, MO, USA) and mounted onto a glass slide with VECTASHIELD (Vector Laboratories, CA, USA). The mount was secured by placing a cover slip (Marienfeld-Superior, Baden-Wurttemberg, Germany) on top of the specimen. The edges of the cover slip were covered with nail polish and the slide was allowed to dry in the dark. Serial sections of the zebrafish were imaged using Leica TCS SP5 II confocal microscope (Leica

Microsystems, Hesse, Germany) to visualise the dissemination of DiI-stained MDA-MB-231 cells from the yolk into the body at 5× magnification (excitation: 543nm; emission: 550-640nm). Percentage of metastatic MDA-MB-231 cells (outside the yolk) was obtained by measuring fluorescence in the z-stack images using 'analyse particle' function in ImageJ v1.50i software.

3.15 Target prediction analysis for miRNA

TargetscanHuman v7.1 online software (http://www.targetscan.org) (Agarwal et al., 2015) was used to determine predicted target proteins of miR-6744-5p using default parameters. The list of predicted targets was generated and used for gene-annotation enrichment using DAVID Functional Annotation Tool (https://david.ncifcrf.gov/home.jsp) (Huang et al., 2009). The UniProtKB Keywords database was used in DAVID software to obtain major association clusters containing the predicted target genes. To obtain the hypothetical signalling pathways regulated by the miRNA, KEGG pathway database was used in DAVID software.

3.16 Vector design

For luciferase assay, pmirGLO Dual-Luciferase miRNA Target Vectors (Promega, WI, USA) containing miR-6744-5p wild-type and mutated predicted target site in NAT1 3'UTR were prepared. Firstly, DNA fragments of wild-type and mutated NAT1 3'UTR were synthesised by a vendor, First BASE Laboratories Sdn. Bhd., Malaysia. Both fragments were 149 base pairs (bp) in length and contained Pme1 restriction site at 5' end and Xba1 restriction site at 3' end. The mutated fragment contained scrambled sequence at the predicted target site. These fragments were then cloned into the pmirGLO Dual-Luciferase miRNA Target Expression Vector, and the constructs, wild-type and mutated, were sequence verified by the same service provider.

3.17 Dual Luciferase Reporter Assay

Dual Luciferase Reporter Assay System (Promega, WI, USA) was used to validate miR-6744-5p targeting of NAT1 3'UTR. MCF-7 cells were harvested, and 0.3×10^6 cells were plated in a well in 6-well plate with 2.0 mL of complete growth medium. After 24 h, the cells were transfected with either miRNA mimic or mimic negative control according to the established protocol. Additionally, each transfection group was co-transfected with 50.0 ng of either the wild-type or mutated construct by adding the construct into the transfection tube after the addition of the transfection reagent and prior to the 15 minutes incubation at room temperature. After 48 h of co-transfection, normalised luciferase activity was measured according to manufacturer's protocol using Dual-Luciferase Reporter Assay System. Firstly, Dual-Glo Luciferase Buffer and Dual-Glo Luciferase Substrate were mixed to produce the Dual-Glo Luciferase Reagent for the assay. Meanwhile, transfected cells were harvested using trypsin and centrifuged to produce a cell pellet in a microcentrifuge tube. The supernatant was discarded, and the pellet was resuspended in 100 µL of PBS. Then, 100.0 µL of Dual-Glo Luciferase Reagent was mixed to the cell suspension and the mixture was incubated at room temperature in the dark. After 10 minutes, the firefly luminescence was measured using Glomax Multi - Luminescence Multimode and recorded. Immediately after the measurement, 50.0 µL of Dual-Glo Stop & Glo Reagent was added to the mixture and mixed well. The sample was incubated for an additional 10 minutes in the dark before the *Renilla* luminescence was measured and recorded. This measurement acts as the internal control as it is constitutively expressed by the transfected cells. To obtain the luciferase activity, the ratio of firefly luciferase reporter to *Renilla* luciferase reporter was calculated and normalised to the control samples.

3.18 Statistical significance

Statistical analysis was calculated using paired Student's t-test to determine *p*-value, where $p<0.05$ was considered significant, and experiments were carried out with three independent replicates unless otherwise stated. For miRNA microarray, one-way between-subject ANOVA was carried out, with ANOVA p-value <0.05 considered to be significant.

CHAPTER 4: RESULTS

4.1 A stable anoikis-resistant variant of the luminal A type breast cancer cell line MCF-7 was generated

4.1.1 MCF-7-AR6 sub-cell line was generated from MCF-7

To elucidate miRNAs regulating anoikis in breast cancer, an anoikis-resistant variant of the MCF-7 cell line, MCF-7-AR6, was generated. MCF-7 cells were detached from normal tissue culture flask using trypsin before being suspended in a well in ULA 6-well plate. After 72 h in suspension, aggregates of tumourspheres were visible compared to when the cells were transferred to the ULA plate at 0 h (Figure 4.1). The cells were transferred to a normal tissue culture plate to allow the surviving cells to grow, before the process was repeated for a total of six cycles to establish MCF-7-AR6.

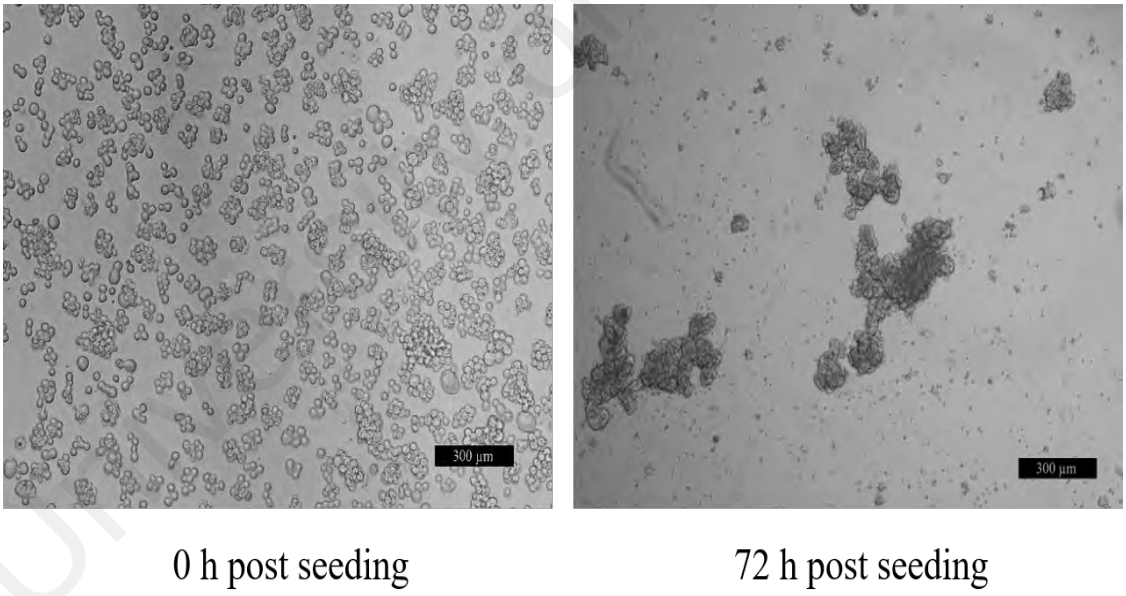

Figure 4.1: Appearance of MCF-7 in anchorage-independent condition. Representative images of MCF-7 when transferred to the ULA plate at 0 h and at 72 h post-seeding.

4.1.2 MCF-7-AR6 shows higher resistance to anoikis and increased migration ability compared to MCF-7

MCF-7-AR6 was compared to the parental MCF-7 cell line, and MCF-7-AR6 was found to be more resistant to anoikis (Figure 4.2). To determine anoikis resistance, anoikis was induced by subjecting the cells to suspension before carrying out viability and caspase-3/7 activity assay. Viability assay measured surviving population after 48 h in suspension while caspase-3/7 activity assay measured the early apoptotic event of caspase-3/7 activation after 24 h in suspension. MCF-7-AR6 showed significantly higher viability (145.1±6.3% compared to MCF-7) and lower caspase-3/7 activity (63.8±8.3% compared to MCF-7). Furthermore, MCF-7-AR6 also showed increased migration in wound healing assay (32.2±8.0% area recovered compared to 15.4±5.9% in MCF-7).

4.2 Elucidation of miRNAs dysregulated during acquisition of anoikis resistance in MCF-7

4.2.1 A list of 22 miRNAs was identified to be upregulated and downregulated in MCF-7-AR6

Next, miRNA microarray was performed to determine the changes in the miRNA expression in MCF-7-AR6 due to the acquisition of higher anoikis resistance. A total of 22 miRNAs were found to be differentially expressed with a fold change of >2.5 or <-2.5 (Figure 4.3). Out of these, 15 miRNAs were upregulated, and 7 miRNAs were downregulated (Table 4.1).

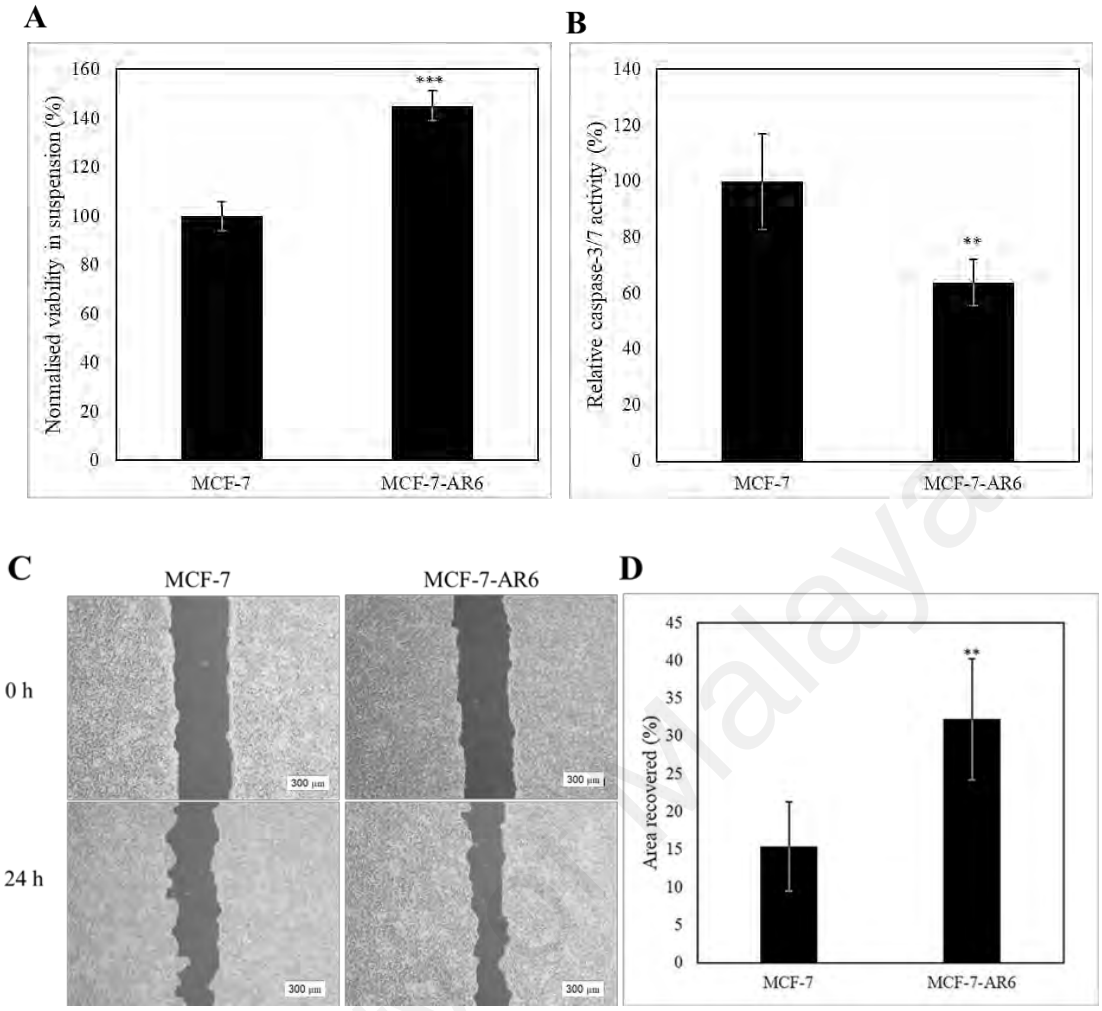

Figure 4.2: Comparison of MCF-7-AR6 to MCF-7. Comparative analysis was done by measuring (A) viability after 48 h in suspension and (B) caspase-3/7 activity of MCF-7 and MCF-7-AR6 after 24 h in suspension. (C) Representative images of wound healing assay and (D) scratch area recovery of MCF-7 and MCF-7-AR6 after 24 h. Data are presented as mean±standard deviation (SD), and statistically significant differences compared to MCF-7 as the control are denoted by (**) for $p<0.01$ or (***) for $p<0.001$.

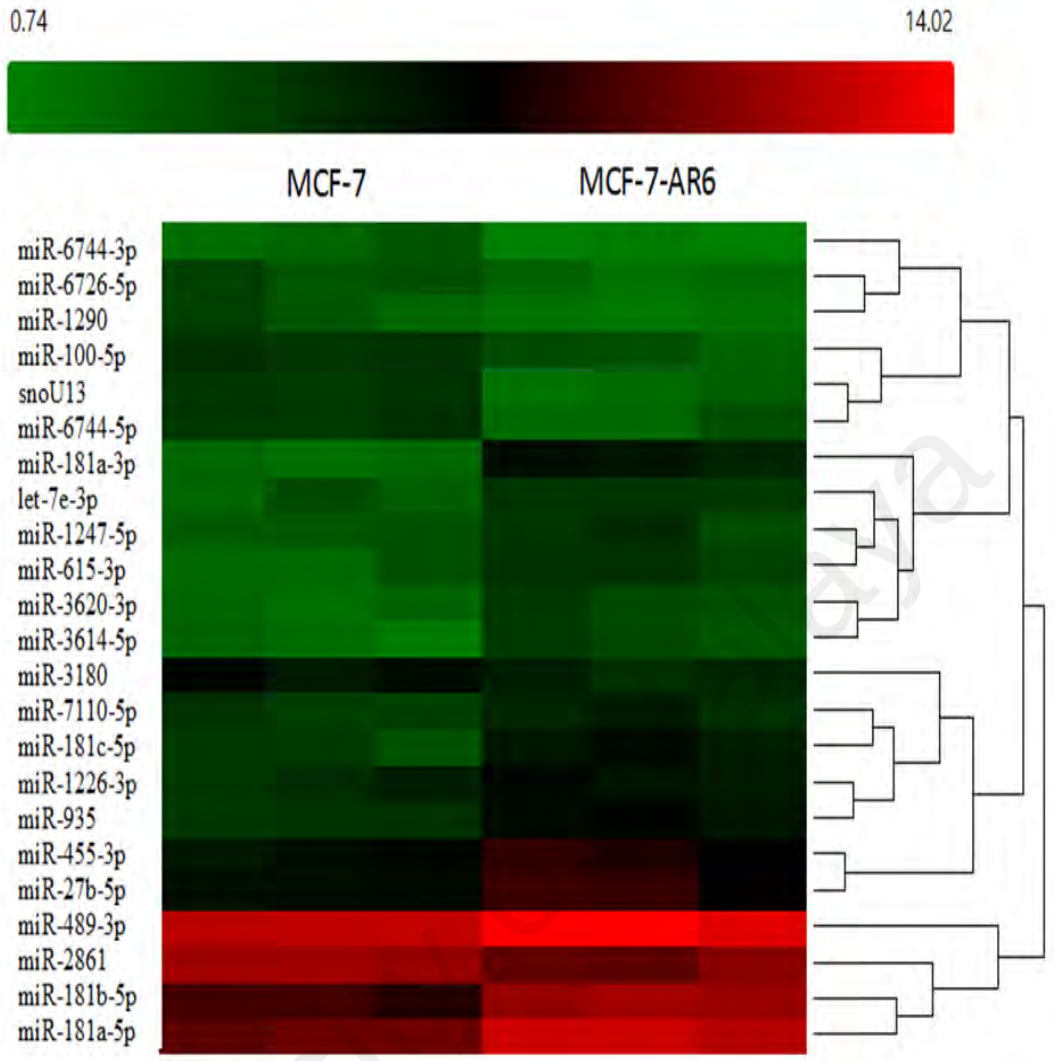

Figure 4.3: miRNA microarray comparison of MCF-7-AR6 to MCF-7. Hierarchical cluster heat map of miRNAs that were differentially expressed in MCF-7-AR6 when compared to MCF-7. Red and green spectrum is used to represent signal strength, with red denoting high and green denoting low signal. Affymetrix Transcriptome Analysis Console v3.0 was used to analyse the results using one-way between-subject ANOVA, with ANOVA p-value <0.05, and fold change >2.5 or <-2.5.

Table 4.1: Summary of miRNA microarray results

miRNA	Fold-change	ANOVA *p*-value
miR-6744-5p	-5.97	0.012
miR-2861	-3.04	0.039
miR-6744-3p	-2.96	0.017
miR-1290	-2.88	0.048
miR-6726-5p	-2.81	0.019
miR-100-5p	-2.67	0.012
miR-3180	-2.58	0.041
miR-455-3p	2.54	0.036
miR-1226-3p	2.54	0.045
miR-7110-5p	2.54	0.045
miR-3620-3p	2.8	0.012
miR-1247-5p	3.06	0.044
miR-489-3p	3.28	0.006
miR-181c-5p	3.75	0.011
miR-3614-5p	3.86	0.026
miR-935	4.05	0.002
let-7e-3p	4.16	0.012
miR-181b-5p	4.36	0.001
miR-27b-5p	4.49	0.029
miR-181a-5p	5.91	0.001
miR-615-3p	7.33	0.016
miR-181a-3p	19.6	0.000

Differential expression of miRNAs in MCF-7-AR6 compared to MCF-7 presented as fold-change for miRNAs with ANOVA p-value <0.05. Positive fold-change denotes upregulation while negative fold-change denotes downregulation.

4.2.2 miR-935 and miR-6744-5p were quantitatively confirmed to be downregulated and upregulated in MCF-7-AR6 respectively using RT-qPCR.

From the list of dysregulated miRNAs, a miRNA upregulated in MCF-7-AR6, miR-935, and a miRNA downregulated in MCF-7-AR6, miR-6744-5p, were chosen for further analysis owing to their possible novel role in regulating anoikis. To provide quantitative validation for the change in expression seen during microarray, RT-qPCR was performed. The results of RT-qPCR were consistent with the microarray findings, confirming the upregulation of miR-935 and downregulation of miR-6744-5p (Figure 4.4).

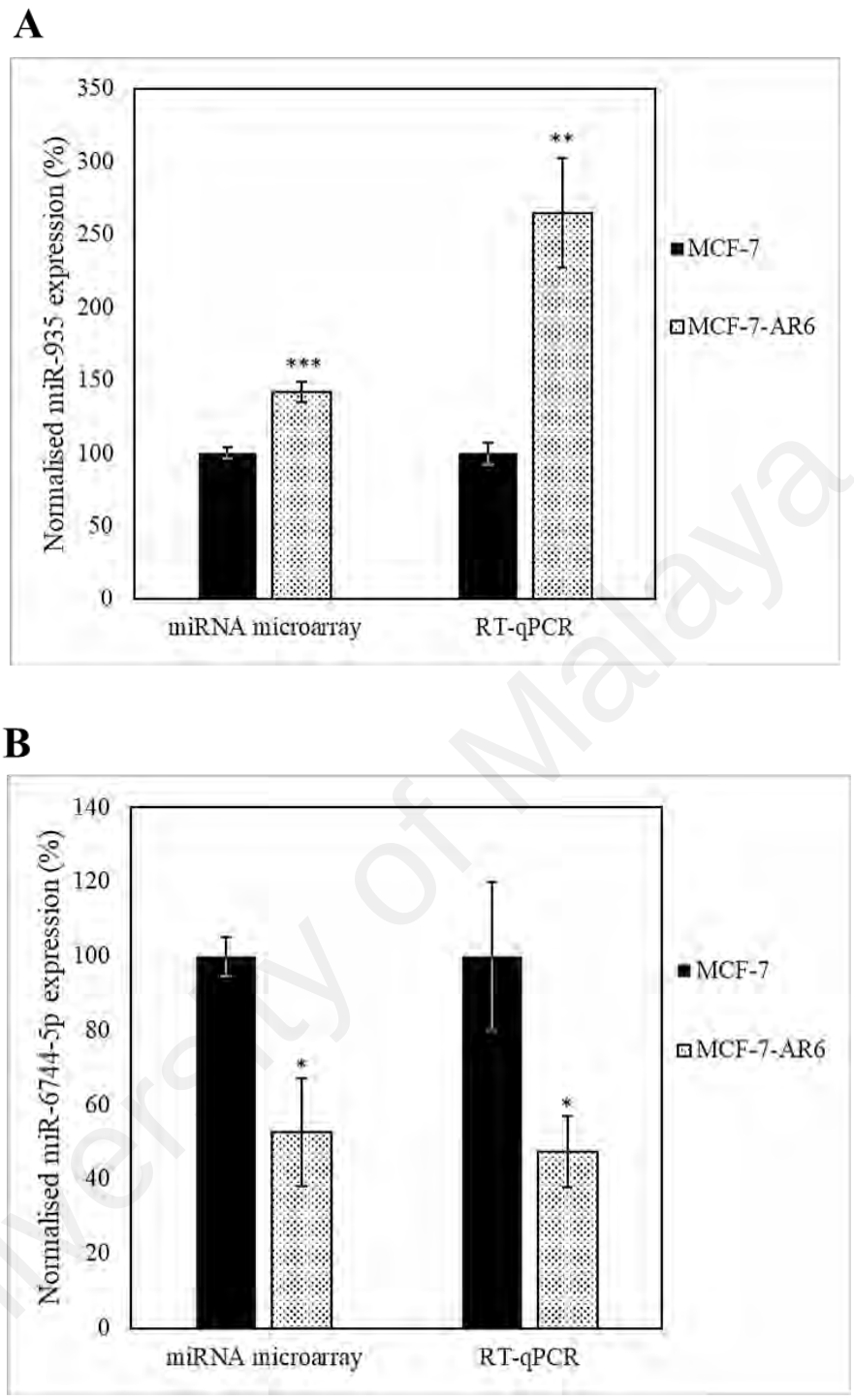

Figure 4.4: RT-qPCR validation of miR-935 and miR-6744-5p dysregulation. Differential expression in MCF-7-AR6 shown by miRNA microarray of the selected miRNAs, (A) miR-935 and (B) miR-6744-5p, was validated with RT-qPCR. Data are presented as mean±SD, and statistically significant differences compared to MCF-7 as the control are denoted by (*) for $p<0.05$, (**) for $p<0.01$ or (***) for $p<0.001$.

4.3 Overexpression and knockdown of miR-935 and miR-6744-5p was effectively demonstrated using mimics and inhibitor

The overexpression and knockdown studies of the selected miRNAs were carried out using transfection with miRIDIAN miRNA mimics and miRIDIAN miRNA inhibitors. Before proceeding into functional analysis of miR-935 and miR-6744-5p, the effectiveness of the transfection method was confirmed by measuring miRNA fold change upon transfection using RT-qPCR. The transfections were performed on two different breast cancer cell lines, which are the luminal A type MCF-7 and the triple-negative type MDA-MB-231. While MCF-7 is a non-invasive breast cancer cell line that expresses E-cadherin, MDA-MB-231 is invasive and does not express E-cadherin, exhibiting mesenchymal-like traits (Nagaraja et al., 2006). The results showed that the desired change in expression was achieved in both cell lines after transfection with miRNA mimics and inhibitors for miR-935 and miR-6744-5p (Figure 4.5).

4.4 miR-935 and miR-6744-5p do not affect proliferation of MCF-7 and MDA-MB-231 in adherent condition

Before analysing the effects of miR-935 and miR-6744-5p in regulating anoikis in MCF-7 and MDA-MB-231, the ability of these miRNAs to affect cell proliferation was tested in normal adherent culture condition. Based on proliferation assay, it was found that the overexpression and knockdown of miR-935 and miR-6744-5p did not have a significant effect on the proliferation of MCF-7 (Figure 4.6) and MDA-MB-231 cells (Figure 4.7).

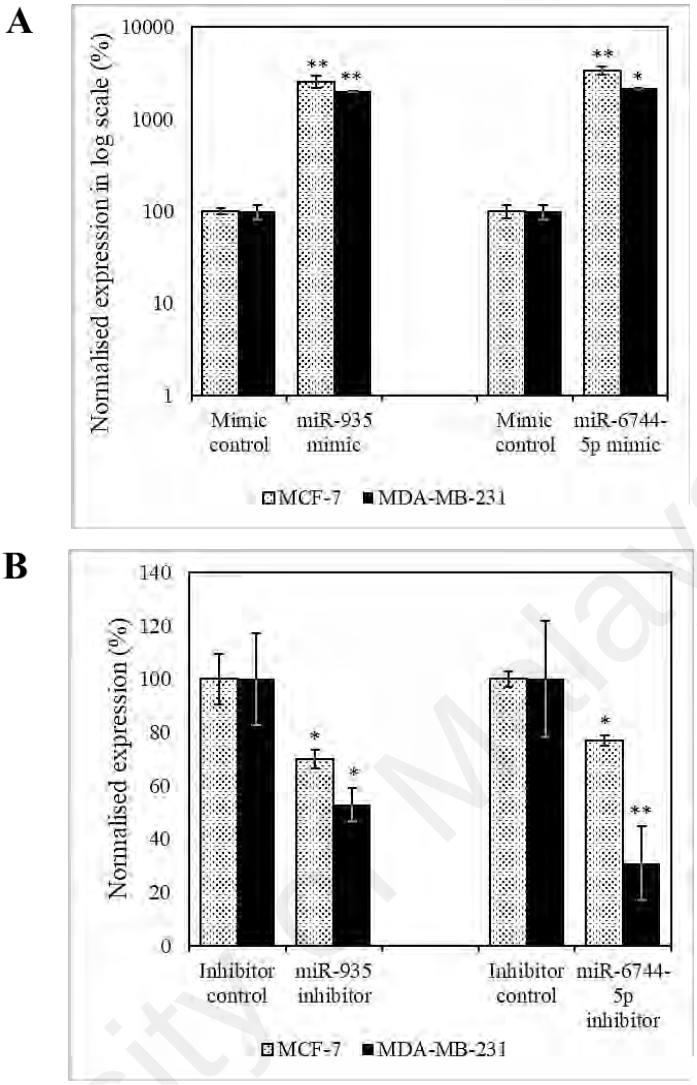

Figure 4.5: Overexpression and knockdown of miR-935 and miR-6744-5p in MCF-7 and MDA-MB-231. Measurement for (A) overexpression (mimic) and (B) knockdown (inhibitor) of the selected miRNAs, miR-935 and miR-6744-5p, using RT-qPCR. The expression of the miRNAs was calculated using ΔΔCq method with RNU6B as the reference gene. Data are presented as mean±SD, and statistically significant differences compared to mimic and inhibitor controls are denoted by (*) for $p<0.05$ or (**) for $p<0.01$.

4.5 miR-935 does not regulate anoikis in MCF-7 and MDA-MB-231

Since miR-935 was found to be upregulated in MCF-7-AR6, it was hypothesised that miR-935 played an oncogenic role by inhibiting anoikis in breast cancer cells. To test this, overexpression and knockdown of miR-935 was done using miR-935 mimic and inhibitor respectively in MCF-7 (Figure 4.8) and MDA-MB-231 (Figure 4.9).

Overexpression and knockdown of miR-935 did not have any significant effects in the induction of anoikis or the migration ability of MCF-7. Similarly, no significant changes were observed in MDA-MB-231, suggesting that miR-935 does not play a role in regulating anoikis.

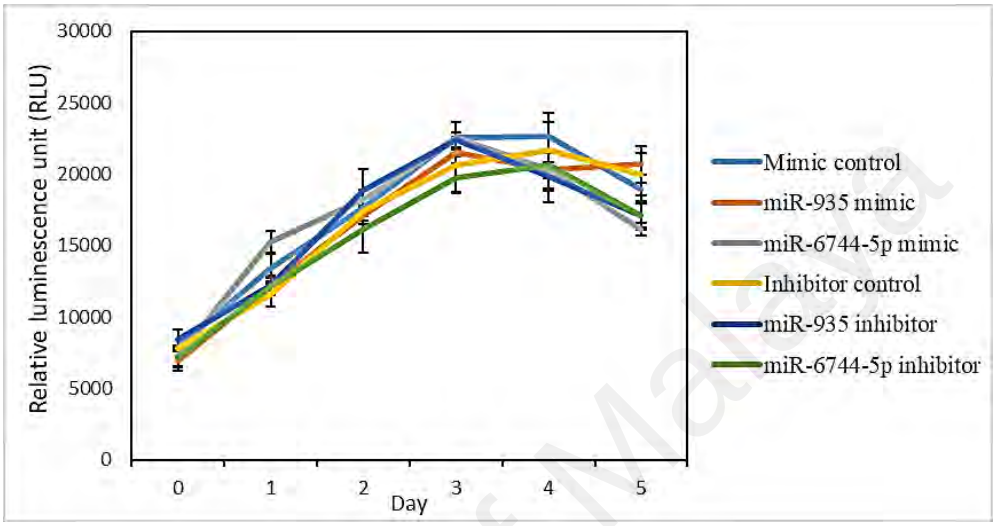

Figure 4.6: Proliferation assay of transfected MCF-7. The proliferation of MCF-7 cells with overexpression (mimic) and knockdown (inhibitor) of miR-935 and miR-6744-5p was measured over 5 days and compared to mimic and inhibitor controls.

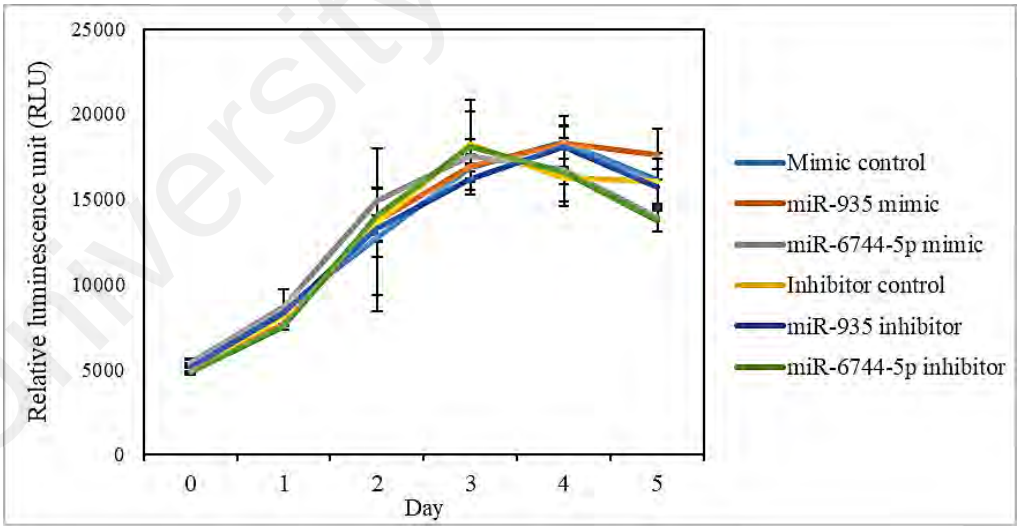

Figure 4.7: Proliferation assay of transfected MDA-MB-231. The proliferation of MDA-MB-231 cells with overexpression (mimic) and knockdown (inhibitor) of miR-935 and miR-6744-5p was measured over 5 days compared to mimic and inhibitor controls.

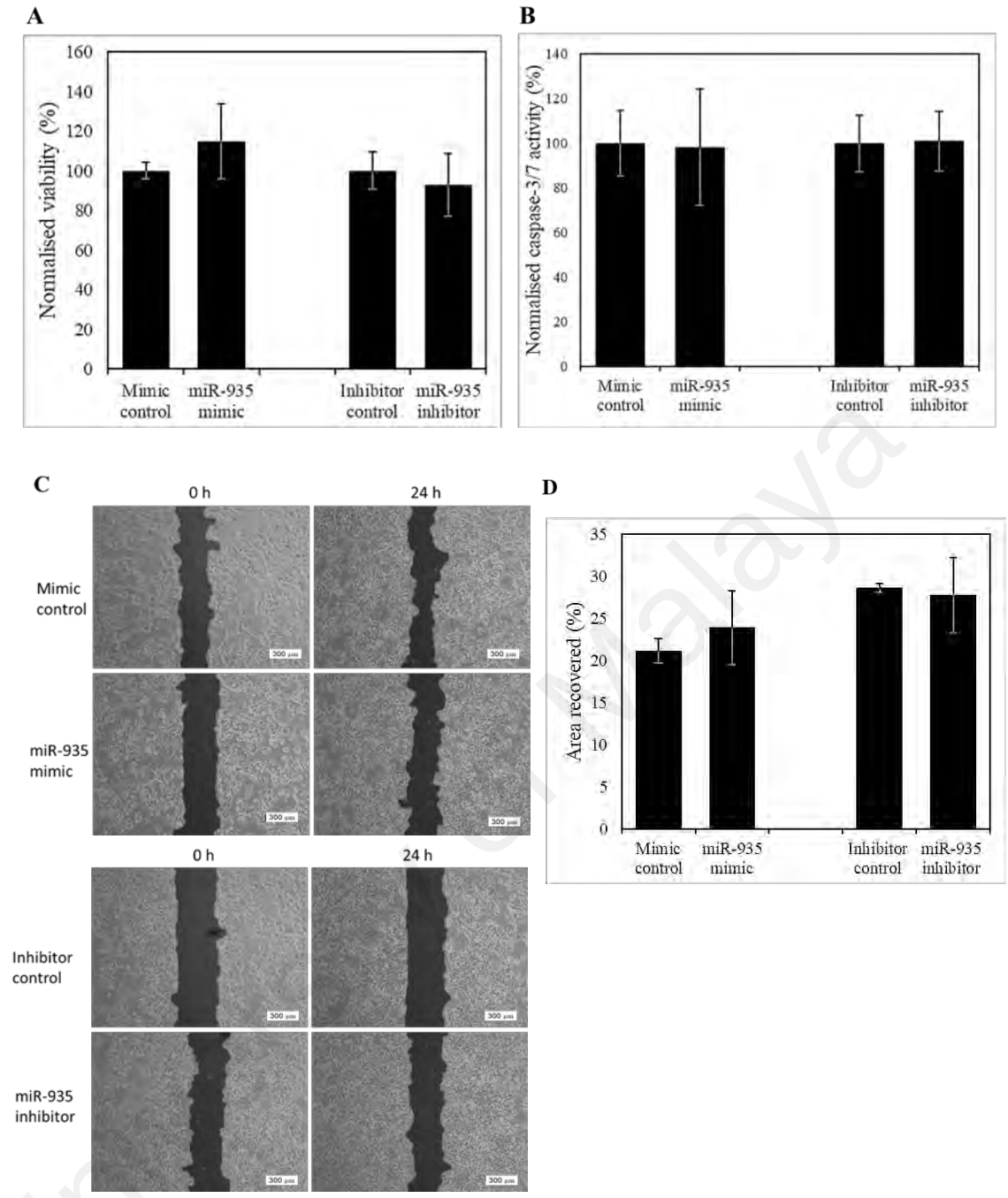

Figure 4.8: Overexpression and knockdown of miR-935 in MCF-7**.** Comparative analysis of overexpression (mimic) and knockdown (inhibitor) of miR-935 was done by measuring (A) viability after 48 h in suspension and (B) caspase-3/7 activity after 24 h in suspension and comparing to mimic and inhibitor controls. (C) Representative images for wound healing assay and (D) scratch area recovery of transfected MCF-7 after 24 h. Data are presented as mean±SD.

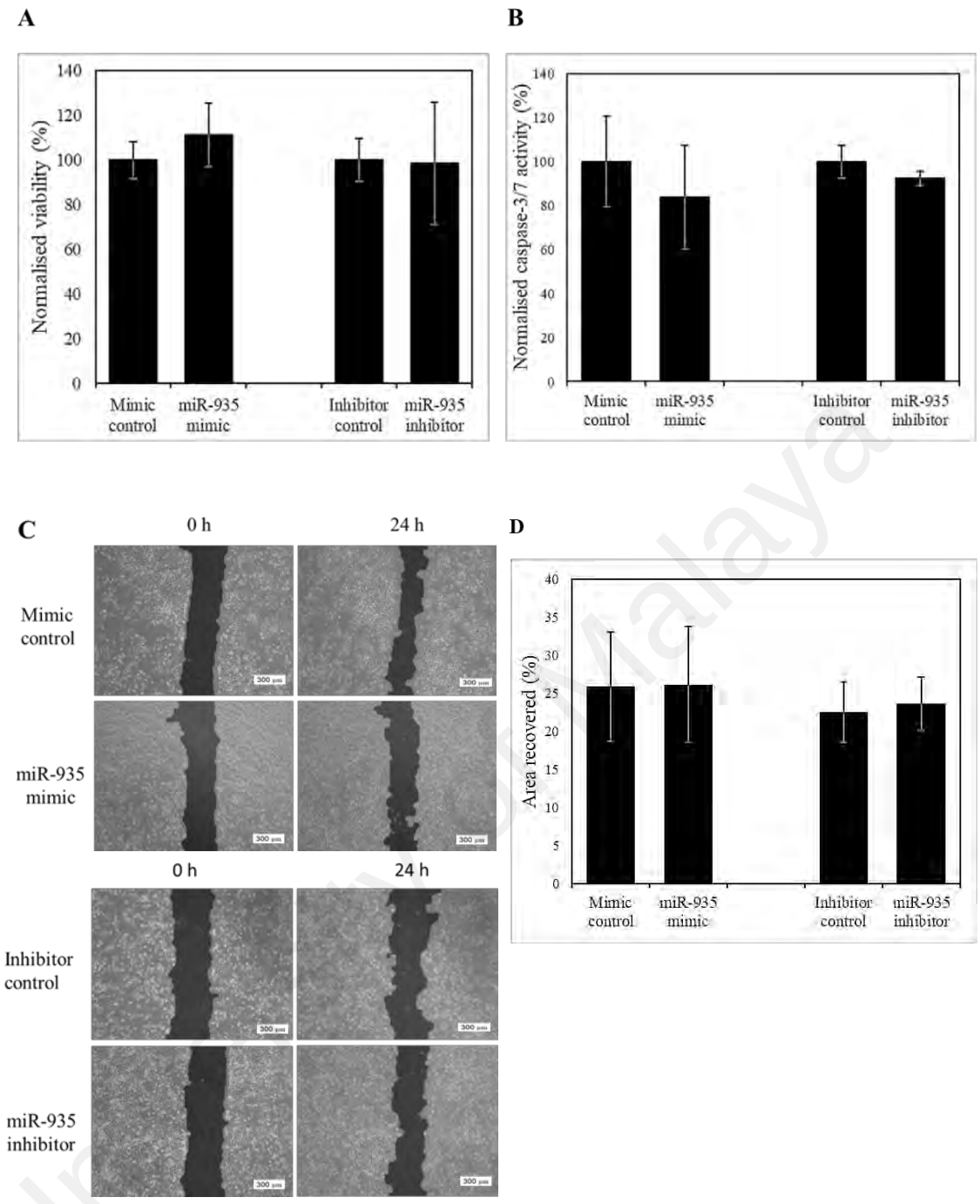

Figure 4.9: Overexpression and knockdown of miR-935 in MDA-MB-231. Comparative analysis of overexpression (mimic) and knockdown (inhibitor) of miR-935 was done by measuring (A) viability after 48 h in suspension and (B) caspase-3/7 activity after 24 h in suspension and comparing to mimic and inhibitor controls. (C) Representative images for wound healing assay and (D) scratch area recovery of transfected MDA-MB-231 after 24 h. Data are presented as mean±SD.

4.6 miR-6744-5p regulates anoikis sensitivity in MCF-7

miR-6744-5p was downregulated in MCF-7-AR6. As such, it was hypothesised that miR-6744-5p played a tumour suppressive role by promoting anoikis in breast cancer. To test this hypothesis, overexpression and knockdown of miR-6744-5p was carried out in MCF-7 cell line.

4.6.1 Overexpression of miR-6744-5p increases anoikis while its knockdown decreases anoikis

Upon transfection with miR-6744-5p mimic and inhibitor, the transfected MCF-7 cells were exposed to anchorage-independent condition to induce anoikis. Based on viability assay and caspase-3/7 activity assay, it was confirmed that overexpression of miR-6744-5p increased anoikis in MCF-7 (Figure 4.10), which showed lower amount of surviving cells (81.2±5.0% compared to control) and higher caspase-3/7 activity (200.5±2.1% compared to control). Meanwhile, the knockdown of miR-6744-5p decreased anoikis in MCF-7, which showed higher amount of surviving cells (144.6±12.0% compared to control) and lower caspase-3/7 activity (64.8±6.6% compared to control).

4.6.2 Overexpression of miR-6744-5p inhibits migration while its knockdown increases migration

To test the effects of miR-6744-5p on MCF-7's migration ability, wound healing assay was carried out with transfected cells. Corresponding to the results seen for anoikis sensitivity (Figure 4.11), overexpression of miR-6744-5p in wound healing assay showed lower recovery at 24 h (14.9±1.5% compared to 21.1±1.5% in control) while knockdown showed higher recovery at 24 h (40.4±3.7% compared to 28.6±0.5% in control).

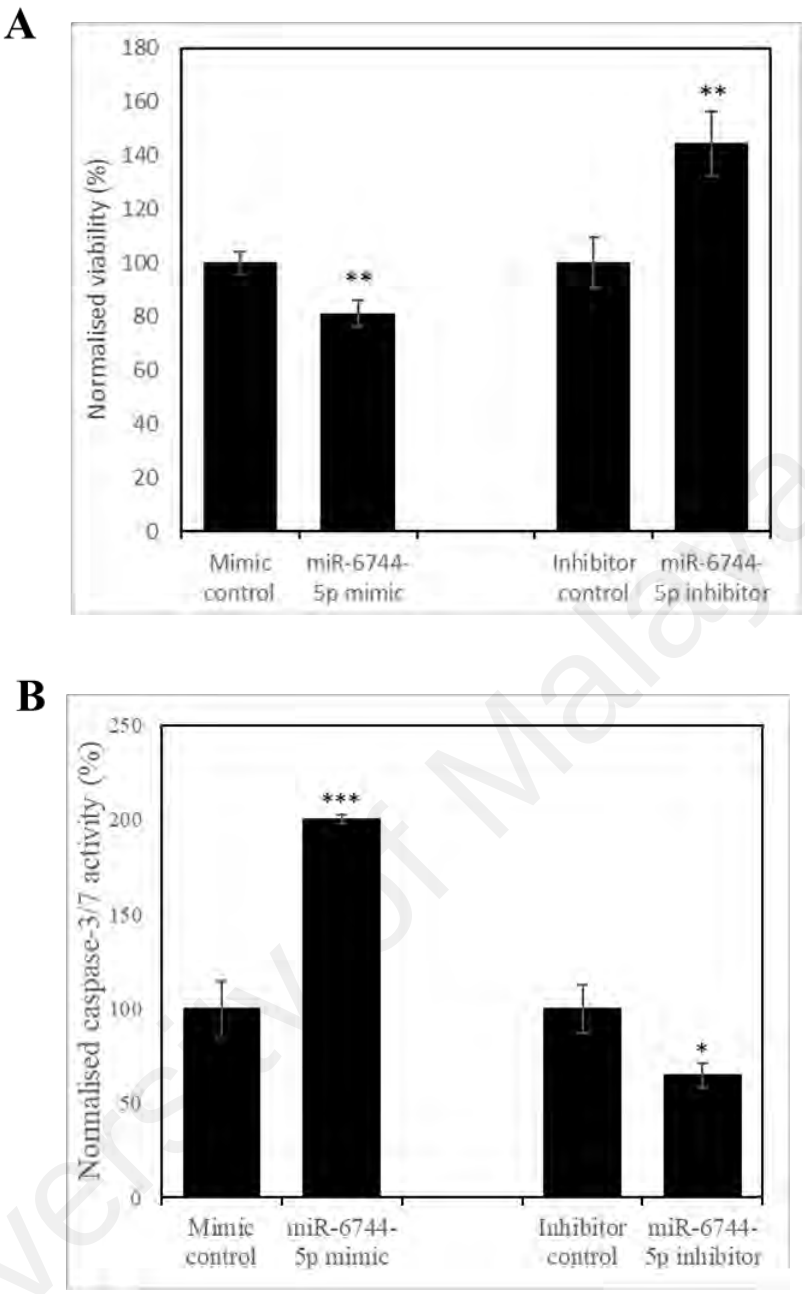

Figure 4.10: Anoikis during overexpression and knockdown of miR-6744-5p in MCF-7. Comparative analysis of overexpression (mimic) and knockdown (inhibitor) of miR-6744-5p was done by measuring (A) viability after 48 h in suspension and (B) caspase-3/7 activity after 24 h in suspension. Data are presented as mean±SD, and statistically significant differences compared to mimic and inhibitor controls are denoted by (*) for $p<0.05$, (**) for $p<0.01$ or (***) for $p<0.001$.

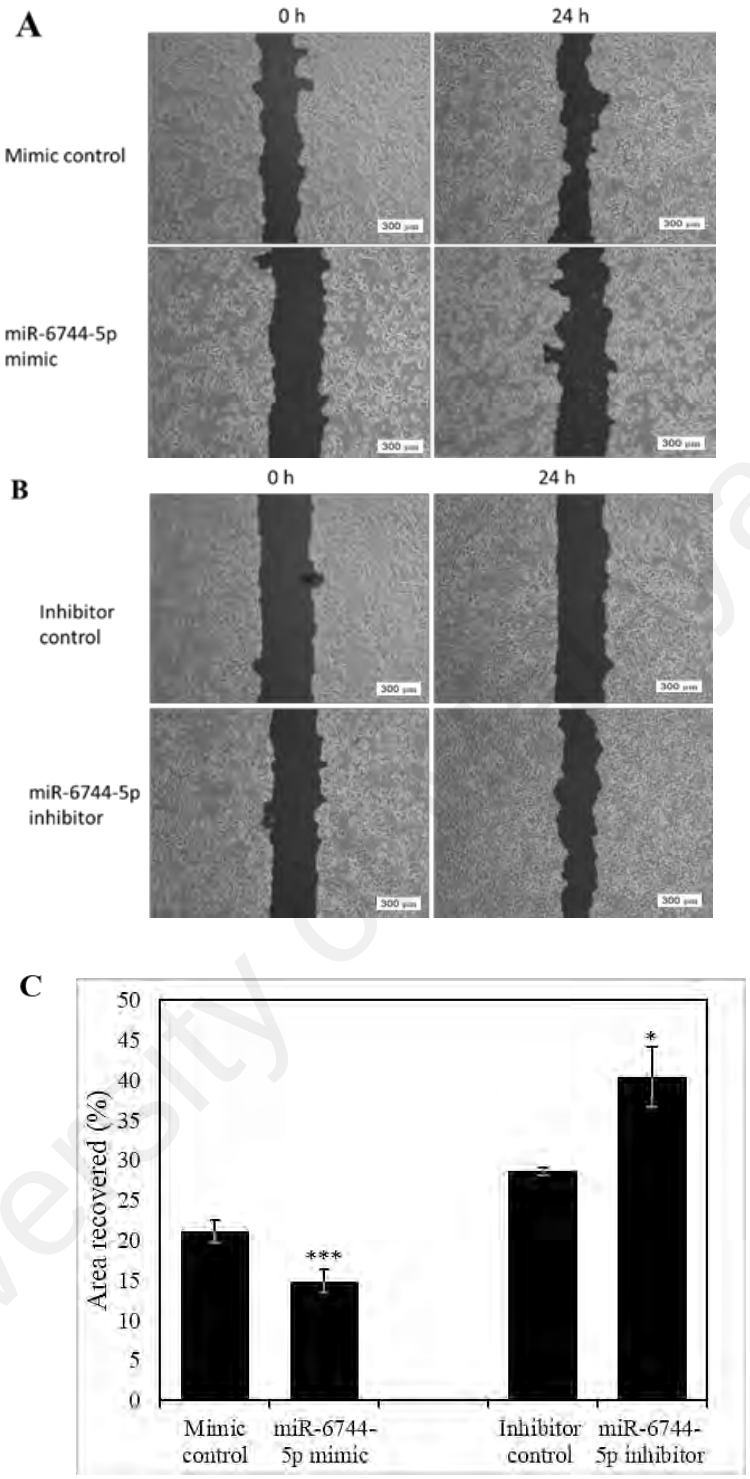

Figure 4.11: Overexpression and knockdown of miR-6744-5p for wound healing assay in MCF-7. Representative images of wound healing assay for (A) miR-6744-5p overexpression (mimic) and (B) knockdown (inhibitor). (C) Comparison of scratch area recovery of transfected MCF-7 after 24 h. Data are presented as mean±SD, and statistically significant differences compared to mimic and inhibitor controls are denoted by (*) for $p<0.05$ or (***) for $p<0.001$.

4.6.3 miR-6744-5p regulates the expression of E-cadherin

E-cadherin is an important cell surface receptor that ensures activation of anoikis in the event of cellular detachment. As such, since miR-6744-5p promotes anoikis and reduces migration, western blot was carried out to compare the expression of E-cadherin during the overexpression and knockdown studies (Figure 4.12). From the analysis of western blot using total proteins from transfected cells, E-cadherin was found to have increased expression during miR-6744-5p overexpression (153.5±13.9% compared to control) and decreased expression during miR-6744-5p knockdown (55.4±7.1% compared to control). This shows the role of miR-6744-5p in promoting anoikis in MCF-7 takes places through the regulation of E-cadherin expression.

4.7 miR-6744-5p regulates anoikis in MDA-MB-231

Considering the effects of miR-6744-5p in MCF-7, its capability to promote anoikis in another type of breast cancer was determined. For this purpose, overexpression and knockdown of miR-6744-5p was done in MDA-MB-231 cell line.

4.7.1 Overexpression of miR-6744-5p promotes anoikis

MDA-MB-231 cells were transfected with miR-6744-5p mimic and inhibitor before anoikis was induced. Viability and caspase-3/7 activity assays showed that overexpression of miR-6744-5p significantly decreased surviving population of cells (64.7±6.2% compared to control) and increased caspase-3/7 activation (163.5±19.9% compared to control). However, unlike seen in MCF-7, the knockdown of miR-6744-5p did not show any phenotypic effects (Figure 4.13).

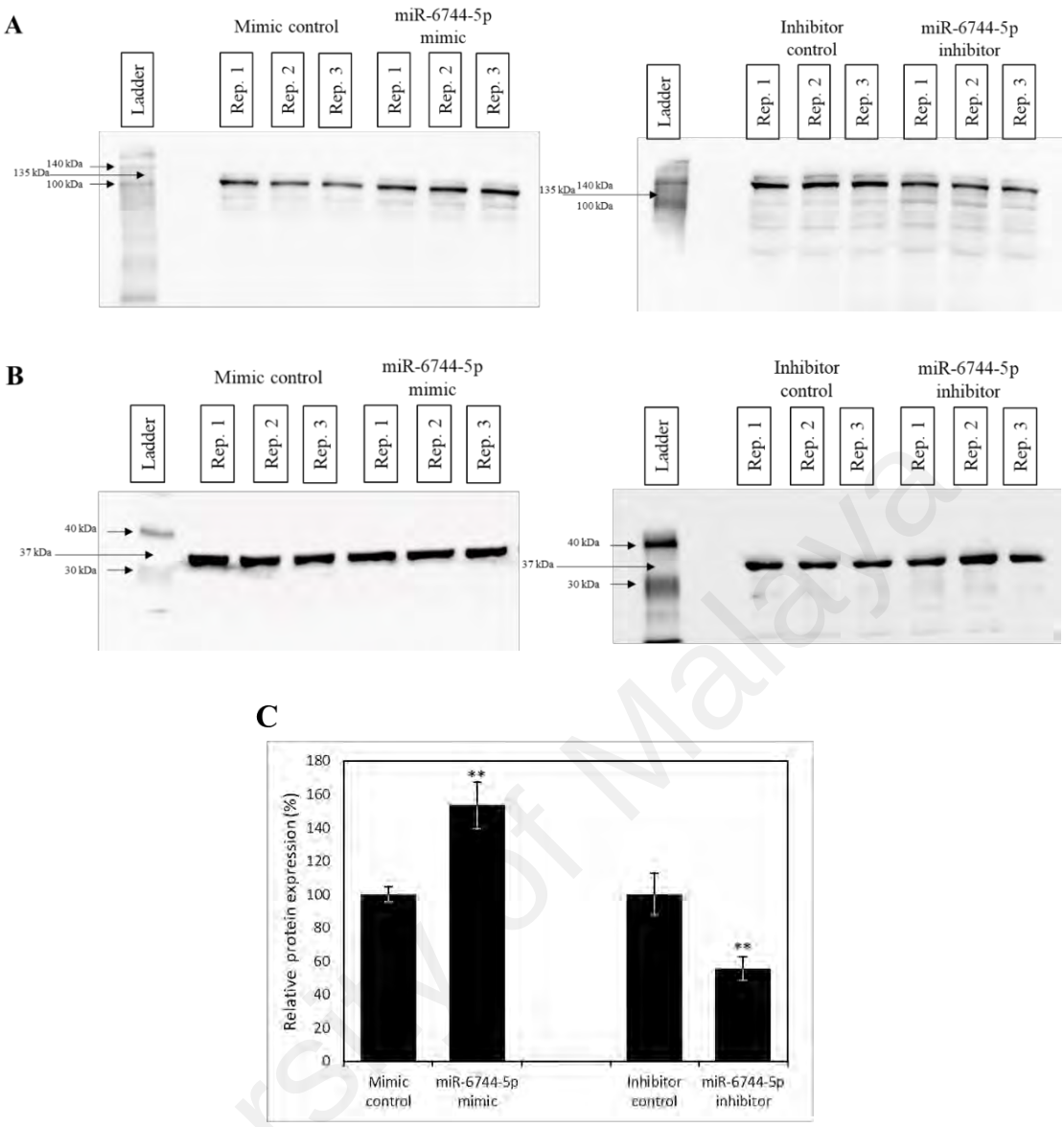

Figure 4.12: Expression of E-cadherin during overexpression and knockdown of miR-6744-5p in MCF-7. Western blot images of (A) E-cadherin and (B) GAPDH during overexpression (mimic) and knockdown (inhibitor) of miR-6744-5p. (C) Relative protein expression of E-cadherin was calculated from band intensity and normalised to the internal control, GAPDH. Data are presented as mean±SD, and statistically significant differences compared to mimic and inhibitor controls are denoted by (*) for $p<0.05$ or (**) for $p<0.01$.

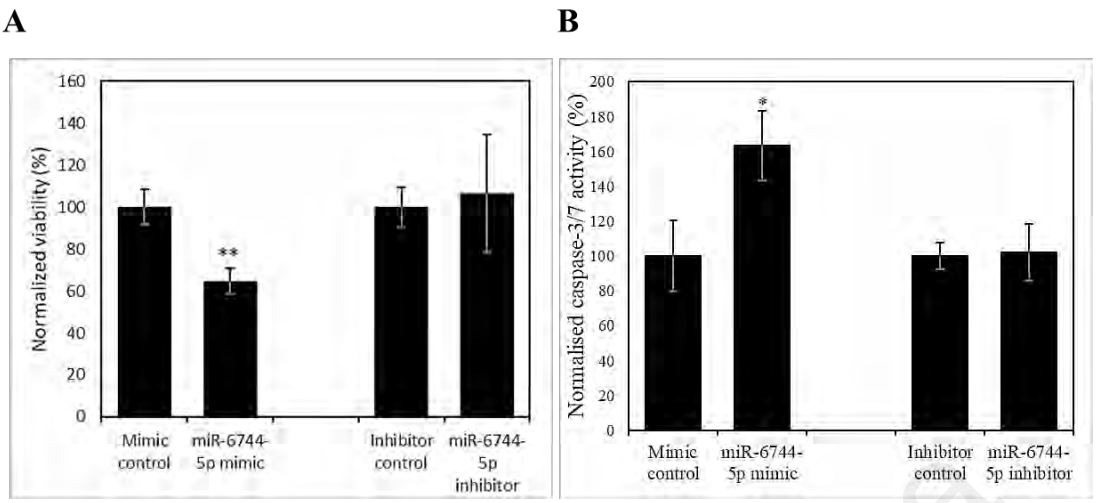

Figure 4.13: Anoikis during overexpression and knockdown of miR-6744-5p in MDA-MB-231. Comparative analysis of overexpression (mimic) and knockdown (inhibitor) of miR-6744-5p was done by measuring (A) viability after 48 h in suspension and (B) caspase-3/7 activity in MDA-MB-231 after 24 h in suspension. Data are presented as mean±SD, and statistically significant differences compared to mimic and inhibitor controls are denoted by (*) for $p<0.05$ or (**) for $p<0.01$.

4.7.2 Overexpression of miR-6744-5p inhibits migration

Consistent with the findings for anoikis regulation, overexpression of miR-6744-5p in MDA-MB-231 inhibited migration during wound healing assay, with lower recovery at 24 h (15.1±4.2% compared to 26.1±7.4% in control). The knockdown of miR-6744-5p did not have any significant effects (Figure 4.14).

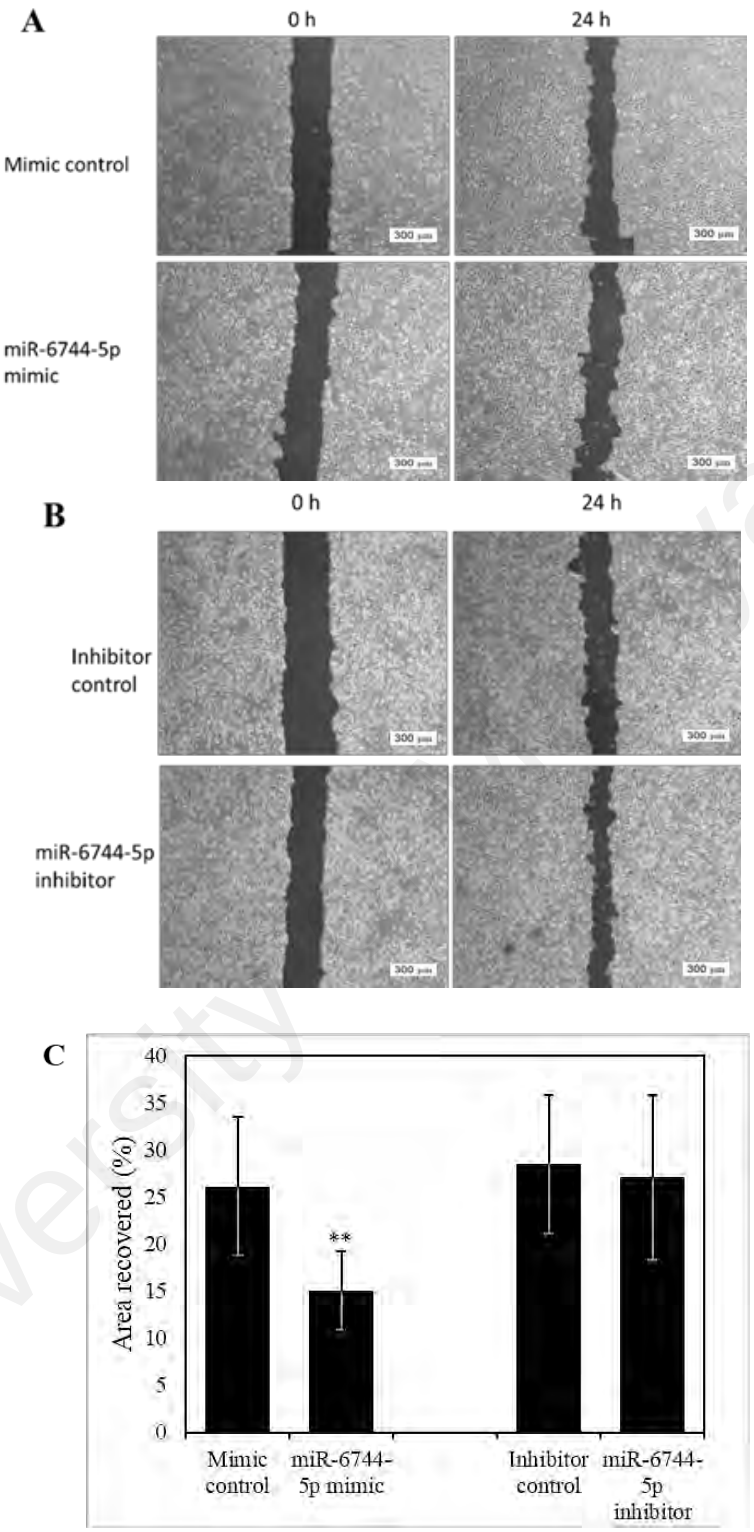

Figure 4.14: Overexpression and knockdown of miR-6744-5p for wound healing assay in MDA-MB-231. Representative images of wound healing assay for (A) overexpression (mimic) and (B) knockdown (inhibitor) of miR-6744-5p. (C) Comparison of scratch area recovery of transfected MDA-MB-231 after 24 h. Data are presented as mean±SD, and statistically significant differences compared to mimic and inhibitor controls are denoted by (**) for $p<0.05$.

4.7.3 miR-6744-5p induces morphological changes without the re-expression of E-cadherin.

During the overexpression of miR-6744-5p, morphological changes were observed in MDA-MB-231 cells. The cells began to shift from expressing spindle-like protruding edges to becoming more rounded (Figure 4.15). Further analysis through western blot showed that MDA-MB-231 did not re-express the epithelial marker E-cadherin or show significant changes in the expression of the mesenchymal marker vimentin during the overexpression of miR-6744-5p, suggesting that the change was not due to reversal of EMT (Figure 4.16).

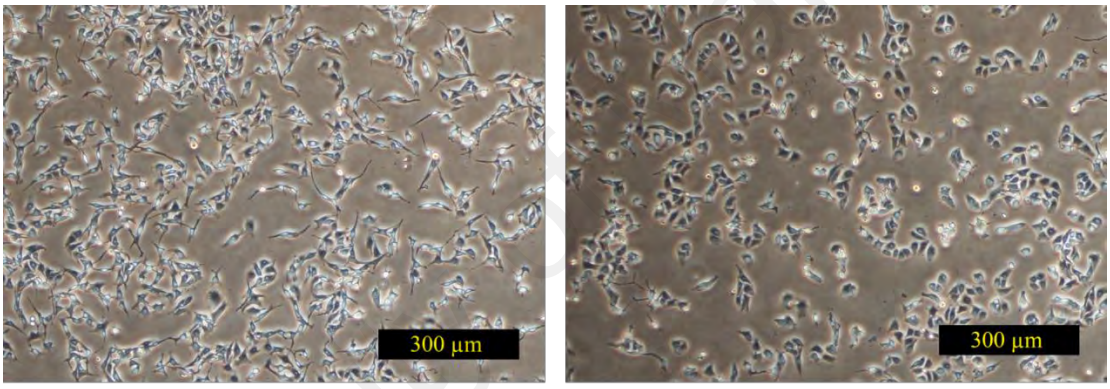

Figure 4.15: Morphological changes in transfected MDA-MB-231. Image of transfected MDA-MB-231 cells overexpressing miR-6744-5p (mimic) with rounded edges compared to the cells transfected with mimic control with protruding spindle-like edges.

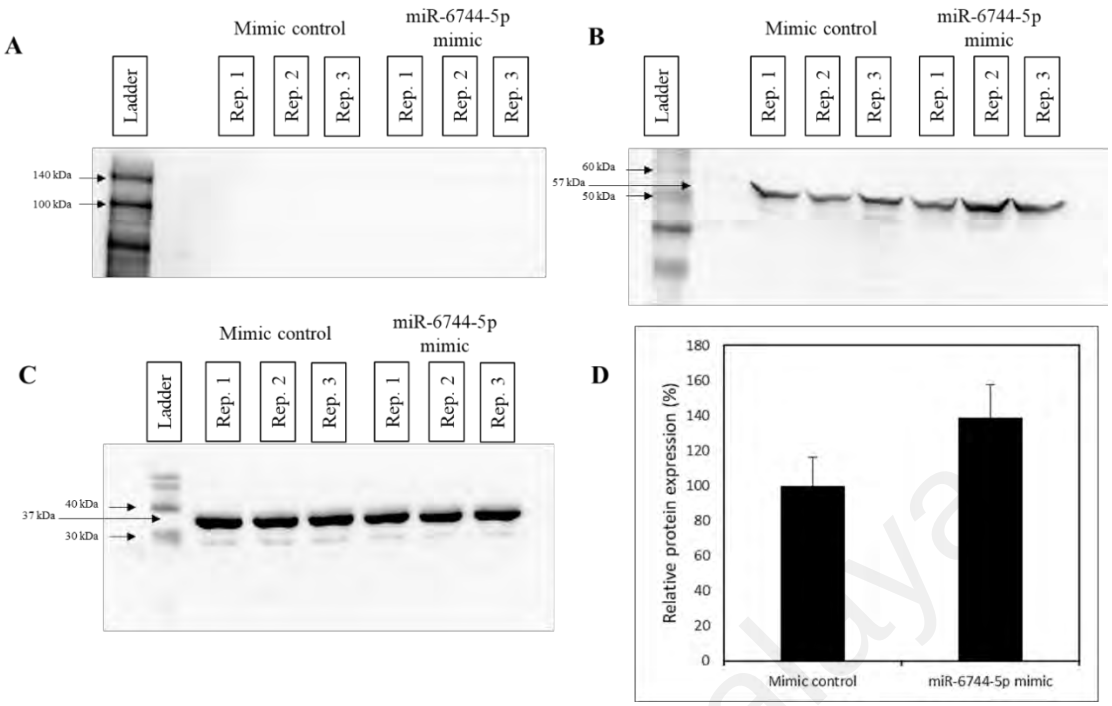

Figure 4.16: miR-6744-5p does not induce MET. Western blot images of (A) E-cadherin, (B) vimentin and (C) GAPDH during overexpression of miR-6744-5p (mimic) compared to mimic control. (D) Relative protein expression of vimentin was calculated from band intensity and normalised to the internal control, GAPDH.

4.6.4 miR-6744-5p impedes invasiveness

The overexpression of miR-6744-5p increased anoikis while the knockdown did not have any effects in MDA-MB-231. As such, since MDA-MB-231 is an invasive cell line, overexpression of miR-6744-5p was carried out to test its ability to restrict invasion using transwell invasion assay, as an *in vitro* model (Figure 4.17), and zebrafish metastasis assay, as an *in vivo* model (Figure 4.18). Both experiments showed that overexpression of miR-6744-5p significantly inhibited invasion. In transwell invasion assay, reduced number of invaded cells was observed (57.3±31.9 compared to 151±34.7 in control). Meanwhile in zebrafish metastasis model, lower percentage of cells was observed to have metastasised out of the original injection site at the zebrafish yolk (22.2±18.3% compared to 41.0±14.6% in control).

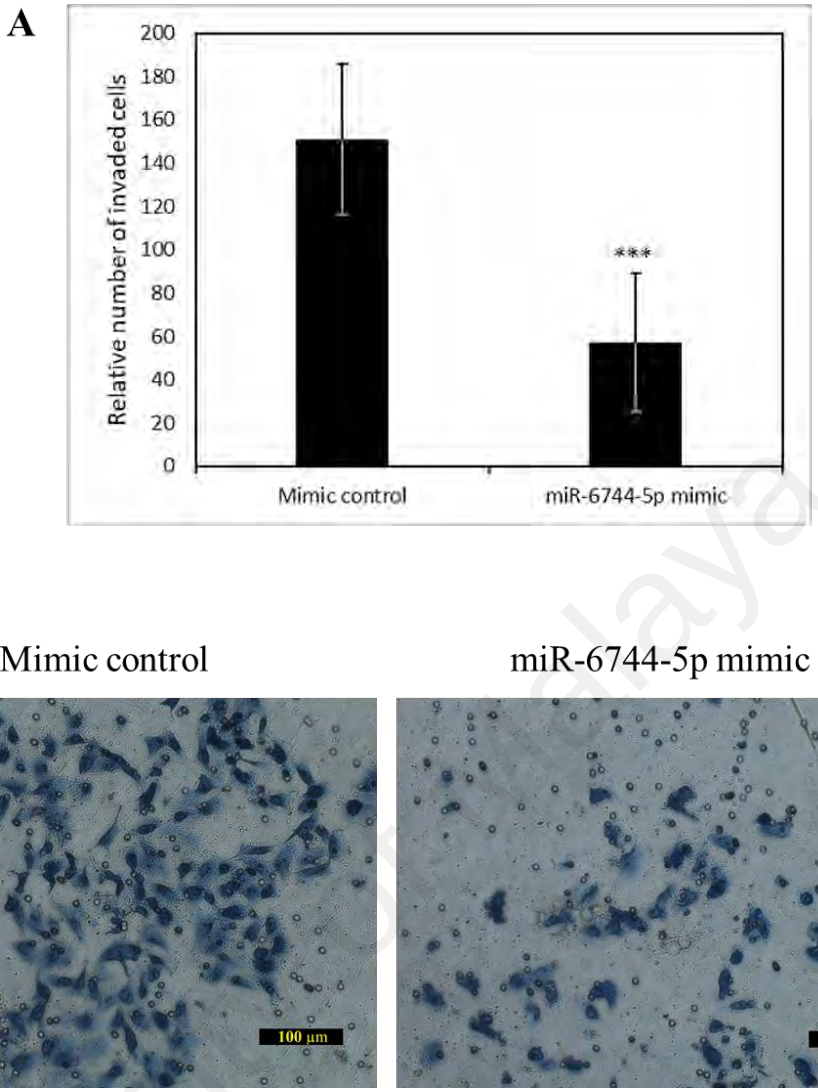

Figure 4.17: miR-6744-5p impedes invasiveness of MDA-MB-231 *in vitro*. (A) Relative number of MDA-MB-231 cells overexpressing miR-6744-5p (mimic) that invaded the Matrigel in transwell invasion assay and (B) representative images of the invading MDA-MB-231 cells overexpressing miR-6744-5p (mimic) compared to mimic control. Data are presented as mean±SD, and statistically significant difference compared to mimic control is denoted by (***) for $p<0.001$.

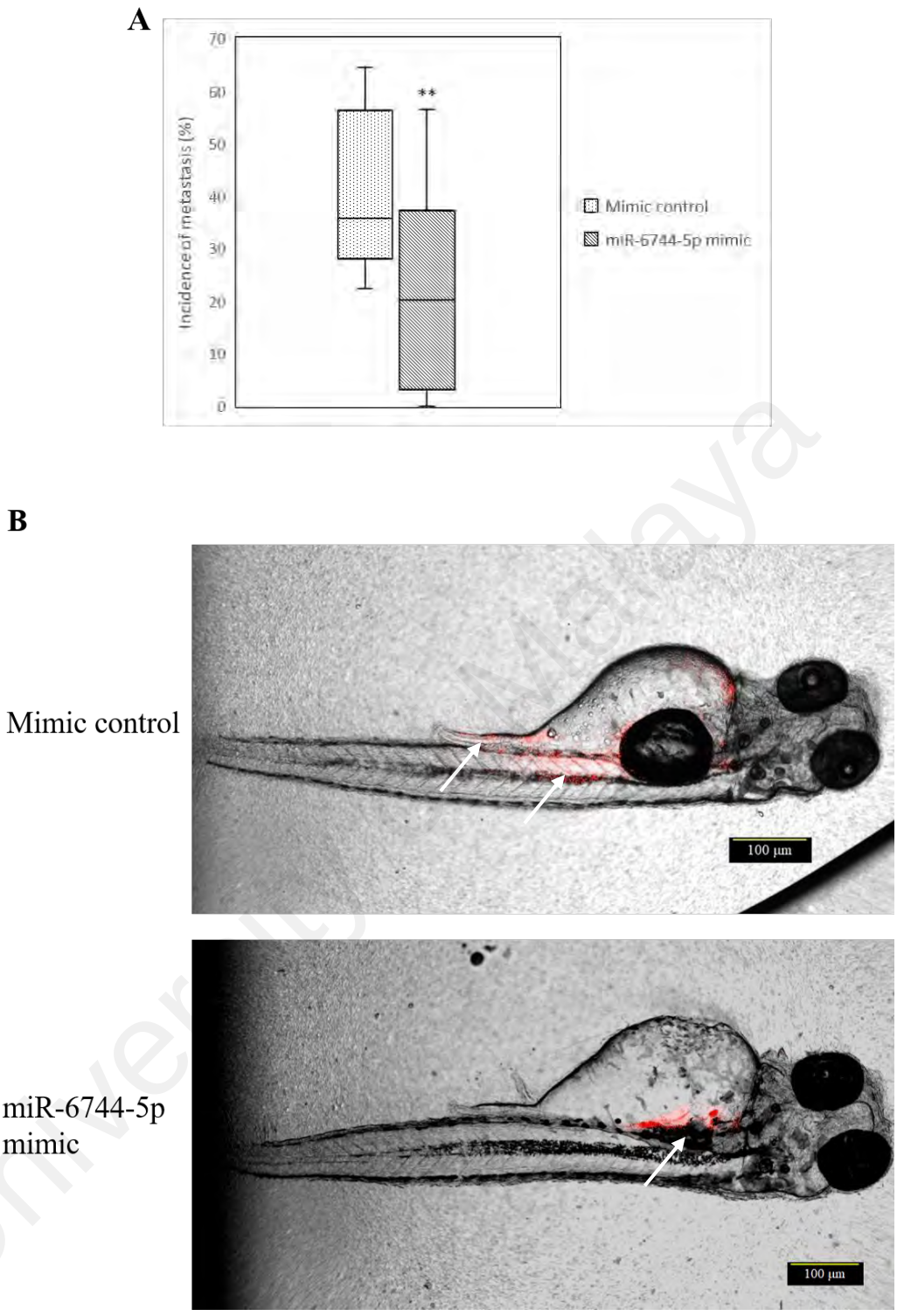

Figure 4.18: miR-6744-5p impedes invasiveness of MDA-MB-231 *in vivo*. (A) Incidence of metastasis in zebrafish model measured by percentage of DiI (red) stained MDA-MB-231 cells, transfected with mimic control (n=10) or miR-6744-5p mimic (n=12), that have metastasized out of the yolk to the rest of the body and tail and (B) representative images of the zebrafish metastasis model at 48 hpi (arrows indicate red-stained MDA-MB-231 cells transfected with mimic control or miR-6744-5p mimic). Data are presented as mean±SD, and statistically significant difference compared to mimic control is denoted by (**) for $p<0.01$.

4.8 NAT1 protein is confirmed to be the target of miR-6744-5p.

4.8.1 miR-6744-5p is predicted to bind to NAT1 3'UTR

To illuminate how miR-6744-5p carries out its anoikis-promoting effects, *in silico* analysis was done using publicly available online software for miRNA target prediction and pathway analysis, which are TargetscanHuman v7.1, DAVID Functional Annotation Tool 6.8 and KEGG PATHWAY database (Huang et al., 2009; Agarwal et al., 2015).

Firstly, TargetscanHuman was used to obtain a list of predicted targets for miR-6744-5p. The threshold for the context++ score, a score for the algorithm used for miRNA target prediction, was set at -0.04. Based on the criteria, 99 genes were found to be possible target of miR-6744-5p. Next, gene-annotation enrichment was carried out with the list of predicted target genes using DAVID Functional Annotation Tool to elucidate major cellular processes and signalling pathways associated with the genes. From the analysis, five major clusters of association among the target genes were identified, which are cell signalling, nucleus and transcription, miRNA processing, cell membrane and glycoprotein (Table 4.2). Meanwhile, the signalling pathways associated with the target genes were shown to primarily control proliferation and apoptosis (Figure 4.19).

These target genes, however, have not been experimentally validated to be miR-6744-5p's target genes. As such, since most of these targets are likely to be false positives, a literature review was conducted on published studies to identify genes with known role in anoikis regulation in breast cancer. This led to the discovery of similar *in vitro* results in studies on overexpression and knockdown of the NAT1 enzyme (Wakefield et al., 2008; Tiang et al., 2010; Tiang et al., 2011). NAT1 is a predicted target of miR-6744-5p with a context++ score of -0.66 and an 8mer binding site on position 30 to 37 on its 3'UTR. As an enzyme that metabolises xenobiotics, NAT1 transfers acetyl group to its substrates such as arylamine and hydrazine. Based on KEGG PATHWAY database

analysis, NAT1 is also involved in chemical carcinogenesis through the formation of DNA adducts. Thus, from literature review and *in silico* predicted interaction, NAT1 was chosen for validation steps.

Table 4.2: Functional annotation clustering of miR-6744-5p target genes

Annotation cluster	Enrichment score	Target genes
Cell signalling	1.3	18
Nucleus and transcription	0.63	33
miRNA processing	0.49	5
Cell membrane	0.15	35
Glycoprotein	0.08	23

Predicted target genes of miR-6744-5p were grouped based on their respective functions and association using DAVID Functional Annotation Tool. The higher the score, the more enriched is the cluster. Each cluster may contain overlapping genes.

4.8.2 miR-6744-5p directly binds to NAT1 3'UTR

To validate NAT1 targeting by miR-6744-5p, fragments of 3'UTR of *NAT1* gene containing the wild-type sequence and the mutated sequence of the predicted target site were synthesised with PmeI and XbaI restriction sites. These fragments were then cloned into pmirGLO Dual-Luciferase miRNA Target Expression Vector, which was confirmed by the sequencing results (Figure 4.20). The luciferase assay in MCF-7 showed the overexpression of miR-6744-5p significantly reduced luciferase activity in cells co-transfected with vector containing wild-type NAT1 3'UTR, whereas no significant difference was observed with vector containing mutated NAT1 3'UTR (Figure 4.21). As such, the luciferase assay provided confirmation for the interaction between miR-6744-5p and NAT1 3'UTR.

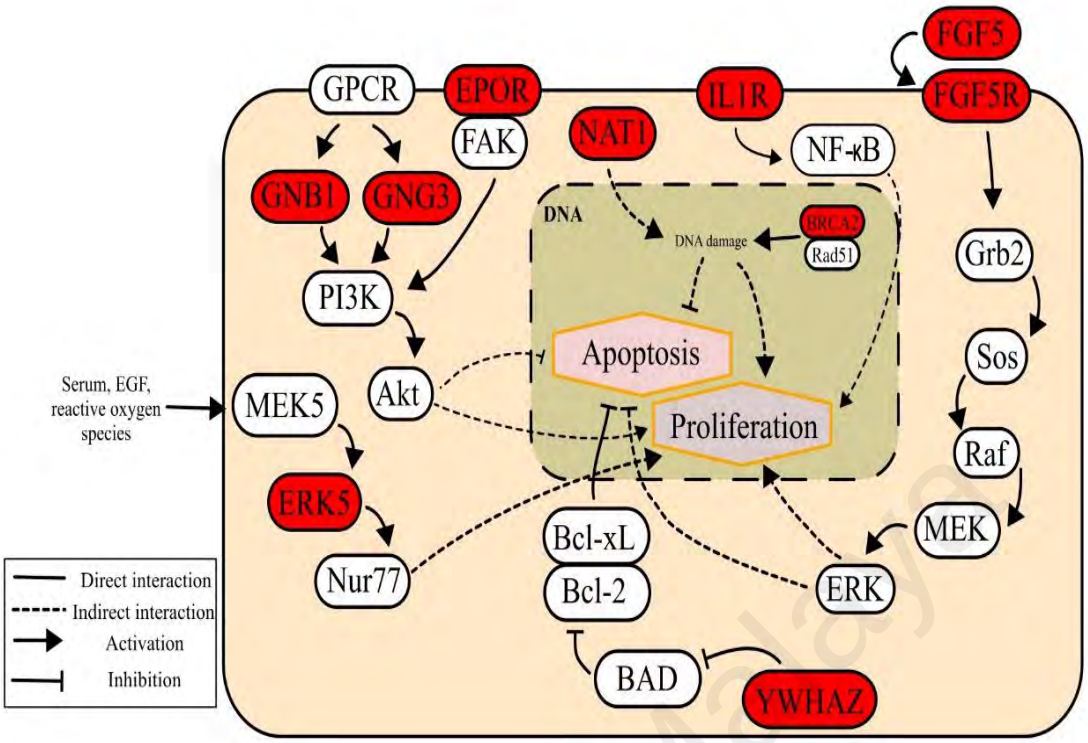

Figure 4.19: Hypothetical network of major pathways regulated by miR-6744-5p's predicted target proteins. A visual representation for the role of miR-6744-5p predicted target genes (highlighted in red) in regulating apoptosis and proliferation through direct and indirect interactions based on DAVID Functional Annotation Tool and KEGG PATHWAY database.

A

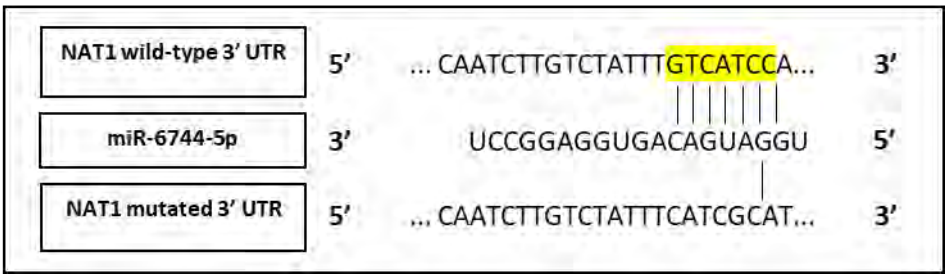

B

```
7201  GGACGAGGTGCCTAAAGGACTGACCGGCAAGTTGGACGCCCGCAAGATCCGCGAGATTCT
7261  CATTAAGGCCAAGAAGGGCGGCAAGATCGCCGTGTAATTCTAGTTGTTTAAACAATCTTG
7321  TCTATTTGTCATCCAGCTCACCAGTTATCAACTGACGACCTATCATGTATCTTCTGTACC
7381  CTTACCTTATTTTGAAGAAAATCCTAGACATCAAATCATTTCACCTATAAAAATGTCATC
7469  ATATATAATTTCTAGAGTCGACCTGCAGG
```

C

```
7201  GGACGAGGTGCCTAAAGGACTGACCGGCAAGTTGGACGCCCGCAAGATCCGCGAGATTCT
7261  CATTAAGGCCAAGAAGGGCGGCAAGATCGCCGTGTAATTCTAGTTGTTTAAACAATCTTG
7321  TCTATTTCATCGCATGCTCACCAGTTATCAACTGACGACCTATCATGTATCTTCTGTACC
7381  CTTACCTTATTTTGAAGAAAATCCTAGACATCAAATCATTTCACCTATAAAAATCAGGAT
7469  ATATATAATTTCTAGAGTCGACCTGCAGG
```

Figure 4.20: Sequencing of pmirGLO construct. (A) Insert sequence of NAT1 wild-type 3' UTR with predicted target site containing base complementarity (highlighted in yellow) with miR-6744-5p and NAT1 mutated 3' UTR. Confirmation of successful insertion of inserts containing (B) NAT1 wild-type 3'UTR and (C) mutated 3'UTR into the pmirGLO vector at position 7306 (highlighted in green) provided by sequencing results.

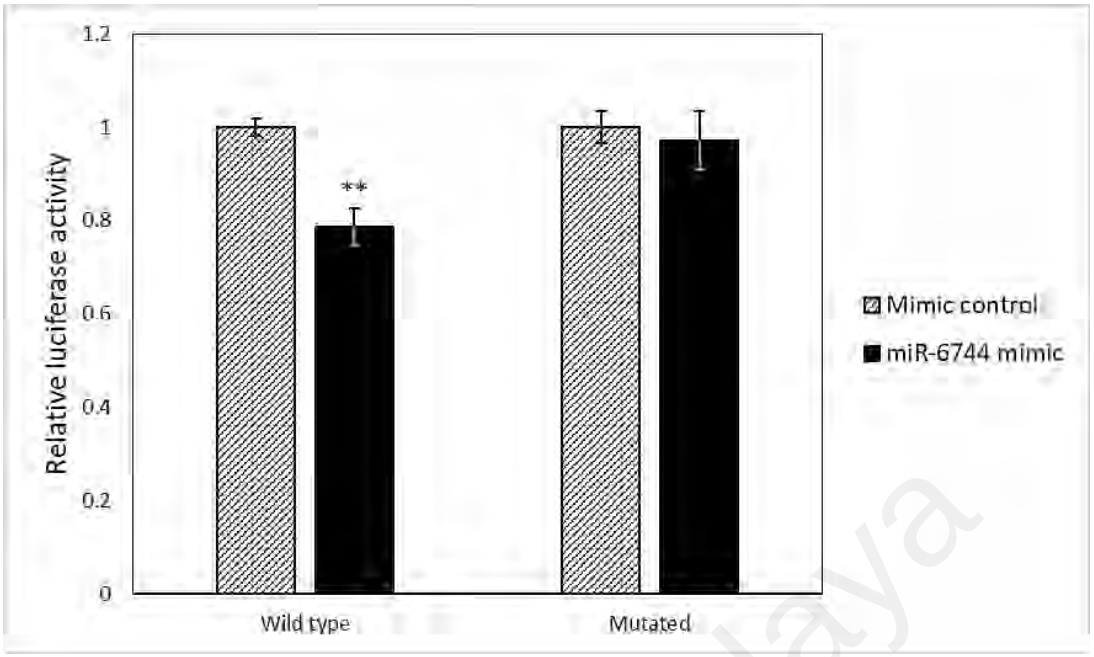

Figure 4.21: Luciferase assay validation of miR-6744-5p and NAT1 3'UTR binding in MCF-7. Relative luciferase activity, normalized to *Renilla* luciferase activity, was measured in MCF-7 cells transfected with wild type or mutated pmirGLO construct after co-transfection with mimic control or miR-6744-5p mimic. Data are presented as mean±SD, and statistically significant difference compared to mimic control is denoted by (**) for $p<0.01$.

4.8.3 miR-6744-5p overexpression downregulates NAT1 protein level

To confirm downregulation of NAT1 by miR-6744-5p, the expression of NAT1 protein during overexpression and knockdown of miR-6744-5p was evaluated in MCF-7 (Figure 4.22). Firstly, western blot showed that when miR-6744-5p was overexpressed, NAT1 expression was reduced (59.3±19.8% compared to control). On the other hand, during knockdown of miR-6744-5p, NAT1 expression was increased (140.7±13.9% compared to control). Additionally, overexpression of miR-6744-5p was also shown to decrease the expression of NAT1 in MDA-MB-231 (Figure 4.23), although the overall expression of NAT1 was very low compared to MCF-7 and required overexposure for band visibility.

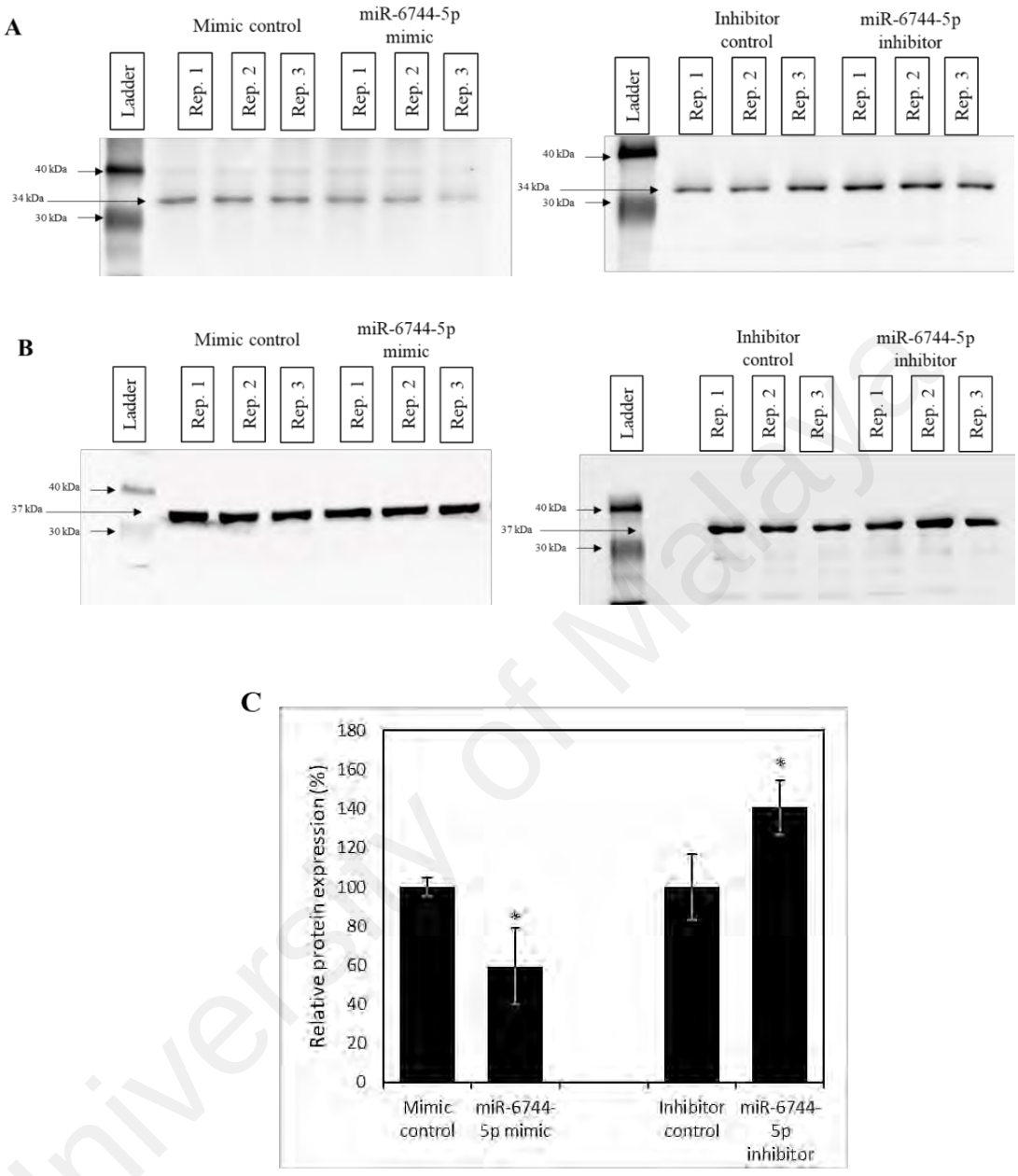

Figure 4.22: Expression of NAT1 during overexpression and knockdown of miR-6744-5p in MCF-7. Western blot images of (A) NAT1 and (B) GAPDH during overexpression (mimic) and knockdown (inhibitor) of miR-6744-5p in MCF-7. (C) Relative protein expression of NAT1 was calculated from band intensity and normalised to the internal control, GAPDH. Data are presented as mean±SD, and statistically significant differences compared to mimic and inhibitor controls are denoted by (*) for $p<0.05$.

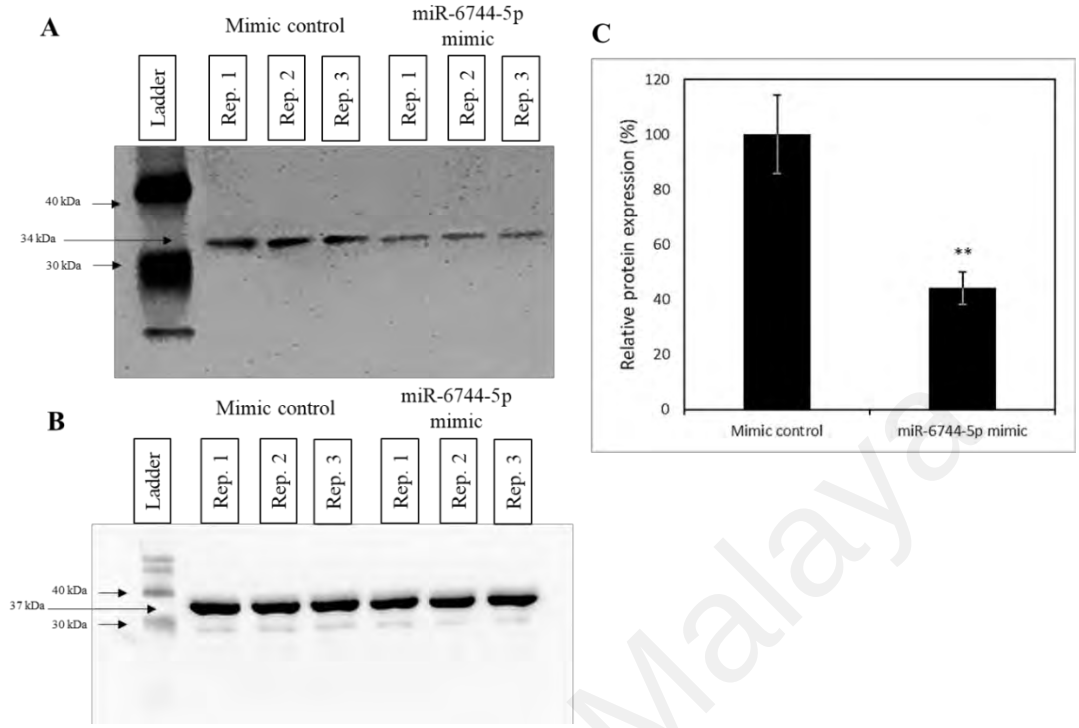

Figure 4.23: Expression of NAT1 during overexpression and knockdown of miR-6744-5p in MDA-MB-231. Western blot images of (A) NAT1 and (B) GAPDH during overexpression (mimic) of miR-6744-5p in MDA-MB-231. (C) Relative protein expression of NAT1 was calculated from band intensity and normalised to the internal control, GAPDH. Data are presented as mean±SD, and statistically significant difference compared to mimic control is denoted by (**) for $p<0.01$.

CHAPTER 5: DISCUSSION

In the attempt to reveal novel roles of miRNA in cancer, this study on miRNAs regulating anoikis resistance in breast cancer was carried out. miRNAs have gained immense attention recently, with research findings harbouring far-ranging implications on various areas within the biotechnology field. Meanwhile, unlike other cellular events that receive prominent attention in cancer research, anoikis remains relatively overlooked. Acquisition of anoikis resistance in cancer cells is often accompanied by EMT and subsequently metastasis, making anoikis an early barrier for cancer cells to break to become more invasive.

The study was initiated by using MCF-7, a luminal A type breast cancer cell line, to generate a stable anoikis resistant sub-cell line (MCF-7-AR6). Through repeated cycles of exposure to anchorage-independent state and normal adherent condition, a stable anoikis resistant sub-cell line, MCF-7-AR6, was generated. The extended exposure to suspension for 72 h ensures that only cells that are highly resistant to anoikis survive while repeating the cycle multiple times increases the chances to obtain cells that are stably resistant to anoikis for a long term. Subjecting cancer cells to additional stringent growth conditions and studying the resulting molecular changes in genetic expression sheds light on how cancer cells often adapt to variable microenvironment in the human body during tumourigenesis. As such, this strategy has allowed the identification of how miRNA expression is manipulated to achieve anoikis resistance.

To confirm that MCF-7-AR6 is more resistant to anoikis compared to the parental MCF-7 cell line, viability assay, caspase-3/7 activity assay and wound healing assay were carried out. Viability assay was done after 48 h in suspension to induce anoikis by comparing the amount of surviving cells. This assay was done using CellTiter-Glo Luminescent Cell Viability Assay kit which approximates the amount of living cells by

producing a luminescent signal proportional to adenosine triphosphate (ATP) in the sample.

On the other hand, caspase-3/7 activity assay was carried out after 24 h in suspension to compare the onset of apoptosis, as the activation of caspase-3/7 is an early event in apoptosis. For this assay, Caspase-Glo3/7 Assay kit was used. The reagent used in this assay contains the substrate for caspase-3/7, which is then broken down to release luminescence, directly correlated to the amount of active caspase-3/7 that are present in each sample. In MCF-7, this kit measures only the activity of capase-7 as this cell line does not express caspase-3.

Thirdly, wound healing assay was also carried to compare migration ability between the two groups. Although this assay is not directly relevant to cancer cell viability and death, migration ability requires the reorganisation of the cytoskeleton and integrin dynamics, serving as a quick and effective model to study cell-cell and cell-ECM interactions (Rodriguez et al., 2005; Vicente-Manzanares et al., 2009). Additionally, the assay is carried out using low serum media to rule out the effects of proliferation on wound recovery. Through these three assays, MCF-7-AR6 was confirmed to be more resistant to anoikis compared to the parental MCF-7.

The next step was to analyse the change in miRNA expression that occurred during the acquisition of anoikis resistance in MCF-7. By comparing MCF-7-AR6 to MCF-7 using miRNA microarray, a list of miRNAs with possible roles in anoikis regulation was identified. The change in expression level, when compared to the parental cell line, may be due to active roles played by the miRNAs in regulating survival in anchorage-independent growth. For example, as MCF-7-AR6 is more resistant to anoikis, it can be hypothesised that miRNAs that are upregulated inhibit anoikis, and miRNAs that are downregulated promote anoikis. Additionally, the findings from the miRNA microarray

also need to be quantitatively validated first using RT-qPCR before the dysregulation and role of the miRNAs can be confirmed through *in vitro* analysis.

A cursory literature review revealed that many of the miRNAs in the list with high fold change have been well established to regulate various oncogenic phenotypes across different cancer types. Among the top upregulated miRNAs are the members of the miR-181 family, miR-181a-3p, miR-181a-5p and miR-181b-5p. As mentioned in Chapter 2, members of this family have been prominently studied for their various roles in both promoting and suppressing tumourigenesis. The high fold change of these miRNAs is unsurprising as they are functionally similar in inhibiting anoikis and are also expressed together as clusters (Servin-Gonzalez et al., 2015). The mechanism of how these miRNAs regulate anoikis is explained in Chapter 2.3.4.2, which has been validated in breast cancer. As such, miR-181a-3p was not chosen for further analysis.

Another miRNA that was upregulated in MCF-7-AR6 is miR-615-3p. Although there are no studies of miR-615 in breast cancer, studies on gastric and non-small cell lung cancer (NSCLC) have revealed a dual role for miR-615-3p. Firstly, miR-615-3p was shown to be oncogenic in a study conducted on gastric cancer patients (Wang et al., 2018). The overexpression of miR-615-3p and reduced expression of its target gene, the RNA-binding protein CELF2, were revealed through microarray on gastric cancer tissues. Further analysis showed that the high expression of miR-615-3p correlated with the advanced stages of gastric cancer, and its ectopic expression led to increased survival, proliferation and invasion of gastric cancer cells. On the other hand, a study carried out in NSCLC found miR-615 to have an opposing tumour suppressive role (Pu et al., 2017). Unlike the study on gastric cancer, a microarray on NCSLC patient samples found miR-615-3p to be downregulated. Furthermore, overexpression and knockdown studies

showed miR-615-3p suppressed various oncogenic phenotypes in breast cancer cell lines including anoikis resistance.

Similar to many miRNAs in cancer, miR-27b-5p has been associated with conflicting roles in different cancer types. Notably, miR-27b-5p has shown both oncogenic and tumour suppressive roles within the same cancer type. In a study using mice model to determine the clinical significance of miR-27b-5p expression in breast cancer, the authors found that suppression of this miRNA resulted in tumour regression and increased expression of the receptor Nischarin (Jin et al., 2013). Furthermore, *in vitro* analysis of miR-27b-5p also provided evidence for its role in inhibiting anoikis to promote survival in anchorage-independent condition. The authors supported their findings with data from breast cancer patients which showed the high expression of miR-27b-5p and low expression of Nischarin was correlated with shorter recurrence-free survival. While this study positively identified miR-27b-5p to be oncogenic and suppress anoikis, two other studies have provided evidence to the contrary. Although these studies were not functional analyses, miR-27b-5p was found to be significantly downregulated in breast cancer tissues and can even be used as a biomarker to discriminate lower-grade from higher grade breast cancer samples (Tsuchiya et al., 2006; Lehmann et al., 2015).

Unlike the number of upregulated miRNAs, relatively fewer downregulated miRNAs were revealed from the miRNA microarray on MCF-7-AR6. Of these, miR-2861 and miR-1290 exhibited high fold change and have been previously studied in several cancer types. The tumour suppressive role of miR-2861 was recently shown to occur through the EGFR mediated pathway. By overexpressing miR-2861 in cervical cancer cells, Xu and colleagues were able to demonstrate a marked decrease in proliferation, migration and invasion of the cancer cells through the involvement of the PI3K/Akt pathway (Xu et al.,

2016). Additionally, the study also found the downregulation of this miRNA in cervical cancer tissues, which further corroborated its role as a tumour suppressor miRNA.

As for miR-1290, studies in breast cancer have shown it to have reduced expression in breast cancer cells expressing ERα (ER-positive) (Endo et al., 2013). Upon further investigations, it was proven that miR-1290 targets NAT1, making this the first study to implicate NAT1 as a target for a downregulated miRNA in breast cancer (Endo et al., 2014). Interestingly, conflicting evidence on miR-1290's role in breast cancer was also shown through the analysis of serum miRNA, during which miR-1290 was found to be upregulated in cancer patients (Hamam et al., 2016). Similarly, studies on other cancer types have also portrayed miR-1290 as an oncomiR instead. For example, according to studies in laryngeal carcinoma, prostate cancer and NSCLS, miR-1290 is upregulated in tumour cells, promotes tumourigenesis and correlates with poor overall survival (Huang et al., 2015; Janiszewska et al., 2015; Zhang et al., 2016).

From the review of existing studies on the dysregulated miRNAs in MCF-7-AR6, the focus of this study was narrowed down to miR-935, an upregulated miRNA, and miR-6744-5p, a downregulated miRNA, based on their high fold change and novelty in anoikis regulation and breast cancer. Before the functions of these selected miRNAs were studied, the upregulation and downregulation of expression was first quantitatively validated using RT-qPCR. The results were in agreement with the findings from microarray, confirming the dysregulation of miR-935 and miR-6744-5p in MCF-7-AR6 when compared to MCF-7. Thus, functional analysis of these miRNAs was carried out in two breast cancer cell lines of different subtypes, which are the luminal A type MCF-7 and triple-negative type MDA-MB-231 cell lines.

Proliferation assay was first carried out with the overexpression and knockdown of miR-935 and miR-6744-5p, which showed no impact on the rate of proliferation in both

MCF-7 and MDA-MB-231. This ensures that any phenotypic changes observed during the assessment of anoikis are not due to the difference in growth rate upon the overexpression or knockdown of these miRNAs.

Disappointingly, the overexpression and knockdown of miR-935 did not exert any significant changes in inducing anoikis in both cell lines despite its high fold change discovered in MCF-7-AR6. This was shown through viability, caspase-3/7 activity and wound healing assays, suggesting that miR-935 does not regulate anoikis in the breast cancer cells. Interestingly, miR-935 has been found to be upregulated in gastric cancer in a study which demonstrated the miRNA's ability to inhibit anoikis and promote cancer cell proliferation (Yang et al., 2016). This occurs through the direct targeting and downregulation of the tumour suppressor protein SOX7, which was also similarly reported in hepatocellular carcinoma (Liu et al., 2017).

The genomic context of miR-935 may explain why it was upregulated in MCF-7-AR6 but did not affect anoikis. Intragenic miRNAs are miRNAs found in the exons or introns of host genes, which can control its expression through co-transcription (Franca et al., 2016). miR-935 is located in an exon on chromosome 19 (chr19). As an intragenic miRNA, the expression of miR-935 is related to its host gene, which codes for calcium voltage-gated channel auxiliary subunit gamma 8 (CACNG8) (Hinske et al., 2014). CACNG8 associates with AMPA glutamate receptor and is primarily found in the brain, functioning as ion channels. Although no direct role in tumourigenesis has been established for CACNG8, both AMPA receptor and CACNG8 are known to play important roles in the classical MAPK/ERK pathway. In fact, glutamate-mediated AMPA receptor activation has been explicitly linked to higher invasion and migration of pancreatic cancer cells (Herner et al., 2011). It is worth noting that CACN8 is also a predicted target for miR-6744-3p, a miRNA that was downregulated in MCF-7-AR6 and

is derived from the same precursor as miR-6744-5p. As such, it is hypothetically possible for miR-935 to be upregulated due to increased co-expression with CACNG8 in MCF-7-AR6. Moreover, there is also the limited possibility that miR-935 is involved in other cellular processes in breast cancer unrelated to anoikis.

Meanwhile, miR-6744-5p, the second miRNA chosen for further analysis, is a relatively new miRNA that was annotated in 2012, with no existing functional studies at present (Ladewig et al., 2012). Based on its downregulation in MCF-7-AR6, miR-6744-5p was hypothesised to play a tumour suppressive role by promoting anoikis. To test this hypothesis, overexpression and knockdown studies of the miRNA was carried out using miRNA mimics and inhibitor in MCF-7.

Firstly, overexpression of miR-6744-5p in MCF-7 was found to promote anoikis, decrease migration and increase the protein expression of E-cadherin, whereas knockdown achieved the opposite outcomes as expected. As mentioned in Chapter 2, E-cadherin is an important epithelial marker and a cell surface receptor playing a pivotal duty of regulating cell-cell interaction and anoikis regulation. Its loss leads to EMT, which enables cancer cells to adopt mesenchymal-like characteristics to resist anoikis and metastasise. As such, increase in the expression of E-cadherin upon overexpression of miR-6744-5p was in line with the predicted hypothesis as it prevents cells from surviving the disassociation from neighbouring cells into an anchorage-independent condition.

Next, the experiments were repeated in MDA-MB-231, a triple-negative breast cancer cell line lacking E-cadherin expression, to test if miR-6744-5p can induce similar results. The knockdown of miR-6744-5p did not show any significant changes in terms of both anoikis induction and cell migration. This may be due to a low endogenous expression of miR-6744-5p in MDA-MB-231, and knockdown of the miRNA achieved no functional loss.

On the other hand, overexpression of miR-6744-5p not only increased anoikis sensitivity and reduced migration but also caused change in cell morphology. The cells began to lose their spindle-like protrusions to acquire comparatively rounded edges, which reduces motility and increases cell-cell contact. Membrane protrusions seen in cancer cells, such as filopodia, lamellipodia and invadopodia, house the focal adhesion complexes and various receptors such as integrins, making them highly necessary for ECM recognition. Furthermore, these cellular protrusions have also been demonstrated to modulate breast cancer cell *in vivo* spreading and migration. As such, the loss of these structures may greatly contribute to suppressing cancer cell motility and invasion. It was initially thought that the change in morphology is an indication that E-cadherin expression was being restored in this mesenchymal-like cancer cell line, marking MET. Indeed, the reverse has been observed in breast cancer cells during EMT, wherein cells exhibited significant loss of E-cadherin and adoption of elongated mesenchymal-like morphology (Xie et al., 2012). However, this was not the case, as the expression of the epithelial marker, E-cadherin, was not restored in MDA-MB-231, nor were there any changes to the mesenchymal marker, vimentin. Together, these results indicate that miR-6744-5p induces morphological changes in MDA-MB-231, but it was not sufficient to drive MET.

The next analysis conducted was related to cancer cell invasion. Unlike MCF-7, MDA-MB-231 is a highly invasive breast cancer cell line (Nagaraja et al., 2006). As such, the effects of miR-6744-5p on invasiveness were tested using this cell line. Transwell-invasion assay revealed that the overexpression of miR-6744-5p significantly reduced the invasiveness of MDA-MB-231 compared to control. The transwell-invasion assay is an *in vitro* set up to measure the invasive capability of cells (Marshall, 2011). Suspension of serum-starved cells is placed in an insert above a layer of Matrigel, a gelatinous mixture of proteins analogous to the ECM. The Matrigel forms a barrier that separates the cells in the insert from a provided chemoattractant, which in this case is growth medium with a

high percentage of serum. As such, the cells must traverse through the Matrigel to reach the bottom layer of the insert where the chemoattractant is fully accessible. The cells that have invaded the bottom after 24 h are then stained and visualised. The more invasive the cells are, the more cells will be visualised in the insert.

Similarly, miR-6744-5p also significantly inhibited invasiveness *in vivo*, demonstrated through a zebrafish larva metastasis model. Although not a suitable model to study tumour regression, zebrafish provides a microenvironment that is equipped with a functioning circulatory system in the host organism, providing an excellent model to study cancer cell invasion and metastasis. Similarities between the zebrafish and human genome also mean that the xenotransplantation of cancer cells is supported by interaction with the zebrafish stroma and tolerance by the zebrafish, providing a time- and cost-effective model for researchers to study cancer cell behaviour (Chen et al., 2017). Unsurprisingly, the zebrafish larva model is becoming vastly popular and being used in an increasing number of studies on various cancer traits, such as metastasis and angiogenesis (Brown et al., 2017). Especially for metastasis, zebrafish larva model offers a practical alternative for *in vivo* validation by using fluorescent-labelled cancer cells. This is because optical transparency can be induced with the use of PTU to inhibit melanogenesis in zebrafish, which allows easier imaging of cancer cells during the course of the experiment (Teng et al., 2013). Furthermore, the metastatic potential observed in zebrafish has also been shown to be parallel to the effects seen in mice, making it a highly versatile model.

For this experiment, transfected MDA-MB-231 cells were stained with a stable lipophilic membrane dye, DiI, and injected into the yolk sac of 48 hpf zebrafish embryos. The yolk is responsible to provide nutrients for the zebrafish embryos for the first five days and is well capable to sustain xenotransplanted cancer cells (Veinotte et al., 2014).

Injection of cells into this location in the zebrafish embryos provide the cells access to the circulatory system as well, establishing a starting point for invasive cancer cells to metastasise. At 48 hpi, the zebrafish embryos were euthanised and imaged using fluorescent confocal microscopy. The analysis of the combined z-stack images allows discerning the metastatic spread of the cancer cells away from the yolk of the zebrafish and into its circulatory system throughout its body. By comparing the percentage of fluorescent cells outside of the yolk with the control group, it was established that the overexpression of miR-6744-5p was able to significantly impede invasiveness of MDA-MB-231 cells.

Since the experiments so far have provided sufficient evidence to support miR-6744-5p's tumour suppressive role, the next question that was tackled was how the miRNA functions to exhibit its effects in breast cancer. For this purpose, *in silico* target prediction analysis and *in vitro* validation was used concurrently to determine the target gene of miR-6744-5p. Firstly, a list of putative target genes was obtained for miR-6744-5p using TargetScanHuman software. This software uses an algorithm to predict target 3'UTR binding efficacy, using a set of conditions to determine binding sites and the respective context++ scores (Agarwal et al., 2015). The score is calculated for each of the predicted target sites and presented as a cumulative number, after taking into account conditions such as 3'UTR length, seed-pairing stability and open reading frame (ORF) length.

From this analysis, 99 genes were listed as probable targets of miR-6744-5p. To illuminate possible connections between these target genes, the list was then fed into the gene-annotation enrichment software, DAVID (Huang et al., 2009). This software runs an analysis on all the terms and signalling pathways that are associated with each of the genes and attempts to find similarities among them. The functional annotation clustering revealed terms that were relevant to anoikis, such as cell signalling, cell membrane and

glycoprotein. Furthermore, the software was also used to highlight signalling pathways that are hypothetically regulated by the target genes, which are the PI3K/Akt and MAPK/ERK pathways. Examples of target genes implicated in these pathways are receptor EPOR and transducer GNB1 that activate PI3K/Akt pathway and growth factor FGF5 and its receptor FGFR that activate MAPK/ERK pathway. Unsurprisingly, these pathways are regularly associated with cancer cell malignancy as they govern a wide array of processes including survival and proliferation. Furthermore, the majority of miRNAs regulating anoikis have been shown to target components of these major pathways to exert their effects (Malagobadan & Nagoor, 2015).

Additionally, there were also some predicted target proteins that are known to contribute to carcinogenesis by causing DNA damage either directly or indirectly, such as NAT1 and BRCA2. Based on a literature review on these target genes, NAT1 appeared to be the best candidate for validation as miR-6744-5p target gene. NAT1 is a xenobiotic-metabolizing enzyme highly overexpressed in ER-positive breast cancer (Adam et al., 2003; Wakefield et al., 2008). In addition to NAT1 being one of the top predicted targets in TargetScanHuman, similarities were also observed in studies exploring the function of NAT1 in breast cancer cells. One of these studies was by Tiang *et al.* (2011), which demonstrated that knockdown of NAT1 caused loss of spindle-like protrusions and reduced transwell invasion without MET in three triple-negative breast cancer cell lines including MDA-MB-231 (Tiang et al., 2011). As such, NAT1 was chosen for further analysis.

Based on luciferase assay and western blot, it was confirmed that miR-6744-5p directly targets and downregulates NAT1. Luciferase assay was conducted to confirm the interaction and binding between miR-6744-5p and NAT1 3'UTR region. To achieve this, luciferase assay was carried out with vectors coding for luciferase enzyme in tandem with

either NAT1 wild-type 3'UTR fragment with the binding site or mutated 3'UTR fragment without the binding site. If there was binding between miR-6744-5p and NAT1 3'UTR, the luciferase enzyme will be reduced in expression compared to the control as the binding causes degradation of luciferase-NAT1 3'UTR mRNA transcript. The results of the luciferase assay confirmed this, as less luminescence was produced by the enzyme in cells co-transfected with the wild-type vector and miR-6744-5p mimic compared to the control.

On the other hand, western blot showed that there was indeed downregulation of NAT1 when miR-6744-5p was overexpressed in MCF-7 and MDA-MB-231. However, compared to MCF-7, the expression of NAT1 in MDA-MB-231 was too low for proper visualisation. This was consistent with findings of other studies that NAT1 expression and activity is higher in ER-positive breast cancer, such as MCF-7, compared to triple-negative breast cancer, such as MDA-MB-231 (Carlisle & Hein, 2018). Regardless, this does not indicate that NAT1 does not have a functional role in MDA-MB-231, as many studies on NAT1 have been carried out with this cell line (Tiang et al., 2010; Endo et al., 2014; Carlisle & Hein, 2018; Carlisle et al., 2018; Wang et al., 2018). As such, a more suitable way to measure downregulation of NAT1 in MDA-MB-231 would be to either measure NAT1 activity or its mRNA expression.

This project has identified the functional role of miR-6744-5p in promoting anoikis sensitivity and established that miR-6744-5p directly targets and downregulates NAT1. However, addressing the direct role of NAT1 enzyme in the regulation of anoikis by miR-6744-5p will require additional studies, such as the overexpression and knockdown of NAT1 without the target 3'UTR site. Other studies have attempted the knockdown of NAT1 enzyme in breast and colon cancer cells, producing comparably identical *in vitro* results to that seen during the overexpression of miR-6744-5p (Tiang et al., 2010; Tiang

et al., 2011; Tiang et al., 2015). Indeed, it was such findings that led to the hypothesis that miR-6744-5p exerts its role through the downregulation of NAT1 enzyme.

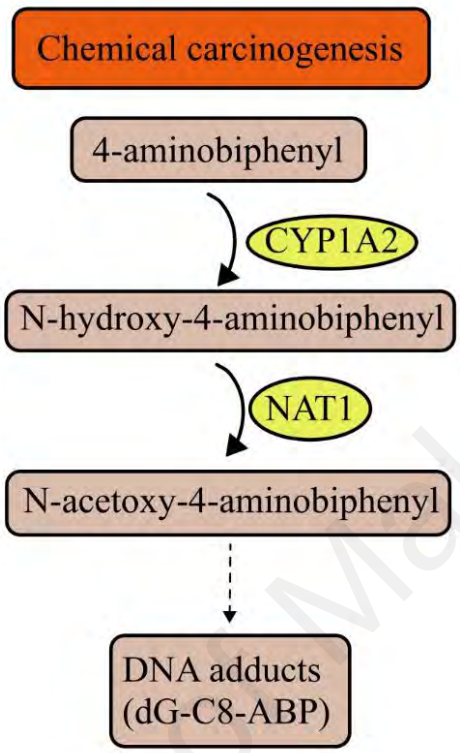

Figure 5.1: Chemical carcinogenesis by NAT1. A summary of the metabolism of aromatic amines/amides by NAT1 to form DNA adducts, contributing to genomic instability.

Although NAT1 has been identified as a target in cancer therapy, the link between the acetylation function of NAT1 enzyme and oncogenic phenotype observed when NAT1 is overexpressed is in need of further clarification (Rodrigues-Lima et al., 2012). Among the possible mechanism by which NAT1 could contribute to anoikis resistance is by causing DNA damage through chemical carcinogenesis. As an enzyme that adds acetyl group to its substrate, NAT1 is involved in the conversion of 4-aminobiphenyl into DNA adduct (Figure 5.1), a carcinogenic compound that has been popularly associated with red meat consumption (Xiao et al., 2016). Moreover, a recent study has also unravelled evidence suggesting NAT1 inhibits reactive oxygen species (ROS) to suppress apoptosis

(Wang et al., 2018). In this study using colon cancer cells, NAT1 was found to be necessary to stabilize and increase gain-of-function p53 during glucose starvation, leading to increased survival and resistance to anoikis. Lastly, NAT1 has also shown an inferred interaction with ICAM1, a CAM upregulated in triple-negative breast cancer, in a recent interactome analysis performed in HEK293T cells (Guo et al., 2014; Huttlin et al., 2015). However, the exact nature of this interaction has not been explored.

Research on breast cancer and NAT1 enzyme has only begun to gain momentum, and it is expected that NAT1's role as an oncogene and a cancer therapeutic target will achieve further clarification in the near future. Interestingly, another miRNA that targets NAT1 in ER-positive breast cancer, miR-1290, was also found to be downregulated in MCF-7-AR6 during miRNA microarray analysis, suggesting the importance of suppressing various inhibitors of NAT1 enzyme for cancer cells to resist anoikis (Endo et al., 2014). It is necessary to highlight here that while this study has identified a target of miR-6744-5p, the role of a miRNA goes beyond a single target, as miRNAs can target multiple genes to become an oncomiR or a tumour suppressive miRNA. For example, miR-34a, a prolific tumour suppressor miRNA, is reported to target more than 700 genes associated with cancer cell malignancy (Slabáková et al., 2017).

CHAPTER 6: CONCLUSION

Overall, this project has revealed a novel miRNA, miR-6744-5p, as a tumour suppressor miRNA that regulates anoikis in luminal A and triple-negative breast cancer. Overexpression and knockdown of miR-6744-5p were able to promote and inhibit anoikis respectively in MCF-7. Furthermore, the overexpression of miR-6744-5p was able to increase anoikis and impede invasiveness of the metastatic MDA-MB-231. The target gene, NAT1, has been previously found to be associated with aggressive breast cancer phenotypes, although the exact molecular mechanism involved is yet to be elucidated. As such, the findings of this study have provided enlightenment on how breast cancer cells are able to manipulate miRNA expression to inhibit anoikis.

Although NAT1 was identified and validated as the target of miR-6744-5p, the direct link between them in anoikis regulation is yet to be established which will require NAT1 overexpression and knockdown studies. Furthermore, it is also highly likely that miR-6744-5p also targets other genes, which results in the net effects that were observed. This will require additional studies to determine the network of targets regulated by this miRNA, such as microarrays. As for miR-6744-5p, having identified this miRNA as a tumour suppressor miRNA in breast cancer can be useful in therapeutic and prognostics application.

Therapeutic uses in cancer treatment have various challenges to attain feasibility, including effective and safe delivery methods. Furthermore, the role of miR-6744-5p in tumour regression in a higher animal model needs to be carried out before proceeding any further, as the zebrafish model used in this project is only preliminary. Meanwhile, the prognostic use of miR-6744-5p can be more immediate. Profiling and validating circulating miRNA level in breast cancer patients can prove to be a faster and efficient way of following patients' response to a particular cancer treatment. With concerted

efforts from the scientific community, there is no doubt that miRNA-based application will find their way to cancer therapeutics and prognostics in the near future.

REFERENCES

Acs, B., Zambo, V., Vizkeleti, L., Szasz, A. M., Madaras, L., Szentmartoni, G., . . . Tokes, A. M. (2017). Ki-67 as a controversial predictive and prognostic marker in breast cancer patients treated with neoadjuvant chemotherapy. *Diagnostic Pathology, 12*(1), 20.

Adam, P. J., Berry, J., Loader, J. A., Tyson, K. L., Craggs, G., Smith, P., . . . Terrett, J. A. (2003). Arylamine N-acetyltransferase-1 is highly expressed in breast cancers and conveys enhanced growth and resistance to etoposide in vitro. *Molecular Cancer Research, 1*(11), 826-835.

Agarwal, V., Bell, G. W., Nam, J. W., & Bartel, D. P. (2015). Predicting effective microRNA target sites in mammalian mRNAs. *Elife, 4,* e05005.

Amato, F., Tomaiuolo, R., Nici, F., Borbone, N., Elce, A., Catalanotti, B., . . . Castaldo, G. (2014). Exploitation of a very small peptide nucleic acid as a new inhibitor of miR-509-3p involved in the regulation of cystic fibrosis disease-gene expression. *BioMed Research International, 2014*, 610718.

Aoudjit, F., & Vuori, K. (2001). Matrix attachment regulates FAS-induced apoptosis in endothelial cells. *The Journal of Cell Biology, 152*(3), 633-644.

Auyeung, V. C., Ulitsky, I., McGeary, S. E., & Bartel, D. P. (2013). Beyond secondary structure: Primary-sequence determinants license pri-miRNA hairpins for processing. *Cell, 152*(4), 844-858.

Avalos, Y., Canales, J., Bravo-Sagua, R., Criollo, A., Lavandero, S., & Quest, A. F. (2014). Tumor suppression and promotion by autophagy. *BioMed Research International, 2014*, 603980.

Blazie, S. M., Geissel, H. C., Wilky, H., Joshi, R., Newbern, J., & Mangone, M. (2017). Alternative polyadenylation directs tissue-specific mirna targeting in caenorhabditis elegans somatic tissues. *Genetics, 206*(2), 757-774.

Bray, F., Ferlay, J., Soerjomataram, I., Siegel, R. L., Torre, L. A., & Jemal, A. (2018). Global cancer statistics 2018: GLOBOCAN estimates of incidence and mortality worldwide for 36 cancers in 185 countries. *CA: A Cancer Journal for Clinicians, 68*(6), 394-424.

Brown, H. K., Schiavone, K., Tazzyman, S., Heymann, D., & Chico, T. J. (2017). Zebrafish xenograft models of cancer and metastasis for drug discovery. *Expert Opinion on Drug Discovery, 12*(4), 379-389.

Bulfoni, M., Turetta, M., Del Ben, F., Di Loreto, C., Beltrami, A. P., & Cesselli, D. (2016). Dissecting the heterogeneity of circulating tumor cells in metastatic breast cancer: Going far beyond the needle in the haystack. *International Journal of Molecular Sciences, 17*(10), 1775.

Burstein, H. J. (2005). The distinctive nature of HER2-positive breast cancers. *The New England Journal of Medicine, 353*(16), 1652-1654.

Cancer Genome Atlas, N. (2012). Comprehensive molecular portraits of human breast tumours. *Nature, 490*(7418), 61-70.

Carlisle, S. M., & Hein, D. W. (2018). Retrospective analysis of estrogen receptor 1 and Nacetyltransferase gene expression in normal breast tissue, primary breast tumors, and established breast cancer cell lines. *International Journal of Oncology, 53*(2), 694-702.

Carlisle, S. M., Trainor, P. J., Doll, M. A., Stepp, M. W., Klinge, C. M., & Hein, D. W. (2018). Knockout of human arylamine N-acetyltransferase 1 (NAT1) in MDA-MB-231 breast cancer cells leads to increased reserve capacity, maximum mitochondrial capacity, and glycolytic reserve capacity. *Molecular Carcinogenesis, 57*(11), 1458-1466.

Chakraborty, C., Sharma, A. R., Sharma, G., Doss, C. G. P., & Lee, S. S. (2017). Therapeutic miRNA and siRNA: moving from bench to clinic as next generation medicine. *Molecular Therapy - Nucleic Acids, 8*, 132-143.

Chen, J. L., David, J., Cook-Spaeth, D., Casey, S., Cohen, D., Selvendiran, K., . . . Hays, J. L. (2017). Autophagy induction results in enhanced anoikis resistance in models of peritoneal disease. *Molecular Cancer Research, 15*(1), 26-34.

Chen, L., Groenewoud, A., Tulotta, C., Zoni, E., Kruithof-de Julio, M., van der Horst, G., . . . Ewa Snaar-Jagalska, B. (2017). A zebrafish xenograft model for studying human cancer stem cells in distant metastasis and therapy response. *Methods in Cell Biology, 138*, 471-496.

Chen, Y., Gao, D. Y., & Huang, L. (2015). In vivo delivery of miRNAs for cancer therapy: Challenges and strategies. *Advanced Drug Delivery Reviews, 81*, 128-141.

Cho, N. (2016). Molecular subtypes and imaging phenotypes of breast cancer. *Ultrasonography, 35*(4), 281-288.

Christopher, A. F., Kaur, R. P., Kaur, G., Kaur, A., Gupta, V., & Bansal, P. (2016). MicroRNA therapeutics: Discovering novel targets and developing specific therapy. *Perspective in Clinical Research, 7*(2), 68-74.

Cifuentes, D., Xue, H., Taylor, D. W., Patnode, H., Mishima, Y., Cheloufi, S., . . . Giraldez, A. J. (2010). A novel miRNA processing pathway independent of Dicer requires Argonaute2 catalytic activity. *Science, 328*(5986), 1694-1698.

Coates, A. S., Winer, E. P., Goldhirsch, A., Gelber, R. D., Gnant, M., Piccart-Gebhart, M., . . . Panel, M. (2015). Tailoring therapies--improving the management of early breast cancer: St Gallen international expert consensus on the primary therapy of early breast cancer 2015. *Annals of Oncology, 26*(8), 1533-1546.

Cuk, K., Zucknick, M., Madhavan, D., Schott, S., Golatta, M., Heil, J., . . . Burwinkel, B. (2013). Plasma microRNA panel for minimally invasive detection of breast cancer. *PLoS ONE, 8*(10), e76729.

Daige, C. L., Wiggins, J. F., Priddy, L., Nelligan-Davis, T., Zhao, J., & Brown, D. (2014). Systemic delivery of a miR34a mimic as a potential therapeutic for liver cancer. *Molecular Cancer Therapeutics, 13*(10), 2352-2360.

Daniel, A. R., Hagan, C. R., & Lange, C. A. (2011). Progesterone receptor action: Defining a role in breast cancer. *Expert Review of Endocrinology & Metabolism, 6*(3), 359-369.

De Gregorio, A., Friedl, T. W. P., Huober, J., Scholz, C., De Gregorio, N., Rack, B., . . . Fehm, T. (2017). Discordance in human epidermal growth factor receptor 2 (HER2) phenotype between primary tumor and circulating tumor cells in women with HER2-negative metastatic breast cancer. *JCO Precision Oncology, 1*(1), 1-12.

Delgado, M., & Tesfaigzi, Y. (2013). BH3-only proteins, Bmf and Bim, in autophagy. *Cell Cycle, 12*(22), 3453-3454.

Ebert, M. S., & Sharp, P. A. (2010). MicroRNA sponges: Progress and possibilities. *RNA, 16*(11), 2043-2050.

Ellsworth, R. E., Blackburn, H. L., Shriver, C. D., Soon-Shiong, P., & Ellsworth, D. L. (2017). Molecular heterogeneity in breast cancer: State of the science and implications for patient care. *Seminars in Cell and Developmental Biology, 64*, 65-72.

Endo, Y., Toyama, T., Takahashi, S., Yoshimoto, N., Iwasa, M., Asano, T., . . . Yamashita, H. (2013). miR-1290 and its potential targets are associated with characteristics of estrogen receptor alpha-positive breast cancer. *Endocrine-Related Cancer, 20*(1), 91-102.

Endo, Y., Yamashita, H., Takahashi, S., Sato, S., Yoshimoto, N., Asano, T., . . . Toyama, T. (2014). Immunohistochemical determination of the miR-1290 target arylamine N-acetyltransferase 1 (NAT1) as a prognostic biomarker in breast cancer. *BMC Cancer, 14*, 990.

Engstrom, M. J., Opdahl, S., Hagen, A. I., Romundstad, P. R., Akslen, L. A., Haugen, O. A., . . . Bofin, A. M. (2013). Molecular subtypes, histopathological grade and survival in a historic cohort of breast cancer patients. *Breast Cancer Research and Treatment, 140*(3), 463-473.

Esau, C., Davis, S., Murray, S. F., Yu, X. X., Pandey, S. K., Pear, M., . . . Monia, B. P. (2006). miR-122 regulation of lipid metabolism revealed by in vivo antisense targeting. *Cell Metabolism, 3*(2), 87-98.

Fayanju, O. M., Park, K. U., & Lucci, A. (2018). Molecular genomic testing for breast cancer: Utility for surgeons. *Annals of Surgical Oncology, 25*(2), 512-519.

Ferlay, J., Colombet, M., Soerjomataram, I., Dyba, T., Randi, G., Bettio, M., . . . Bray, F. (2018). Cancer incidence and mortality patterns in Europe: Estimates for 40 countries and 25 major cancers in 2018. *European Journal of Cancer, 103*, 356-387.

Ferlay, J., Soerjomataram, I., Dikshit, R., Eser, S., Mathers, C., Rebelo, M., . . . Bray, F. (2015). Cancer incidence and mortality worldwide: Sources, methods and major patterns in GLOBOCAN 2012. *International Journal of Cancer, 136*(5), E359-386.

Ferreira, M. M., Ramani, V. C., & Jeffrey, S. S. (2016). Circulating tumor cell technologies. *Molecular Oncology, 10*(3), 374-394.

Filipowicz, W., Jaskiewicz, L., Kolb, F. A., & Pillai, R. S. (2005). Post-transcriptional gene silencing by siRNAs and miRNAs. *Current Opinion in Structural Biology, 15*(3), 331-341.

Franca, G. S., Vibranovski, M. D., & Galante, P. A. (2016). Host gene constraints and genomic context impact the expression and evolution of human microRNAs. *Nature Communications, 7*, 11438.

Frisch, S. M., & Francis, H. (1994). Disruption of epithelial cell-matrix interactions induces apoptosis. *Journal of Cell Biology, 124*(4), 619-626.

Frisch, S. M., Schaller, M., & Cieply, B. (2013). Mechanisms that link the oncogenic epithelial-mesenchymal transition to suppression of anoikis. *Journal of Cell Science, 126*(1), 21-29.

Gallardo, A., Lerma, E., Escuin, D., Tibau, A., Munoz, J., Ojeda, B., . . . Peiro, G. (2012). Increased signalling of EGFR and IGF1R, and deregulation of PTEN/PI3K/Akt pathway are related with trastuzumab resistance in HER2 breast carcinomas. *British Journal of Cancer, 106*(8), 1367-1373.

Godone, R. L. N., Leitao, G. M., Araujo, N. B., Castelletti, C. H. M., Lima-Filho, J. L., & Martins, D. B. G. (2018). Clinical and molecular aspects of breast cancer: Targets and therapies. *Biomedicine & Pharmacotherapy, 106*, 14-34.

Gong, C., Bauvy, C., Tonelli, G., Yue, W., Deloménie, C., Nicolas, V., . . . Mehrpour, M. (2012). Beclin 1 and autophagy are required for the tumorigenicity of breast cancer stem-like/progenitor cells. *Oncogene, 32*, 2261.

Grimson, A., Farh, K. K., Johnston, W. K., Garrett-Engele, P., Lim, L. P., & Bartel, D. P. (2007). MicroRNA targeting specificity in mammals: Determinants beyond seed pairing. *Molecular Cell, 27*(1), 91-105.

Guo, P., Huang, J., Wang, L., Jia, D., Yang, J., Dillon, D. A., . . . Auguste, D. T. (2014). ICAM-1 as a molecular target for triple negative breast cancer. *PNAS, 111*(41), 14710-14715.

Ha, M., & Kim, V. N. (2014). Regulation of microRNA biogenesis. *Nature Reviews Molecular Cell Biology, 15*, 509.

Haenssen, K. K., Caldwell, S. A., Shahriari, K. S., Jackson, S. R., Whelan, K. A., Klein-Szanto, A. J., & Reginato, M. J. (2010). ErbB2 requires integrin alpha5 for anoikis resistance via Src regulation of receptor activity in human mammary epithelial cells. *Journal of Cell Science, 123*(8), 1373-1382.

Hamam, R., Ali, A. M., Alsaleh, K. A., Kassem, M., Alfayez, M., Aldahmash, A., & Alajez, N. M. (2016). microRNA expression profiling on individual breast cancer patients identifies novel panel of circulating microRNA for early detection. *Scientific Reports, 6*, 25997.

Hamam, R., Hamam, D., Alsaleh, K. A., Kassem, M., Zaher, W., Alfayez, M., . . . Alajez, N. M. (2017). Circulating microRNAs in breast cancer: Novel diagnostic and prognostic biomarkers. *Cell Death & Disease, 8*(9), e3045.

Han, J., Lee, Y., Yeom, K. H., Kim, Y. K., Jin, H., & Kim, V. N. (2004). The Drosha-DGCR8 complex in primary microRNA processing. *Genes & Development, 18*(24), 3016-3027.

Hanahan, D., & Weinberg, R. A. (2011). Hallmarks of cancer: The next generation. *Cell, 144*(5), 646-674.

Herner, A., Sauliunaite, D., Michalski, C. W., Erkan, M., De Oliveira, T., Abiatari, I., . . . Kleeff, J. (2011). Glutamate increases pancreatic cancer cell invasion and migration via AMPA receptor activation and Kras-MAPK signaling. *International Journal of Cancer, 129*(10), 2349-2359.

Hinske, L. C., Franca, G. S., Torres, H. A., Ohara, D. T., Lopes-Ramos, C. M., Heyn, J., . . . Galante, P. A. (2014). miRIAD-integrating microRNA inter- and intragenic data. *Database (Oxford), 2014*, bau099.

Howe, E. N., Cochrane, D. R., & Richer, J. K. (2011). Targets of miR-200c mediate suppression of cell motility and anoikis resistance. *Breast Cancer Research, 13*(2), 45.

Hua, H., Zhang, H., Kong, Q., & Jiang, Y. (2018). Mechanisms for estrogen receptor expression in human cancer. *Experimental Hematology & Oncology, 7*, 24.

Huang, W., Sherman, B. T., & Lempicki, R. A. (2009). Bioinformatics enrichment tools: Paths toward the comprehensive functional analysis of large gene lists. *Nucleic Acids Research, 37*(1), 1-13.

Huang, X., Yuan, T., Liang, M., Du, M., Xia, S., Dittmar, R., . . . Wang, L. (2015). Exosomal miR-1290 and miR-375 as prognostic markers in castration-resistant prostate cancer. *European Urology, 67*(1), 33-41.

Huttlin, E. L., Ting, L., Bruckner, R. J., Gebreab, F., Gygi, M. P., Szpyt, J., . . . Gygi, S. P. (2015). The BioPlex network: A systematic exploration of the human interactome. *Cell, 162*(2), 425-440.

Iglesias, J. M., Beloqui, I., Garcia-Garcia, F., Leis, O., Vazquez-Martin, A., Eguiara, A., . . . Martin, A. G. (2013). Mammosphere formation in breast carcinoma cell lines depends upon expression of E-cadherin. *PLoS ONE, 8*(10), e77281.

Iorio, M. V., & Croce, C. M. (2012). MicroRNA dysregulation in cancer: Diagnostics, monitoring and therapeutics. A comprehensive review. *EMBO Molecular Medicine, 4*(3), 143-159.

Jabbari, N., Reavis, A. N., & McDonald, J. F. (2014). Sequence variation among members of the miR-200 microRNA family is correlated with variation in the ability to induce hallmarks of mesenchymal-epithelial transition in ovarian cancer cells. *Journal of Ovarian Research, 7*, 12.

Jaeger, B. A. S., Neugebauer, J., Andergassen, U., Melcher, C., Schochter, F., Mouarrawy, D., . . . Rack, B. (2017). The HER2 phenotype of circulating tumor cells in HER2-positive early breast cancer: A translational research project of a prospective randomized phase III trial. *PLoS ONE, 12*(6), e0173593.

Janiszewska, J., Szaumkessel, M., Kostrzewska-Poczekaj, M., Bednarek, K., Paczkowska, J., Jackowska, J., . . . Jarmuz-Szymczak, M. (2015). Global miRNA expression profiling identifies miR-1290 as novel potential oncomir in laryngeal carcinoma. *PLoS ONE, 10*(12), e0144924.

Jenning, S., Pham, T., Ireland, S. K., Ruoslahti, E., & Biliran, H. (2013). Bit1 in anoikis resistance and tumor metastasis. *Cancer Letters, 333*(2), 147-151.

Jin, L., Wessely, O., Marcusson, E. G., Ivan, C., Calin, G. A., & Alahari, S. K. (2013). Prooncogenic factors miR-23b and miR-27b are regulated by Her2/Neu, EGF, and TNF-alpha in breast cancer. *Cancer Research, 73*(9), 2884-2896.

Jo, M. H., Shin, S., Jung, S. R., Kim, E., Song, J. J., & Hohng, S. (2015). Human argonaute 2 has diverse reaction pathways on target RNAs. *Molecular Cell, 59*(1), 117-124.

Jonas, S., & Izaurralde, E. (2015). Towards a molecular understanding of microRNA-mediated gene silencing. *Nature Reviews Genetics, 16*(7), 421-433.

Kim, Y. N., Koo, K. H., Sung, J. Y., Yun, U. J., & Kim, H. (2012). Anoikis resistance: An essential prerequisite for tumor metastasis. *International Journal of Cell Biology, 2012*, 306879.

Kodahl, A. R., Lyng, M. B., Binder, H., Cold, S., Gravgaard, K., Knoop, A. S., & Ditzel, H. J. (2014). Novel circulating microRNA signature as a potential non-invasive multi-marker test in ER-positive early-stage breast cancer: A case control study. *Molecular Oncology, 8*(5), 874-883.

Kovacs, E. M., Ali, R. G., McCormack, A. J., & Yap, A. S. (2002). E-cadherin homophilic ligation directly signals through Rac and phosphatidylinositol 3-kinase to regulate adhesive contacts. *Journal of Biological Chemistry, 277*(8), 6708-6718.

Kumar, S., Mapa, K., & Maiti, S. (2014). Understanding the effect of locked nucleic acid and 2'-O-methyl modification on the hybridization thermodynamics of a miRNA-mRNA pair in the presence and absence of AfPiwi protein. *Biochemistry, 53*(10), 1607-1615.

Ladewig, E., Okamura, K., Flynt, A. S., Westholm, J. O., & Lai, E. C. (2012). Discovery of hundreds of mirtrons in mouse and human small RNA data. *Genome Research, 22*(9), 1634-1645.

Lamouille, S., Xu, J., & Derynck, R. (2014). Molecular mechanisms of epithelial-mesenchymal transition. *Nature Reviews Molecular Cell Biology, 15*(3), 178-196.

Lau, M. T., Klausen, C., & Leung, P. C. K. (2011). E-cadherin inhibits tumor cell growth by suppressing PI3K/Akt signaling via β-catenin-Egr1-mediated PTEN expression. *Oncogene, 30*, 2753.

Lee, C. H., Yu, C. C., Wang, B. Y., & Chang, W. W. (2016). Tumorsphere as an effective in vitro platform for screening anti-cancer stem cell drugs. *Oncotarget, 7*(2), 1215-1226.

Lee, H. J., Seo, A. N., Kim, E. J., Jang, M. H., Kim, Y. J., Kim, J. H., . . . Park, S. Y. (2015). Prognostic and predictive values of EGFR overexpression and EGFR copy number alteration in HER2-positive breast cancer. *British Journal of Cancer, 112*(1), 103-111.

Lee, R. C., Feinbaum, R. L., & Ambros, V. (1993). The C. elegans heterochronic gene lin-4 encodes small RNAs with antisense complementarity to lin-14. *Cell, 75*(5), 843-854.

Lehmann, T. P., Korski, K., Gryczka, R., Ibbs, M., Thieleman, A., Grodecka-Gazdecka, S., & Jagodzinski, P. P. (2015). Relative levels of let-7a, miR-17, miR-27b, miR-125a, miR-125b and miR-206 as potential molecular markers to evaluate grade, receptor status and molecular type in breast cancer. *Molecular Medicine Reports, 12*(3), 4692-4702.

Lim, E., Vaillant, F., Wu, D., Forrest, N. C., Pal, B., Hart, A. H., . . . Lindeman, G. J. (2009). Aberrant luminal progenitors as the candidate target population for basal tumor development in BRCA1 mutation carriers. *Nature Medicine, 15*(8), 907-913.

Liu, X., Li, J., Yu, Z., Li, J., Sun, R., & Kan, Q. (2017). miR-935 promotes liver cancer cell proliferation and migration by targeting SOX7. *Oncology Research, 25*(3), 427-435.

Luey, B. C., & May, F. E. (2016). Insulin-like growth factors are essential to prevent anoikis in oestrogen-responsive breast cancer cells: Importance of the type I IGF receptor and PI3-kinase/Akt pathway. *Molecular Cancer, 15*, 8.

Lumachi, F., Luisetto, G., M.M. Basso, S., Basso, U., Brunello, A., & Camozzi, V. (2011). Endocrine therapy of breast cancer. *Current Medicinal Chemistry, 18*(4), 513-522.

Macfarlane, L. A., & Murphy, P. R. (2010). MicroRNA: Biogenesis, function and role in cancer. *Current Genomics, 11*(7), 537-561.

Malagobadan, S., & Nagoor, N. H. (2015). Evaluation of microRNAs regulating anoikis pathways and its therapeutic potential. *BioMed Research International, 2015*, 716816.

Marshall, J. (2011). Transwell((R)) invasion assays. *Methods in Molecular Biology, 769*, 97-110.

Matsusaka, S., Chin, K., Ogura, M., Suenaga, M., Shinozaki, E., Mizunuma, N., . . . Hatake, K. (2012). Detection and HER2 expression of circulating tumor cells in advanced gastric cancer patients. *Journal of Clinical Oncology, 30*(15), 10541-10541.

Meijer, H. A., Smith, E. M., & Bushell, M. (2014). Regulation of miRNA strand selection: Follow the leader? *Biochemistry Society Transactions, 42*(4), 1135-1140.

Michel, J. B., Jondeau, G., & Milewicz, D. M. (2018). From genetics to response to injury: Vascular smooth muscle cells in aneurysms and dissections of the ascending aorta. *Cardiovascular Research, 114*(4), 578-589.

Mishima, Y., Matsusaka, S., Chin, K., Mikuniya, M., Minowa, S., Takayama, T., . . . Hatake, K. (2017). Detection of HER2 amplification in circulating tumor cells of HER2-negative gastric cancer patients. *Target Oncology, 12*(3), 341-351.

Mitra, A., Mishra, L., & Li, S. (2015). EMT, CTCs and CSCs in tumor relapse and drug-resistance. *Oncotarget, 6*(13), 10697-10711.

Mitri, Z., Constantine, T., & O'Regan, R. (2012). The HER2 receptor in breast cancer: Pathophysiology, clinical use, and new advances in therapy. *Chemotherapy Research and Practice, 2012*, 743193.

Molyneux, G., Geyer, F. C., Magnay, F. A., McCarthy, A., Kendrick, H., Natrajan, R., . . . Smalley, M. J. (2010). BRCA1 basal-like breast cancers originate from luminal epithelial progenitors and not from basal stem cells. *Cell Stem Cell, 7*(3), 403-417.

Morozevich, G., Kozlova, N., Cheglakov, I., Ushakova, N., & Berman, A. (2009). Integrin alpha5beta1 controls invasion of human breast carcinoma cells by direct and indirect modulation of MMP-2 collagenase activity. *Cell Cycle, 8*(14), 2219-2225.

Mouw, J. K., Ou, G., & Weaver, V. M. (2014). Extracellular matrix assembly: A multiscale deconstruction. *Nature Reviews Molecular Cell Biology, 15*(12), 771-785.

Mullany, L. E., Herrick, J. S., Wolff, R. K., & Slattery, M. L. (2016). MicroRNA seed region length impact on target messenger RNA expression and survival in colorectal cancer. *PLoS ONE, 11*(4), e0154177.

Nagaraja, G. M., Othman, M., Fox, B. P., Alsaber, R., Pellegrino, C. M., Zeng, Y., . . . Kandpal, R. P. (2006). Gene expression signatures and biomarkers of noninvasive and invasive breast cancer cells: Comprehensive profiles by representational difference analysis, microarrays and proteomics. *Oncogene, 25*(16), 2328-2338.

Nahta, R., Yuan, L. X., Zhang, B., Kobayashi, R., & Esteva, F. J. (2005). Insulin-like growth factor-I receptor/human epidermal growth factor receptor 2 heterodimerization contributes to trastuzumab resistance of breast cancer cells. *Cancer Research, 65*(23), 11118-11128.

Nam, J. W., Rissland, O. S., Koppstein, D., Abreu-Goodger, C., Jan, C. H., Agarwal, V., . . . Bartel, D. P. (2014). Global analyses of the effect of different cellular contexts on microRNA targeting. *Molecular Cell, 53*(6), 1031-1043.

Navin, N., Kendall, J., Troge, J., Andrews, P., Rodgers, L., McIndoo, J., . . . Wigler, M. (2011). Tumour evolution inferred by single-cell sequencing. *Nature, 472*(7341), 90-94.

Ng, E. K., Li, R., Shin, V. Y., Jin, H. C., Leung, C. P., Ma, E. S., . . . Kwong, A. (2013). Circulating microRNAs as specific biomarkers for breast cancer detection. *PLoS ONE, 8*(1), e53141.

O'Brien, J., Hayder, H., Zayed, Y., & Peng, C. (2018). Overview of microRNA biogenesis, mechanisms of actions, and circulation. *Frontiers in Endocrinology (Lausanne), 9*, 402.

Obad, S., dos Santos, C. O., Petri, A., Heidenblad, M., Broom, O., Ruse, C., . . . Kauppinen, S. (2011). Silencing of microRNA families by seed-targeting tiny LNAs. *Nature Genetics, 43*(4), 371-378.

Paoli, P., Giannoni, E., & Chiarugi, P. (2013). Anoikis molecular pathways and its role in cancer progression. *Biochimica et Biophysica Acta (BBA) - Molecular Cell Research, 1833*(12), 3481-3498.

Papadaki, C., Stratigos, M., Markakis, G., Spiliotaki, M., Mastrostamatis, G., Nikolaou, C., . . . Agelaki, S. (2018). Circulating microRNAs in the early prediction of disease recurrence in primary breast cancer. *Breast Cancer Research, 20*(1), 72.

Perron, M. P. (2008). Protein interactions and complexes in human microRNA biogenesis and function. *Frontiers in Bioscience, 13*(13), 2537.

Piscitelli, E., Cocola, C., Thaden, F. R., Pelucchi, P., Gray, B., Bertalot, G., . . . Zucchi, I. (2015). Culture and characterization of mammary cancer stem cells in mammospheres. *Methods in Molecular Biology, 1235*, 243-262.

Polyak, K. (2011). Heterogeneity in breast cancer. *Journal of Clinical Investigation, 121*(10), 3786-3788.

Prat, A., Pineda, E., Adamo, B., Galvan, P., Fernandez, A., Gaba, L., . . . Munoz, M. (2015). Clinical implications of the intrinsic molecular subtypes of breast cancer. *Breast, 24* 26-35.

Pu, H. Y., Xu, R., Zhang, M. Y., Yuan, L. J., Hu, J. Y., Huang, G. L., & Wang, H. Y. (2017). Identification of microRNA-615-3p as a novel tumor suppressor in non-small cell lung cancer. *Oncology Letters, 13*(4), 2403-2410.

Reginato, M. J., Mills, K. R., Paulus, J. K., Lynch, D. K., Sgroi, D. C., Debnath, J., . . . Brugge, J. S. (2003). Integrins and EGFR coordinately regulate the pro-apoptotic protein Bim to prevent anoikis. *Nature Cell Biology, 5*(8), 733-740.

Rivenbark, A. G., O'Connor, S. M., & Coleman, W. B. (2013). Molecular and cellular heterogeneity in breast cancer: Challenges for personalized medicine. *The American Journal of Pathology, 183*(4), 1113-1124.

Rodrigues-Lima, F., Dairou, J., Busi, F., & Dupret, J.-M. (2012). Human Arylamine N-acetyltransferase 1: From Drug Metabolism to Drug Target. In M. Chatterjee & K. Kashfi (Eds.), *Cell Signaling & Molecular Targets in Cancer* (10.1007/978-1-4614-0730-0_2pp. 23-35). New York, NY: Springer New York.

Rodriguez, L. G., Wu, X., & Guan, J. L. (2005). Wound-healing assay. *Methods in Molecular Biology, 294*, 23-29.

Saha Roy, S., & Vadlamudi, R. K. (2012). Role of estrogen receptor signaling in breast cancer metastasis. *International Journal of Breast Cancer, 2012*, 654698.

Saha, S., Panigrahi, D. P., Patil, S., & Bhutia, S. K. (2018). Autophagy in health and disease: A comprehensive review. *Biomedicine & Pharmacotherapy, 104*, 485-495.

Schaffner, F., Ray, A. M., & Dontenwill, M. (2013). Integrin alpha5beta1, the fibronectin receptor, as a pertinent therapeutic target in solid tumors. *Cancers (Basel), 5*(1), 27-47.

Servin-Gonzalez, L. S., Granados-Lopez, A. J., & Lopez, J. A. (2015). Families of microRNAs expressed in clusters regulate cell signaling in cervical cancer. *International Journal of Molecular Sciences, 16*(6), 12773-12790.

Shah, M. Y., Ferrajoli, A., Sood, A. K., Lopez-Berestein, G., & Calin, G. A. (2016). microRNA therapeutics in cancer - An emerging concept. *EBioMedicine, 12*, 34-42.

Shin, J. Y., Hong, S. H., Kang, B., Minai-Tehrani, A., & Cho, M. H. (2013). Overexpression of beclin1 induced autophagy and apoptosis in lungs of K-rasLA1 mice. *Lung Cancer, 81*(3), 362-370.

Slabáková, E., Culig, Z., Remšík, J., & Souček, K. (2017). Alternative mechanisms of miR-34a regulation in cancer. *Cell Death & Disease, 8*, e3100.

Soliman, N. A., & Yussif, S. M. (2016). Ki-67 as a prognostic marker according to breast cancer molecular subtype. *Cancer Biology & Medicine, 13*(4), 496-504.

Sun, Y., Liu, J. H., Sui, Y. X., Jin, L., Yang, Y., Lin, S. M., & Shi, H. (2011). Beclin1 overexpression inhibits proliferation, invasion and migration of CaSki cervical cancer cells. *Asian Pacific Journal of Cancer Prevention, 12*(5), 1269-1273.

Taylor, M. A., Sossey-Alaoui, K., Thompson, C. L., Danielpour, D., & Schiemann, W. P. (2013). TGF-beta upregulates miR-181a expression to promote breast cancer metastasis. *Journal of Clinical Investigation, 123*(1), 150-163.

Teng, Y., Xie, X., Walker, S., White, D. T., Mumm, J. S., & Cowell, J. K. (2013). Evaluating human cancer cell metastasis in zebrafish. *BMC Cancer, 13*, 453.

Tiang, J. M., Butcher, N. J., Cullinane, C., Humbert, P. O., & Minchin, R. F. (2011). RNAi-mediated knock-down of arylamine N-acetyltransferase-1 expression induces E-cadherin up-regulation and cell-cell contact growth inhibition. *PLoS ONE, 6*(2), e17031.

Tiang, J. M., Butcher, N. J., & Minchin, R. F. (2010). Small molecule inhibition of arylamine N-acetyltransferase Type I inhibits proliferation and invasiveness of MDA-MB-231 breast cancer cells. *Biochemical and Biophysical Research Communications, 393*(1), 95-100.

Tiang, J. M., Butcher, N. J., & Minchin, R. F. (2015). Effects of human arylamine N-acetyltransferase I knockdown in triple-negative breast cancer cell lines. *Cancer Medicine, 4*(4), 565-574.

Toloudi, M., Apostolou, P., Chatziioannou, M., & Papasotiriou, I. (2011). Correlation between cancer stem cells and circulating tumor cells and their value. *Case Reports in Oncology, 4*(1), 44-54.

Tsai, J. H., & Yang, J. (2013). Epithelial-mesenchymal plasticity in carcinoma metastasis. *Genes & Development, 27*(20), 2192-2206.

Tsuchiya, Y., Nakajima, M., Takagi, S., Taniya, T., & Yokoi, T. (2006). MicroRNA regulates the expression of human cytochrome P450 1B1. *Cancer Research, 66*(18), 9090-9098.

Vachon, P. H. (2011). Integrin signaling, cell survival, and anoikis: Distinctions, differences, and differentiation. *Journal of Signal Transduction, 2011*, 738137.

Van Poznak, C., Somerfield, M. R., Bast, R. C., Cristofanilli, M., Goetz, M. P., Gonzalez-Angulo, A. M., . . . Harris, L. N. (2015). Use of biomarkers to guide decisions on systemic therapy for women with metastatic breast cancer: American Society of Clinical Oncology clinical practice guideline. *Journal of Clinical Investigation, 33*(24), 2695-2704.

Veinotte, C. J., Dellaire, G., & Berman, J. N. (2014). Hooking the big one: The potential of zebrafish xenotransplantation to reform cancer drug screening in the genomic era. *Disease Models & Mechanisms, 7*(7), 745-754.

Vicente-Manzanares, M., Choi, C. K., & Horwitz, A. R. (2009). Integrins in cell migration--the actin connection. *Journal of Cell Science, 122*(Pt 2), 199-206.

Vieira, A. F., & Schmitt, F. (2018). An update on breast cancer multigene prognostic tests-emergent clinical biomarkers. *Frontiers in Medicine (Lausanne), 5*, 248.

Wakefield, L., Robinson, J., Long, H., Ibbitt, J. C., Cooke, S., Hurst, H. C., & Sim, E. (2008). Arylamine N-acetyltransferase 1 expression in breast cancer cell lines: A potential marker in estrogen receptor-positive tumors. *Genes, Chromosomes & Cancer, 47*(2), 118-126.

Wang, J., Liu, L., Sun, Y., Xue, Y., Qu, J., Pan, S., . . . Zhang, J. (2018). miR-615-3p promotes proliferation and migration and inhibits apoptosis through its potential target CELF2 in gastric cancer. *Biomedicine & Pharmacotherapy, 101*, 406-413.

Wang, L., Minchin, R. F., & Butcher, N. J. (2018). Arylamine N-acetyltransferase 1 protects against reactive oxygen species during glucose starvation: Role in the regulation of p53 stability. *PLoS ONE, 13*(3), e0193560.

Wang, Y., Yu, Y., Tsuyada, A., Ren, X., Wu, X., Stubblefield, K., . . . Wang, S. E. (2011). Transforming growth factor-beta regulates the sphere-initiating stem cell-like feature in breast cancer through miRNA-181 and ATM. *Oncogene, 30*(12), 1470-1480.

Wang, Z. (2017). ErbB receptors and cancer. *Methods in Molecular Biology, 1652*, 3-35.

Wei, J. L., Li, Y. C., Ma, Z. L., & Jin, Y. X. (2016). MiR-181a-5p promotes anoikis by suppressing autophagy during detachment induction in the mammary epithelial cell line MCF10A. *Protein Cell, 7*(4), 305-309.

Wu, C. (2007). Focal adhesion: A focal point in current cell biology and molecular medicine. *Cell Adhesion & Migration, 1*(1), 13-18.

Wu, H., Liang, Y. L., Li, Z., Jin, J., Zhang, W., Duan, L., & Zha, X. (2006). Positive expression of E-cadherin suppresses cell adhesion to fibronectin via reduction of alpha5beta1 integrin in human breast carcinoma cells. *Journal of Cancer Research and Clinical Oncology, 132*(12), 795-803.

Xiao, S., Guo, J., Yun, B. H., Villalta, P. W., Krishna, S., Tejpaul, R., . . . Turesky, R. J. (2016). Biomonitoring DNA adducts of cooked meat carcinogens in human prostate by nano liquid chromatography-high resolution tandem mass spectrometry: Identification of 2-amino-1-methyl-6-phenylimidazo[4,5-b]pyridine DNA adduct. *Analytic Chemistry, 88*(24), 12508-12515.

Xie, G., Yao, Q., Liu, Y., Du, S., Liu, A., Guo, Z., . . . Yuan, Y. (2012). IL-6-induced epithelial-mesenchymal transition promotes the generation of breast cancer stem-like cells analogous to mammosphere cultures. *International Journal of Oncology, 40*(4), 1171-1179.

Xie, J., Burt, D. R., & Gao, G. (2015). Adeno-associated virus-mediated microRNA delivery and therapeutics. *Seminars in Liver Diseases, 35*(1), 81-88.

Xu, J., Wan, X., Chen, X., Fang, Y., Cheng, X., Xie, X., & Lu, W. (2016). miR-2861 acts as a tumor suppressor via targeting EGFR/AKT2/CCND1 pathway in cervical cancer induced by human papillomavirus virus 16 E6. *Scientific Reports, 6*, 28968.

Yang, C., Tabatabaei, Seyed N., Ruan, X., & Hardy, P. (2017). The dual regulatory role of miR-181a in breast cancer. *Cellular Physiology and Biochemistry, 44*(3), 843-856.

Yang, M., Cui, G., Ding, M., Yang, W., Liu, Y., Dai, D., & Chen, L. (2016). miR-935 promotes gastric cancer cell proliferation by targeting SOX7. *Biomedicine & Pharmacotherapy, 79*, 153-158.

Yu, S. J., Hu, J. Y., Kuang, X. Y., Luo, J. M., Hou, Y. F., Di, G. H., . . . Shao, Z. M. (2013). MicroRNA-200a promotes anoikis resistance and metastasis by targeting YAP1 in human breast cancer. *Clinical Cancer Research, 19*(6), 1389-1399.

Yu, Z., Pestell, T. G., Lisanti, M. P., & Pestell, R. G. (2012). Cancer stem cells. *International Journal of Biochemistry & Cell Biology, 44*(12), 2144-2151.

Zhang, W. C., Chin, T. M., Yang, H., Nga, M. E., Lunny, D. P., Lim, E. K., . . . Lim, B. (2016). Tumour-initiating cell-specific miR-1246 and miR-1290 expression converge to promote non-small cell lung cancer progression. *Nature Communications, 7*, 11702.

Zhang, X., Zhang, B., Gao, J., Wang, X., & Liu, Z. (2013). Regulation of the microRNA 200b (miRNA-200b) by transcriptional regulators PEA3 and ELK-1 protein affects expression of Pin1 protein to control anoikis. *Journal of Biological Chemistry, 288*(45), 32742-32752.

Zhang, Y., Wang, Z., & Gemeinhart, R. A. (2013). Progress in microRNA delivery. *Journal of Controlled Release, 172*(3), 962-974.

LIST OF PUBLICATIONS AND PAPERS PRESENTED

PUBLICATIONS:

1. **Malagobadan, S.**, & Nagoor, N. H. (2019). Anoikis. In P. Boffetta & P. Hainaut (Eds.), *Encyclopedia of Cancer* (3rd ed., pp. 75-84): Academic Press.

2. **Malagobadan, S.**, & Nagoor, N. H. (2015). Evaluation of microRNAs regulating anoikis pathways and its therapeutic potential. *BioMed Research International, 2015*, 716816.

PAPERS PRESENTED:

1. **Malagobadan, S.**, & Nagoor, N. H. (2018). *Elucidation of microRNA regulating anoikis in breast cancer.* Paper presented at the International Conference on Biochemistry, Molecular Biology and Biotechnology 2018, 15 – 16th August 2018, Selangor, Malaysia.